FINAL REPORT

Predicting the Mobility and Burial of Underwater Munitions and Explosives of Concern Using the VORTEX Model

ESTCP Project MM-0417

MAY 2008

Jeffrey V. Wilson
Ian McKissick
Sound & Sea Technology, Inc.

Scott A. Jenkins
Joseph Wasyl
Scott A. Jenkins Consultants

Alexandra DeVisser
Barbara Sugiyama
Naval Facilities Engineering Command Engineering Service Center

Approved for public release; distribution unlimited.

Environmental Security Technology Certification Program

Authors

Jeffrey V. Wilson, Sound & Sea Technology, Inc.
Ian McKissick, Sound & Sea Technology, Inc.
Scott A. Jenkins, PhD, Scott A. Jenkins Consultants
Joseph Wasyl, Scott A. Jenkins Consultants
Alexandra DeVisser, Naval Facilities Engineering Command Engineering Service Center
Barbara Sugiyama, Naval Facilities Engineering Command Engineering Service Center

Table of Contents

Authors ii
Table of Contents iii
List of Figures v
List of Tables ix
List of Abbreviations and Acronyms 1
Acknowledgements 3
Executive Summary 4
1. Introduction 7
1.1 Background 9
1.2 Demonstration Hypotheses (expected outcomes) 12
1.3 Program Performance Objectives 13
1.4 Field Demonstration Method 14
1.5 Demonstration Site Selection 15
1.5.1 Pre-Demonstration Testing and Analysis 15
2. Field Demonstration ONE (FRF Duck, NC) 17
2.1 Demonstration Site Description 17
2.1.1 Characteristics of Trailing Edge Coastal Classification 17
2.1.3 Environmental Permitting 17
2.1.4 Field Demonstration Staff 19
2.2 Demonstration Plan 19
2.2.1 Demonstration Layout 19
2.2.2 Surrogates Used 21
2.3 Field Validation Measurements 23
2.3.1 Installation Notes 24
2.3.2 Diving Operations during Installation and First Round of Measurements 25
2.4. Installation Phase Measurement Data (Round One Data) 27
2.4.1 Measurement Method Used 27
2.4.2 Round One Measurement Data 28
2.4.3 Round One Results 34
2.5 Round Two Measurement Data 35
2.6 Round Three Measurement Data 39
2.7 Round Four Measurement Data 45
2.8 Rounds Five and Six Measurement Data 55
2.9 Magnetometer Tests 57
2.10 Recovery 63

3.0 Future Plans 64
3.1 Demobilization 64
3.2 ESTCP UXO Mobility Model Final Report 65
4.0 UXO Mobility Model Validation on FRF Duck Data 65
4.1 Technical Approach 65
4.1.1 Process Model Architecture 65
4.2 Model Initialization 73
4.2.1 Farfield Initialization 73
4.2.1.1 Bathymetry and Construction of Farfield Grid 73
4.2.1.2 Wave and Current Forcing 80
4.2.2 Nearfield Initialization 83
4.2.2.1 Sediment Parameters 83
4.2.2.2 UXO Shape Lattice 84
4.2.2.3 Burial and Migration from Mode 1 Analysis 85
4.3 UXO Migration/Burial Model Performance at FRF Demonstration 87
4.3.1 Model Predictions of UXO Migration and Burial Rates 91
4.3.2 Predictive Skill of Model Predictions 105
5.0 Conclusions 106
6.0 References 110
Appendix A: UXO Mobility Model FORTRAN Code (FRF Duck) 113
Appendix B: FRF Duck Field Test Site Permits 129
Appendix C: Test Hardware 141
Appendix D: Data 145

List of Figures

Figure 1. Site Conceptual Model for UXO showing the UXO Mobility analysis as part of source quantification. 10

Figure 2. UXO Mobility Model output of flow and scour over a 5”/38 projectile surrogate. 11

Figure 3. Duck, NC, is approximately 60 miles south of Norfolk, VA. 16

Figure 4. Coastal classification system with geomorphic types and synthesized model input parameters. The FRF Duck Field Test site is a Type B (Trailing Edge) site. 17

Figure 5. FRF Duck Site Overview showing the Inshore and Offshore Fields. 20

Figure 6. FRF Duck pier, beach, and CRAB vehicle. 21

Figure 7. Surrogate projectile for 5”/38 round. 22

Figure 8. An assembly of 5”/38 surrogates deployed in the FRF Field Demonstration. 22

Figure 9. The 20 mm surrogates deployed are Navy standard inert shapes used in testing ammunition handling systems. 23

Figure 10. The FRF Duck CRAB was used to lower the 5”/38 surrogates into place. 25

Figure 11. The FRF Duck measurement method. 27

Figure 12. Inshore Field Round One measurements. 29

Figure 13. Offshore Field Round One measurements. 30

Figure 14. Round One measurement data for Surrogate #11 shows an example of the largest movement and best triangulation recorded. 31

Figure 15. Round One measurement for Surrogate #16. 32

Figure 16. Round One surrogate movement measurements. 34

Figure 17. Incremental movement for Round Two shows the distance measured from the Round One positions over the 6-week period. 37

Figure 18. Inshore surrogate field, Rounds One and Two Movement. 38

Figure 19. Offshore surrogate field, Rounds One and Two Movement. 39

Figure 20. Survey profiles June-August 2005 indicate slight changes in seafloor level in the Inshore Field and virtually no change in the offshore field. 40

Figure 21. Round Three incremental movement as measured from the locations determined in Round Two. 42

Figure 22. Wave data at FRF, Duck, for Measurement Rounds 1-3 (June-Oct 2006) indicate the absence of major storms during this period. 42

Figure 23. Shore profile changes between installation and Round Three measurements. 43

Figure 24. A comparison of predicted (MM) versus measured movement (Inshore Field, south line). 44

Figure 25. Comparison of predicted (MM) versus measured movement for Offshore Field (north line). 45

Figure 26. Inshore profile changes at FRF Duck July 2005 (red line) thru January 2006 (blue line). There was an average of more than +1 meter of sand (burial) at the inshore site. 47

Figure 27. Summary of Inshore Field movements (installation through Round Four). 49

Figure 28. Summary of Offshore Field movements (installation through Round Four). 50

Figure 29. Surrogate #s 11, 12, 23, and 24 (Round Four). 50

Figure 30. Surrogates 3, 4, 15, and 16 (Round Four). 51

Figure 31. Surrogates 5, 6, 17, and 18 (Round Four). 51

Figure 32. Surrogates 7, 8, 19, and 20 (Round Four). 52

Figure 33. Surrogates 9, 10, 21, and 22 (Round Four) 52

Figure 34. Comparison of measured and predicted movement (Round Four, Inshore Field, south line). 53

Figure 35. Statistics of measured versus modeled UXO movement (June 2005 – Feb 2006, FRF Duck Inshore Field). 54

Figure 36. Burial Simulation of 5"/38 surrogates Rounds 1-4 at FRF Duck, NC, June 2005 to February 2006. 55

Figure 37. Survey profiles 22 Feb through 6 July 2006. 56

Figure 38. Cesium magnetometer and 5”/38 surrogate during in-air calibration testing..... 58

Figure 39. One gamma contour magnetic signature for horizontal 5-inch projectile generated by data collected at 6-foot elevation. 59

Figure 40. One gamma contour magnetic signature for horizontal 20mm projectile generated by data collected at 3-foot elevation. 60

Figure 41. FRF Duck LARC used for towing the magnetometer during the demonstration..... 61

Figure 42. Magnetic data generated by CRAB underway showing UXO targets and the magnetic disturbance generated by the reference pipes. 62

Figure 43. Evidence of biofouling confirms that 5”/38 rounds were at times unburied, which is consistent with Model predictions (Offshore Field recovery, 3-13 April 2007). 64

Figure 44. Vortex Lattice Scour Burial Model after [2]. 66

Figure 45. Hatteras and Ocracoke littoral cells along the outer banks of North Carolina. 68

Figure 46. Critical mass cross-section (a), volume (b), and thickness versus distance (c)..... 69

Figure 47. Vortex induced velocity at any point near the bed: (a) image plane due to the horseshoe vortex system of an imaginary lattice plane, (b) schematic in the vertical plane. 71

Figure 48. Vortex shedding around the ADCP, a vertical cylinder. 72

Figure 49. Regional bathymetry off of the Field Research Facility (FRF), Duck, NC, used for the littoral cell and refraction/diffraction analysis. 74

Figure 50. Wave measurement buoys and other instrumentation locations offshore of FRF..... 75

Figure 51. Refraction/diffraction pattern for storm of 25 October 2005, during UXO mobility experiment at FRF Duck, NC, where H = 3.12m, T = 10.5 sec, and α = 52deg. 77

Figure 52. Refraction/diffraction pattern for storm of 16 September 2005 during UXO mobility experiment at FRF Duck, NC, where H = 2.96m, T = 9.1 sec, α = 11.6 deg. 78

Figure 53. Wave data for Rounds 1-4, Field Demonstration, FRF, Duck, NC: (a) wave height in surf zone, (b) wave period, and (c) wave direction (1 June 2005- 1 March 2006). 79

Figure 54. Beach profile variation during Field Demonstration, FRF Duck, NC, 28 June – 2 September 2005. 81

Figure 55. Beach profile variation during Field Demonstration, FRF, Duck, NC, 28 June 2005 – 22 February 2006. 82

Figure 56. Grain size distribution of sediment, FRF Duck, #B6-S1, 1 September 2005. 84

Figure 57. Vortex and scour field from a Mode 1 simulation of the 5”/38 UXO surrogate. 86

Figure 58. The lay-down pattern of the inshore and offshore fields (black dots signify 5”/38 surrogates, red dots denote reference stakes, and yellow dots are 20 mm surrogates). 88

Figure 59. A 3D rendering of the surrogate deployment, FRF, Duck, NC, June 2005, shows the longshore expanse of bar systems from on-range profiles. 89

Figure 60. Schematic of acoustic directional ranging technique for locating surrogate positions during the FRF Field Demonstration. 91

Figure 61. MM simulation of migration and burial sequence of 5”/38 surrogate #3, Inshore Group, Round One, FRF Duck, 22-27 June 2005. 92

Figure 62. MM simulation of migration and burial sequence of 5”/38 surrogate #11, Offshore Group, Round One, FRF Duck, 22-27 June 2005. 92

Figure 63. MM simulation of migration and burial sequence of 5”/38 surrogate #3, Inshore Group, Round Two, FRF Duck, 27 June – 12 August 2005. 93

Figure 64. MM simulation of migration and burial sequence of 5”/38 surrogate #11, Offshore Group, Round Two, FRF Duck, 27 June – 12 August 2005. 93

Figure 65. MM simulation of migration and burial sequence of 5”/38 surrogate #3, Inshore Group, Round Three, FRF Duck, 12 August – 20 October 2005. 94

Figure 66. MM simulation of migration and burial sequence of 5”/38 surrogate #1, Offshore Group, Round Three, FRF Duck, 12 August – 20 October 2005. 94

Figure 67. MM simulation of migration and burial sequence of 5”/38 surrogate #3, Inshore Group, Round Four, FRF Duck, 20 October 2005 – 16 February 2006. 95

Figure 68. MM simulation of migration and burial sequence of 5”/38 surrogate #1, Offshore Group, Round Four, FRF Duck, 20 October 2005 – 16 February 2006. 95

Figure 69. Predicted versus measured UXO migration in Inshore Field, FRF Duck, NC, Rounds One through Four, 22 June 2005 – 16 February 2006. 100

Figure 70. Predicted versus measured UXO migration in Offshore Field, FRF Duck, NC, Rounds One through Four, 22 June 2005 – 16 February 2006. 101

Figure 71. Predictive skill for all surrogate movement, Rounds 1-4, FRF Duck, NC. (a) Measured probability density function vs. (b) predicted probability density function. 102

Figure 72. MM simulation of migration and burial sequence of 5”/38 UXO surrogate #18 in Inshore Group, during Rounds 5-6 at FRF Duck, NC, 16 February – 3 August 2006. 104

Figure 73.MM simulation of migration and burial sequence of 5”/38 UXO surrogate #23 in Offshore Group during Rounds Five and Six, FRF Duck, NC, 16 February – 3 August 2006.. 104

Figure 74. Predictive skill for surrogate burial, Rounds One through Four, FRF Duck, NC: (a) Measured probability density function, (b) predicted probability density function. 105

Figure 75. Converting Benthos range measurements to surrogate location. 145

Figure 76. Surrogate #7 movement from the initial location, to Round One, and then to Round Two. 147

List of Tables

Table 1. Dates of FRF UXO Field Demonstration Measurements. 8

Table 2. Performance Objectives. 13

Table 3. ESTCP UXO FRF Duck Field Demonstration Points of Contact. 19

Table 4. Round One Surrogate Movement (22-27 June 2005). 33

Table 5. Round Two calculated movement. 36

Table 6. Total vertical profile change for inshore surrogate positions during July to October 2005. 41

Table 7. Round Four measurements show incremental movement since both Round Three and total movement (T). 48

Table 8. Surrogate burial depths as measured on 3 August 2006. 57

Table 9. Round Two measurements determined cumulatively from the installation point to the reference stakes. 146

List of Abbreviations and Acronyms

Acronym	Definition
0817	Navy Pollution Abatement Ashore Research & Development Program
ADCP	Acoustic Doppler Current Profiler
AGD	Applications Guidance Document
ARAMS	Adaptive Risk Assessment Modeling System
ASTM	American Society for Testing and Materials
BPR	Bottom pressure recorders
CATEX	Categorical Exclusion
CFR	U.S. Code of Federal Regulations
CNO	Chief of Naval Operations
CRAB	Coastal Research Amphibious Buggy
DEM/VAL	Demonstration/Validation
Det.	Detachment
DoD	U.S. Department of Defense
DMA	Defense Mapping Agency
DRI	Dive Ranger Interrogator
EPA	U.S. Environmental Protection Agency
ERDC	Engineer Research & Development Center
ESTCP	Environmental Security Technology Certification Program
FRF	Field Research Facility
GPS	Global Positioning System
LARC	Lighter Amphibious Re-supply Cargo
LIDAR	Light Detection And Ranging
Mb	Megabyte
MDT	Mugu Drifter Test
MM	Mobility Model
MMFT	Measurement Method Field Test
MSL	Mean Sea Level
NAD	Navy Ammunition Depot
NAS	Naval Air Station

NAVFAC	Naval Facilities Engineering Command
NAVFAC ESC	Naval Facilities Engineering Command Engineering Service Center
NESDI	Navy Environmental Sustainability Development to Integration
NGDC	National Geophysical Data Center
NGVD	National Geodetic Vertical Datum
NOS	National Ocean Service
NS	Naval Station
NWS	Naval Weapons Station
ONR	Office of Naval Research
NAVFAC Pacific	NAVFAC Pacific Division
PMRF	Pacific Missile Range Facility
SAJ	Dr. Scott A. Jenkins Consulting
SCM	Site Conceptual Model
SEI	Sea Engineering, Inc.
SPAWAR	Space and Naval Warfare Systems Command
SST	Sound & Sea Technology
TAR	Tidewater Atlantic Research, Inc.
UDR	Underwater Diver Receiver
USACE	U.S. Army Corps of Engineers
USAESCH	U.S. Army Engineering and Support Center
USGS	United States Geological Survey
UXO	unexploded ordnance
VSW	Very Shallow Water
VORTEX	Vortex Lattice Model
wrt	with respect to

Acknowledgements

The UXO Mobility Model Demonstration/Validation program was funded by the Environmental Security Technology Certification Program (ESTCP). It was conducted by the Naval Facilities Engineering Command Engineering Service Center (NAVFAC ESC), with support from Sound & Sea Technology, Inc. (SST). Ms. Barbara Sugiyama and Ms. Alexandra DeVisser, with NAVFAC ESC, were the Co-Principle Investigators for this effort. The SST program was lead by Mr. Jeffrey Wilson. The UXO Mobility Model was developed by Dr. Scott Jenkins and Mr. Joe Wasyl of Scott A. Jenkins Consulting. The Model was tested and evaluated by Mr. Dennis Garrood, Mrs. Chanda Daly, and Mr. Eugene Keam of SST. The field work was directed by Mr. William Daly and Mr. Ian McKissick of SST. On-site field demonstration support was provided by Mr. Carl Miller and the staff of the U.S. Army Corps of Engineers (USACE) Field Research Facility (FRF) at Duck, NC. This report was prepared by the combined NAVFAC ESC/SST/SAJ staff.

The original UXO Mobility Model was developed under the Chief of Naval Operation's (CNO) Navy Environmental Sustainability Development to Integration (NESDI) program. The NESDI program is managed for CNO-N45 by the Naval Facilities Engineering Command (NAVFAC). The model upgrades and the field demonstration and validation efforts were funded by the Environmental Security Technology Certification Program (ESTCP).

Executive Summary

A process-based unexploded ordnance (UXO) Mobility Model (MM) was developed and demonstrated at two separate offshore sites. A Trailing Edge geomorphic environment off the east coast of North Carolina at the U.S. Army Corps of Engineers Field Research Facility (FRF), Duck, NC and Biogenic Reef site off the shore of the Pacific Missile Range Facility (PMRF) on Kauai, Hawaii. This report addresses the FRF demonstration where 24 inert surrogate 5”/38 projectiles were placed in the field and their movement was monitored between June 2005 and April 2007. This measured movement was compared to the MM generated simulations of hydrodynamic forcing, UXO migration, and UXO burial using the same parameters. The data showed that they were in general agreement.

The field demonstration was successful in that all the desired data were obtained. The calibration and validation of the MM also was successful – the MM only required minor calibration and the validation showed the predictive skill of the Model, which is derived from the mean squared error between predicted and measured outcomes, to be better than 0.90.

Although the selected site normally is exposed to hurricanes in the summer and nor’easter storms in the winter, the two years of the demonstration experienced unusually mild weather, since the usual hurricanes this time veered into the Gulf of Mexico. Even so, there was adequate movement of the surrogates to provide useful data and allow validation of the MM.

The following conclusions and lessons learned are derived from the demonstration results and the following MM calibration and validation:

- **The trailing edge coast environment of the Outer Banks is a challenging UXO modeling problem that requires very large farfield model grids to adequately resolve the highly variable nearshore bathymetry that ultimately controls the burial/migration evolution.** The far field grid is assembled from a 2,401 x 2,401 point array (5,764,801 grid points) formatted by latitude and longitude using 3 x 3 arc second grid cell resolution and yielding a computational domain of 168.1 km along the x-axis (longitude) and 222.3 km along the y-axis (latitude). This is the largest grid on which the MM has computed UXO transport and burial to date, and was necessitated by the broad-scale longshore fluxes of sediment and mass exchange occurring between the Hatteras and Ocracoke Littoral Cells. Spatial variation in wave forcing over the barrier island system of the Outer Banks is derived from refraction/diffraction analysis over the far field grid based on directional wave measurements from instrumentation maintained by FRF. This instrumentation includes a directional wave buoy in 17m water depth (Sensor #630), pier-mounted pressure sensors at 2m depth, (Sensor # 651), and an Acoustic Doppler Current Profiler (ADCP) with pressure sensor array installed at 8m depth. The nearfield of the model was gridded for a fine to medium coarse sand bottom that was parameterized by 20 grain size bins according to the in situ grain size distribution. The FRF Duck sand is well sorted by the wave action, and mineral analysis indicates it is

predominately quartz of glacial origin. The median grain size is 565 microns with 70 % of the sediment comprised of medium-coarse sand between 450 microns and 750 microns. The UXO surrogates were placed in two groups (inshore group and offshore group) along two cross-shore parallel lines next to FRF profile range lines # 76 and # 85. The inshore field (surrogate #s 1-6 and 13-18) was located on the north side of the FRF Pier in a nominal depth of 2m to 3 m mean sea level(MSL), while the offshore field (surrogate #s 7-12 and 19-24) was laid at depths between 6 m and 7 m MSL.

- **Some of the largest movements of the UXO surrogates (both in the Inshore and Offshore Groups) occurred in the first two days of Round One while burial was minimum immediately after installation.** In this minimal burial state the UXO are particularly susceptible to mobility if sufficiently large waves occur to give rise to a supercritical transport state (Significant Wave Height (*Ho)* $\geq$1.2 m). The high rate of initial migration was subsequently found to be abruptly halted by burial lock-down, after which no further movement of the surrogates occurred. Once the UXO is fully buried, as observed during each diver inspection, subsequent movement is only possible if bottom profile variation results in re-exposure that releases the UXO from burial lock-down and permits it to undergo additional scour and roll progressions. Three such re-exposure events were calculated by the MM during Rounds 1-4 of the experiment, and a forth was calculated for surrogate #23 during Rounds 5-6. <u>The measured movement, and the fact that the recovered surrogates exhibited marine biofouling on their outer surfaces, confirmed these exposure and movement predictions.</u>

- **In the MM, re-exposure of the UXO is the result of a complex interplay between the wave refraction/diffraction time history and the cycloid equilibrium profile (critical mass) algorithms.** Computations of this interplay are only possible in the Mode 3 operation of the MM because it requires time variability in the wave forcing, and spatial variability in the bathymetry. In the FRF model runs of Round 1-6, the time variations of wave height and direction (when shoaled over the broad-shelf bathymetry) produce time variability in the parameters of the bottom profile algorithms. It is that profile variability that can re-expose a UXO and render it susceptible to further migration sequences. The type-b cycloid algorithms in the MM were found to give the best fit to the FRF bottom profiles that are well known for having complex and highly variable bar-trough bed forms. The type-b cycloid has been built into the G-95 (Open Source FORTRAN compiler)/ FRF version of the VORTEX code (Appendix A) that was used exclusively for the model analysis of this study. An interesting feature of the calibrated cycloid profiles using the supporting survey data is that the closure depth was only $h_c \approx 6$ m to 7 m, when normally it is about twice that value. The explanation for this beach profile anomaly was the unusually benign wave forcing that persisted throughout the experiment. The thickness of the critical mass (depth of permanent entombment) is $\zeta_c = 220$ cm for the inshore UXO group; $\zeta_c = 140$ cm for the offshore group; and the critical mass of sand (volume of sand that must be removed to expose buried UXO) is $V_c = 600$ m^3 to 1200 m^3 per meter of shoreline.

- **The most accurate model predictions of *migration* were obtained with surrogate #3 in the Inshore Group and surrogate # 11 in the Offshore Group.** The MM calculation of net movement of surrogate #3 from the beginning of Round One until the end of Round Four was $\xi(i)$ = 915 cm north of its initial placement. This agrees closely with a measured net northerly movement of 9.1 m using acoustic ranging techniques. The net movement of surrogate #11 from the beginning of Round One until the end of Round Four was $\xi(i)$= 443 cm offshore of its initial placement, as compared to a measured value of 4.0 m of offshore movement.

- **The most accurate model predictions of *burial* were obtained during Rounds 5-6 with surrogate #18 in the Inshore Group and surrogate # 23 in the Offshore Group.** Over the course of Rounds 5-6, the bottom profile transitioned from a winter equilibrium to a summer equilibrium and burial depth for surrogate #18 was predicted to decline to $h(i)$ = 43 cm by 3 August 2006. This compared to a measured burial depth of 0.51 m at the time surrogate #18 was extracted. In the Offshore Group, VORTEX predicted active movement for surrogate #23. Here the surrogate was re-exposed circa Julian Day 143 (23 May 2006) and migrated an incremental distance of $\Delta\xi(i)$= 277 cm over a period of about 50 days before become re-buried to a depth of $h(i)$ = 18 cm by the end of Rounds 5-6. This compares to a measured burial depth of 0.15 m for surrogate #23 at the time of extraction.

- **Two approaches were applied to assessing the predictive skill of the quantitative model predictions of the magnitude of migration and burial of UXO surrogates at FRF.** With the first approach, we construct probability density functions of migration and burial magnitudes predicted by the model and compare them with the probability density functions assembled from the observed outcomes of the experiment. With the second approach, we computed a predictive skill factor, R, from the mean squared error between the predicted and measured outcomes.

- **A total of 80 realizations of migration distance were constructed from the diver measurements from Rounds 1-4. These are contrasted with the 96 simulated realizations of migration distance that make up the modeled probability density function.** The peak, spread, and shape of the predicted and measured probability density functions of migration are quite similar. The MM predicts a mean migration distance of 3.5 m as compared to an observed mean of 4.6 m, an agreement within measurement error. The model slightly over-predicts the spread in migration outcomes, predicting a maximum migration distance of 14.3 m and a minimum of 0.5 m; compared to an observed maximum of 12.6 m and an observed minimum of 0.7 m. However, the standard deviation of the modeled migration is slightly less than observed, with the model giving σ_i = 1.9 m versus the observed σ_i = 2.6 m. This is to be expected when comparing a process-based model to stochastics from a field experiment.

- **The measured and predicted burial ensembles were assembled into probability density functions based on 98 separate observations and predictions during Rounds**

1-6. The peak of the measured distribution, its breadth, and shape are all faithfully replicated by the modeled distribution. The model predicts a mean burial depth of 90 cm as compared to an observed mean of 85 cm. The model slightly under-predicts the spread in burial outcomes, predicting a maximum burial depth of 258 cm and a minimum of 11 cm. This compares to an observed maximum of 265 cm and an observed minimum of 2 cm. The standard deviations are virtually the same for both the observed and modeled distributions, σ_i = 58 -59 cm.

- **The skill factor for migration at FRF was calculated at R_ξ = 0.87 and R_h = 0.93 for burial. For coastal processes modeling and mine burial prediction in particular, any skill factor in excess of 0.8 is considered to be a good result.**

1. Introduction

This report is part of the documentation of the Environmental Security Technology Certification Program (ESTCP) Unexploded Ordnance (UXO) Mobility Model (MM) demonstration and validation, and documents the portion of the project conducted at the Army Corps of Engineers (USACE) Field Research Facility (FRF), Duck, North Carolina. The objective of the ESTCP UXO MM demonstration project was to demonstrate and validate the MM for two of the most important coastal classifications:

- Trailing Edge (east coast of the continental United States) and
- Biogenic Reef (typical of tropical island coastlines).

The Trailing Edge environment typically is characterized by areas located on a very wide, shallow continental shelf area with a heavy bottom sediment cover composed of silicon-based sands and sediments which is typical of the east coast of the United States. Biogenic reefs typically exhibit more irregular seafloor shapes crossed by channels and limited sediment covers of detrital carbonate sands. This report documents the first of two major field demonstrations. The second was conducted at the Pacific Missile Range Facility (PMRF), on the west coast of the island of Kauai, HI [1].

The ESTCP UXO Mobility Model project consists of three main parts:

- Refine and update the Navy-developed MM
- Conduct of two field demonstrations to provide calibration/validation data and
- Calibrate/validate the MM using the field demonstration data

This report documents the results of the first of the two major demonstrations, which was conducted at the USACE, FRF, Duck, North Carolina. The second demonstration was conducted at the Pacific Missile Range Facility (PMRF), Kauai, Hawaii, during February to June 2007; that test is reported under separate cover [1].

The basic validation method places a series of surrogate 5”/38 rounds deployed at known locations off the coast and tracks their movement with acoustic pingers and diver tracking systems, while also recording the local current and wave conditions. Once the observed movement was compared to MM predictions for the given environmental conditions, the MM was first calibrated, and then validated. Taken together, these demonstrations provide data to calibrate and validate the MM for the majority of the identified underwater UXO sites in the U.S.

The first field demonstration was conducted at the USACE, Engineer Research & Development Center (ERDC), FRF, Duck, North Carolina. The staff of FRF, Duck, and their specialized handling vehicles and instrumentation provided outstanding support for this demonstration.

The demonstration began on 22 June 2005 and the surrogates were monitored through the winter storm and summer hurricane seasons of 2005-2006 and 2006-2007. Half the demonstration items were recovered in April 2007. Weather, FRF schedule conflicts, and diver equipment difficulties extended final recovery attempts until Sep 2008. It was finally concluded that since the needed data were already obtained, the surrogates posed no environmental risk, and funds were expended, the remaining 12 surrogates should be abandoned in place.

The weather conditions during the two demonstration years were somewhat milder than normal so there were no “extreme events” and no resultant large-scale movements (hundreds of meters migration, UXO washed ashore, etc.). However, there were movements large enough to be usefully measured by the instrumentation system. Measurements of the surrogate movements were conducted every few months, as local operations permitted. The measurement system did reveal movements that were consistent with the MM predictions.

This report describes the installation at the FRF Duck site on 22 June 2005 and seven sets of location measurements taken over the following 28 months (Table 1).

Table 1. Dates of FRF UXO Field Demonstration Measurements.

Operation	Date
Deployment	22 Jun 2005
Round One	28 Jun 2005
Round Two	12 Aug 2005
Round Three	20 Oct 2005
Round Four	15 Feb 2006
Round Five (magnetometer)	25 July 2006
Round Six (limited burial depth check)	3 Aug 2006

Offshore Field Recovery	13 Apr 2007
Inshore Field Recovery	abandoned in place

Despite the extraordinarily high number of extreme hurricanes in 2006 (i.e., Katrina, Rita, et al.), they all passed south of Florida and into the Gulf of Mexico instead of veering up the East Coast. As a result, after a small initial movement, the surrogates were buried by the accretion of the sand and remained buried most of the time during the demonstration period. Fortunately, the migration of sand waves through the site did create intermittent unburial and small-scale movement. The MM predicts that effect and the measurements match the predictions with only minor calibration. The presence of biofouling on the surrogate demonstration items further confirms the occasional exposure.

1.1 Background

Sustainable range management and readiness are vital national security interests, yet are subject to increasingly restrictive regulatory oversight and public concern for safety. In an effort to address these concerns, the Navy through its Navy Environmental Sustainability Development to Implementation (NESDI) Program funded a program to assess the environmental effects of underwater unexploded ordnance (UXO). A site conceptual model (SCM) was developed under this program and is included as Figure 1.

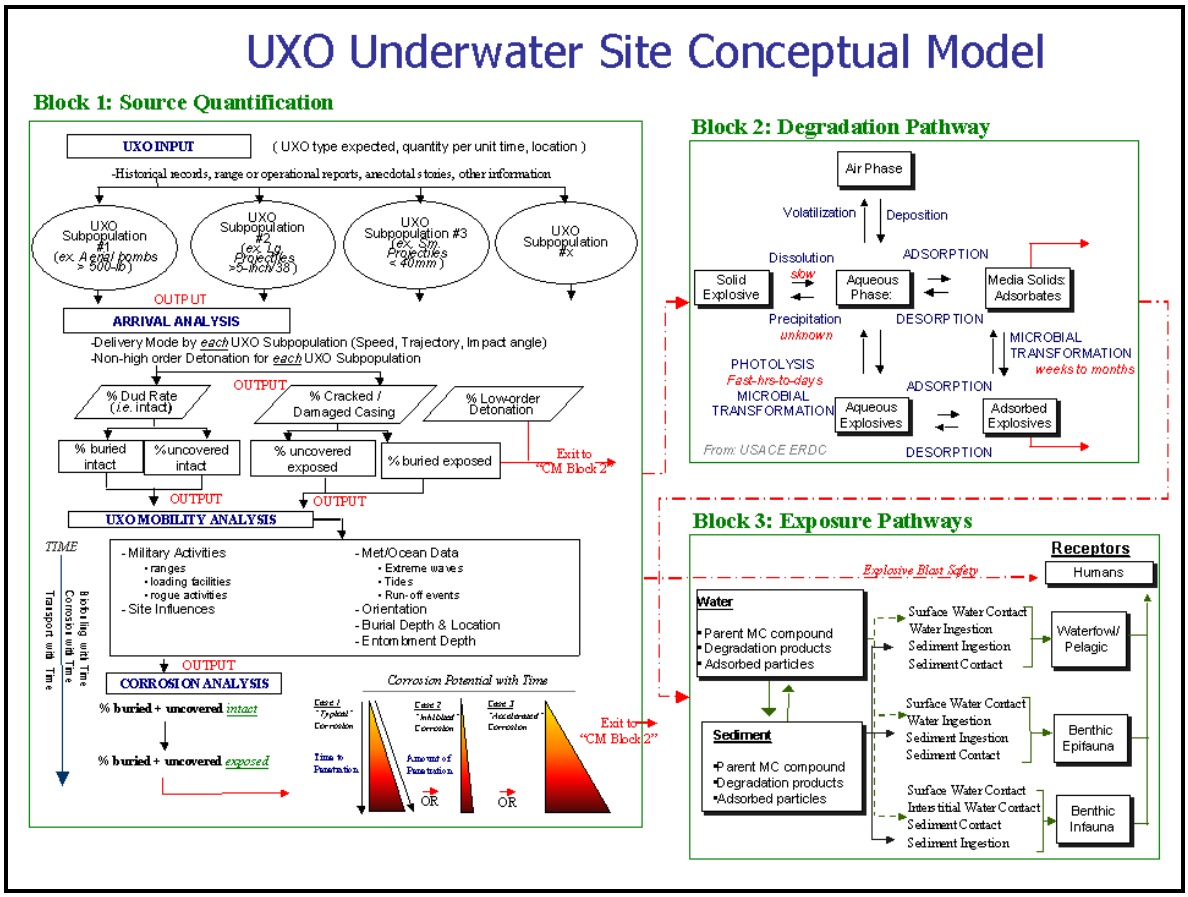

Figure 1. Site Conceptual Model for UXO showing the UXO Mobility analysis as part of source quantification.

After evaluating the SCM at the beginning of the effort against existing scientific data and models, various data gaps were identified. One of these data gaps was the inability to predict the mobility and burial of UXO underwater. To meet this need, the Naval Facilities Command Engineering Service Center (NAVFAC ESC) initiated a project to modify the existing *Vortex Lattice* (VORTEX) *Scour and Burial Model*, which is used to predict mine mobility and burial [2]. The new software is called the UXO Mobility Model (MM). Because of the differences in size, shape, and weight from mines, UXO exhibit both variable responses to ambient coastal dynamics and diverse modes of mobility. The mine-movement model was modified to predict UXO mobility and burial in the underwater environment. Figure 2 shows a plot illustrating the model of the near-field flow over a partially buried UXO (5”/38 round), and the scour associated with the flow.

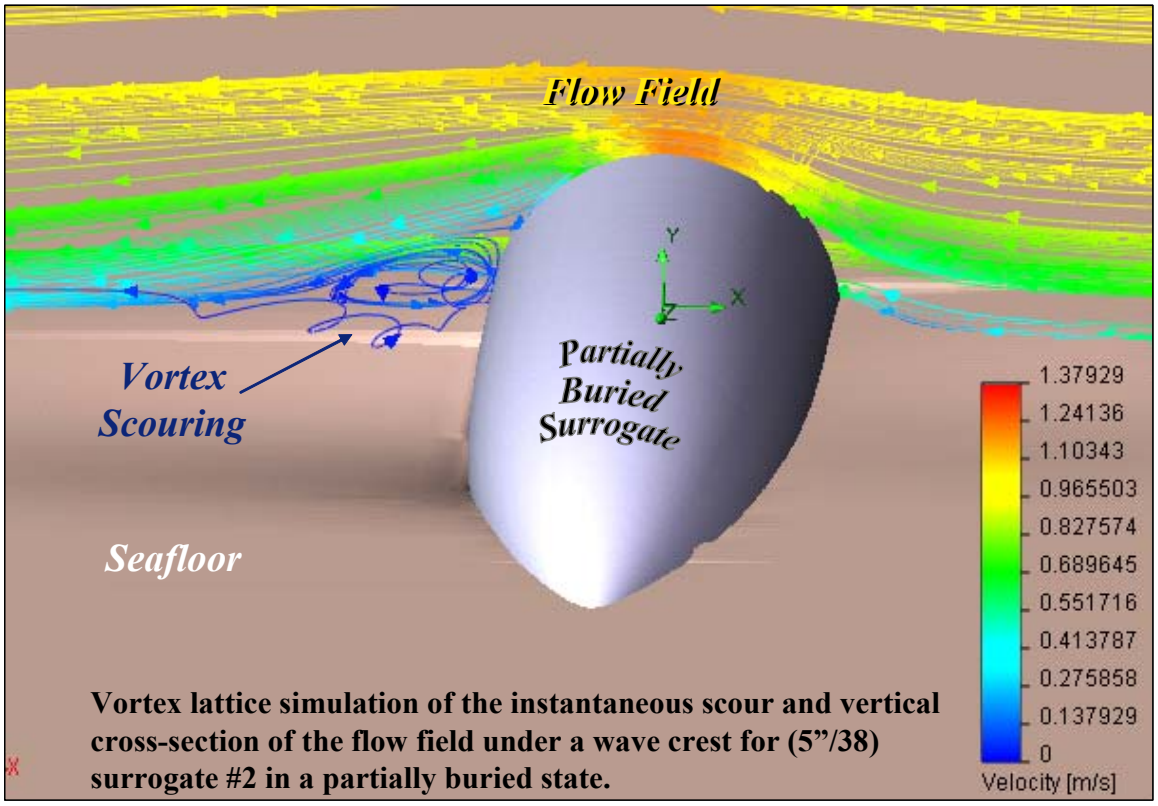

Figure 2. UXO Mobility Model output of flow and scour over a 5”/38 projectile surrogate.

By using the MM, we can resolve the fate of UXO over the broad range of coastal diversity where UXO are known to exist. Additionally, mobility information can be used as part of a risk assessment by using these data to identify the areas and entombment depths likely to contain UXO, thus reducing costs associated with fieldwork focused on physically locating or clearing UXO items.

The ultimate goal is to be able to incorporate UXO mobility and burial model output data into a risk assessment model similar to the Adaptive Risk Assessment Modeling System (ARAMS) developed by the USACE. As an interim step and as a supplement to the overall MM development effort, an “Application Guidance Document (AGD)” is being developed. The AGD outlines a process by which UXO site managers and others can accomplish the following: (a) identify the areas of present UXO risk within or adjacent to their geographic areas of responsibility and (b) use the MM to predict the areas in which UXO will remain entombed and which are at risk of having UXO move into them.

The NESDI Research and Development program supported the MM software development and a limited validation effort at a single collision coastal site adjacent to Mugu Beach, CA,[3] and

conducted a series of Measurement Method Field Tests (MMFT 1 and 2) [4] on the coast of Ocean Shores, Washington, in September 2004 and May 2005.

The Mugu Drifter Test (MDT) was run with only small-diameter UXO (i.e., 20mm inert and surrogate rounds). This location was representative of UXO sites belonging to the collision coastline sub-category, one of the eight coastal sub-categories given in the Geomorphic Coastal Classification system [5]. Data obtained from this test was used to validate the expected movement of small UXO in the Santa Barbara littoral cell, a large open coastal movement area which tends to move small UXO offshore like sand.

The MMFT at Ocean Shores used only larger UXO (5”/38 inert and surrogate rounds). MMFT was a short-term test intended primarily to validate the effectiveness of two measurement methods for tracking UXO movement (i.e., physical tethers and acoustic pingers). The test also provided a calibration for the part of the MM that addresses movement in the high-energy breaking surf zone, again on a collision coastal beach.

The Navy program supported MM development and allowed for short term, surf-zone validation for the collision coastal type. To be useful to DoD planners, the MM needed to be validated for the remaining major coastal types. The data acquired from such validations would enable users to operate the MM as a function of three distinct modes for input data. Thus, the MM can be run with either very limited site data (i.e., Mode 1, using only the collision coastal classification as input) or with more detailed configurations using various levels of site-specific data inputs (i.e., Mode 2 or Mode 3). Choosing one of the three modes also depends on the user’s desire to make site-specific adaptations to the MM’s configuration.

1.2 Demonstration Hypotheses (expected outcomes)

One of the following four outcomes of comparing the results from ESTCP Field Demonstration data to site-specific UXO model predictions was possible:

a. Field observations match predictions within the error bounds of the movement and environmental measurements (i.e., within 10 to 50 percent). Measurements falling within these error bounds signify that the MM is fully validated for that site and the theory is sufficiently sound to warrant using the MM in all three modes of operation at other sites with similar coastal classification. No further MM modifications or dedicated field demonstrations would be required in this instance.
b. Field observations loosely correlate with MM predictions (i.e.>50%). The data therefore indicate that some of the observed behaviors are not included in the MM, which would suggest that the model itself requires additional development and re-testing.
c. There is no clear statistical correlation between field demonstration results and MM predictions, thereby leading to the conclusion that the MM is not applicable to UXO. In that case, another approach would be required.
d. Data collected were inadequate to provide statistically significant conclusions.

The expected outcome for this demonstration was (a) or, possibly, (b). The general success of the early Navy program tests suggested that the negative results of outcome (c) was very unlikely. The previous validations of the MM for mine shapes (including the bomb-shaped versions), the supporting tank test validations from which the theory was derived, and the limited initial validations from the Navy MDT and MMFT indicated that the MM was essentially sound and ready for final field validation.

1.3 Program Performance Objectives

The UXO Mobility Model ESTCP demonstration/validation program main object is to validate the UXO MM. Additionally there are both qualitative and quantitative performance objectives (Table 2):

Qualitative Measures. Given the specialized nature of the MM, however, it is likely that the most cost-effective way to apply the MM will be for NAVFAC ESC and support contractors to remain the Center Of Expertise in this area. This schema ensures MM continuity beyond the specific engineers who developed the software and yet does not incur the expense of refining the software to a more generalized, user-friendly format. It also decreases the possibility of incorrectly using the MM.

Table 2. Performance Objectives.

Type Of Performance Objective	Primary Performance Criteria	Expected Performance (metric)	Performance Objective Met?
Qualitative	MM proves useable by engineers other than software creators.	Review by NAVFAC ESC –selected panel including Navy, Army, and support contractors concludes software is transferable to other users.	Yes. Both NAVFAC ESC and SST staff have been able to use the software (run the MM). However, there is still value from the MM developer (Scott A. Jenkins Consulting) as new applications arise.
	MM provides credible prediction of movement in support of demonstration planning.	Predictions check against general engineering theory and observations at similar sites.	At FRF Duck the MM predictions generally agree with complex movements observed for multiple surrogates.

Quantitative	Field Demonstration collects sufficient quality data to allow validation of MM	> 50% of surrogates are tracked successfully at each site. Movements are measured within +/- 10%.	92% of 120 data points in the 5 main rounds of measurements were successfully collected. Measurements were accurate within 1-2 m (<7% of range). Only a sampling of the 20mm was obtained – but no movement observed.
	MM validation shows good match between predictions and measurements, with coefficients correctable to positive match.	R > 0.8, for a given site.	MM validation by visual match to measurements is very good. Quantitative skill ($R_{movement}$) was 0.87 for movement and R_{burial} was 0.93 for burial – generally excellent.

1.4 Field Demonstration Method

This part of the ESTCP project was conducted at a site located in a Trailing Edge environment on the East Coast of the United States, at the USACE FRF located on the Atlantic Ocean near the town of Duck, North Carolina.

The FRF site is characterized by a long shallow slope to the Continental Shelf and is exposed to Nor'easter storms in the winter and hurricanes in the summer. The environment at this site is well documented and there are excellent support facilities (e.g., pier, crane, instrumentation, etc.). The Army and Navy have both used this site for beach studies and mine movement tests for many years.

At FRF, a series of UXO surrogates were placed on the seafloor in various water depths. Their location and depth of burial (whenever possible) were then monitored by diver inspections at intervals determined by the occurrence of high-energy environmental events (e.g., storms or large local wave events). The samples were left in place through two full local seasonal cycles.

The 5"/38 surrogates were installed at pre-planned distances from the shoreline from the closure depth to just seaward of the low tide line. By then plotting the actual movements of each individual surrogate it was possible to examine trends as a function of location with respect to such meteorological/oceanographic parameters as surf zone characteristics, weather forcing function conditions, local sediment properties, etc.

The 20 mm surrogates were initially placed in small groups near the 5”/38 surrogates. The 20 mm surrogates were not individually tracked, but were to be located and collected when they appeared on the beach, or as they were found during the other measurement processes. The 20 mm surrogates were only used at the FRF Duck site.

The location of the 5”/38 surrogates was tracked by a variety of methods. Each contained a large metal core cast in epoxy and was equipped with an acoustic pinger. Divers used hand-held receivers, as well as a Benthos fixed acoustic tracking system to track the surrogates. Metal detectors were used to further locate the surrogates in conditions of poor visibility or when they were buried. Each location was measured with respect to fixed references by employing acoustic methods, Global Positioning System (GPS) to the Coastal Research Amphibious Buggy (CRAB) vehicle, and tape measures, depending on the local conditions at the time. Those range data were then intersected to obtain fixes on the surrogate locations by triangulation.

The primary metric for a successful field demonstration was to collect data on the movement of all or most of the UXO surrogates and to document the environmental conditions that caused those movements (e.g., currents, waves, and seafloor properties). The primary metric for defining a successful MM validation effort was that the observed movement matched the predicted movement well enough to allow final adjustment of the model parameters to match the observations without changing the basic structure of the model (i.e., assumptions of basic forces and interactions would remain unchanged). The details of the MM calibration and validation process will be described in more detail in Sec. 3 of this report, and in the ESTCP Final Report [6].

1.5 Demonstration Site Selection

The FRF Duck field demonstration site was selected primarily because it represents a Trailing Edge coastal environment and is well instrumented. The demonstration sites were also chosen because they are either under military control or have very limited civilian access. Navy environmental reviews for the California and Washington state tests all showed that there is no significant impact from the short-term testing process, which, in turn, helped to expedite the FRF permitting processes.

Finally, the environments of both sites are already reasonably well documented because of recent offshore test activities there. The FRF at Duck, NC, is an operational Army test facility and has been used in the past for Navy tests of the migration of seafloor mine shapes.

The general site area for the FRF Duck validation is located just north of Cape Hatteras, a region where the Gulf Stream, Nor’easter storms, and hurricanes tend to produce heavy wave action and currents (Figure 3).

1.5.1 Pre-Demonstration Testing and Analysis

Prior to the demonstration, the FRF site was analyzed by running the UXO Mobility Model using available input parameters such as historical wave, current, sediment transport, and other

seafloor data from the site to determine the expected movement of the UXO as a function of location along and across the coastline profile. At the FRF site that analysis was used to set the final location and initial orientation of each surrogate 5”/38 round. That analysis was then used to determine the details of the locations of reference stakes, approaches for use by divers in conducting surveys, etc.

To characterize the bottom sediment characteristics, a preliminary dive was conducted at the FRF site to collect small samples of the seafloor sediment across the demonstration site area. The samples were analyzed for sediment type and a standard grain-size analysis will be performed, since grain size is an important input to the MM. At FRF there are permanently installed instruments to measure waves and currents at the site. There also is an extensive historical database of meteorological and oceanographic information from which to make predictions.

The preliminary dive also baselined local procedures and logistics processes for the initial installation and follow-on monitoring visits.

Figure 3. Duck, NC, is approximately 60 miles south of Norfolk, VA.

2. Field Demonstration ONE (FRF Duck, NC)

2.1 Demonstration Site Description

2.1.1 Characteristics of Trailing Edge Coastal Classification

The following boundary conditions and synthesized model parameters for a Trailing Edge site are shown as Row B in
Figure 4.

Geomorphic Type	Boundary Conditions					Model Parameters		
	Morphology (Example)	Sediment Source	Sediment Sink	Closure Depth	Littoral Cell Dimensions	Grid Cell	Grain Size	Bed Roughness, η_0
A. Collision 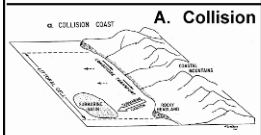	Narrow-Shelf Mountainous Coastal Bluffs (Cailfornia)	Rivers & Bluff Erosion	Submarine Canyons	15 - 18 m	Longshore: 50 km Cross Shore: 1 - 5 km	Farfield: 70 - 90 m Nearfield: 1 - 4 cm	Beach: 0.2 - 0.3 mm Shelf: 0.06 - 0.10 mm	0.5 - 3 cm
B. Trailing Edge 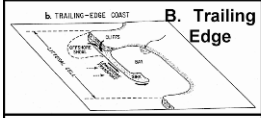	Wide-Shelf Plains (Duck, NC)	Headlands & Shelves	Roll-Over Shoals Spit-Extension	10 -13 m	Longshore: 100 km Cross Shore: 30 - 50 km	Farfield: 40 - 80 m Nearfield: 2 - 7 cm	Beach: 0.2 - 0.4 mm Shelf: 0.06 - 0.15 mm	0.8 - 5 cm
C. Marginal Sea 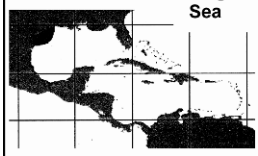	a) Narrow-Shelf Mountainous (Korea) b) Wide-Shelf Plains (Corpus Christi) c) Deltaic tideless (Mississippi) d) Deltaic tidal (Bangladesh) Wide-Shelf	Rivers & Deltas	a) Canyons b) Beaches & Barriers c) Delta & Shelf d) Delta Islands, flats, canyons	Narrow shelf: 7 - 10 m Wide shelf: 4 - 7 m Delta: 3 m	Longshore: a) 5-10 km b) 100 km c) 5-200 km d) var Cross Shore: a) 1 - 5 km b) 50 km c) 20-80 km d) var	Farfield: 10 - 20 m Nearfield: 1 - 3 cm	Beach: 0.06 - 0.21 mm Shelf: 0.01 - 0.09 mm Delta: .005 - .05 mm	a-d) 0.1 - 1 cm d) sand waves
D. Coral Reef Form of Biogenic 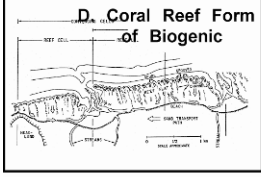	Coral Reef Island (Hawaii)	Carbonate Reef Material Volcanic Headlands	Pocket Beaches & Awa Channels to the Shelf	Reef Platform	Longshore: ~2 km Cross Shore: 0.5 km	Farfield: 100 - 150 m Nearfield: 1 - 20 cm	Beach: 0.2 - 0.4 mm Shelf: 0.03 - 0.1 mm	Reef Platform ~1 m Offshore 1 - 15 cm

Figure 4. Coastal classification system with geomorphic types and synthesized model input parameters. The FRF Duck Field Test site is a Type B (Trailing Edge) site.

2.1.3 Environmental Permitting

The following permits and approvals were obtained:

- NC Department of Environment and Natural Resources – Concurrence with Negative Determination, December 13, 2004
- U.S. Army Corps of Engineers Section 10 Permit, November 16, 2004
- Record of Categorical Exclusion

The permits obtained are provided in Appendix B for reference.

2.1.4 Field Demonstration Staff

Table 3. ESTCP UXO FRF Duck Field Demonstration Points of Contact.

POINT OF CONTACT	ORGANIZATION	E-mail Address	Role In Project
Barbara Sugiyama	NAVFAC ESC	barbara.sugiyama@navy.mil	Principal Investigator
Alexandra De Visser	NAVFAC ESC	alexandra.devisser@navy.mil	Co PI
Jeff Wilson	Sound & Sea Technology	jwilson@soundandsea.com	SST Project Manager, Demonstration Design
Bill Daly	Sound & Sea Technology	wdaly@soundandsea.com	SST Senior Field Test Engineer
Ian McKissick	Sound & Sea Technology	imckissick@soundandsea.com	SST Field Test Engineer, Surrogates, Instruments
Dr. Scott Jenkins	Dr. Scott A. Jenkins Consulting	sjenkins@ucsd.edu	UXO Mobility Model Development, Site Analysis
Dr. William Birkemeier	USACE ERDC FRF	william.birkemeier@usace.army.mil	Field Test Planning, Logistic Support, Diving Ops

2.2 Demonstration Plan

The general approach for the FRF Duck Field Demonstration was to first install the surrogates at pre-planned locations at increasing distance from shore and increasing water depths and then measure their movement from those initial locations.

2.2.1 Demonstration Layout

The 5”/38 surrogates were installed in two groups of twelve, with a general layout for the initial installation as shown in Figure 5. In each field, two rows of six surrogates each were oriented parallel to the major axis of the FRF pier. The positions were established north of the FRF Pier because the expected worst-case movement along the beach was to the south. Because of the scouring effect of the pier pilings there is a trough under the pier that would capture the surrogates in case they should move farther south than predicted. The surrogates labeled 1

through 6 and 13-18 were installed in the inshore approximately 2 m of water (shallow field). The surrogates labeled 7 through 12 and 19-24 were installed in the offshore field in approximately 7 m of water (deep field); these are denoted by the black dots in Figure 5. The distance between deployed rows perpendicular to shore was approximately 20 m. Twelve groups of ten 20mm surrogates, six in the shallow field and six in the deep field, were also deployed in one perpendicular line just south of the southern-most line of 5”/38 surrogates; these are denoted by the yellow dots in Figure 5 and are labeled 20_1 through 20_12. Six reference markers, denoted by the red dots, were used as georeferences for tracking surrogate movement. They were located equally with the two fields: three in the shallow field and three in the deep field.

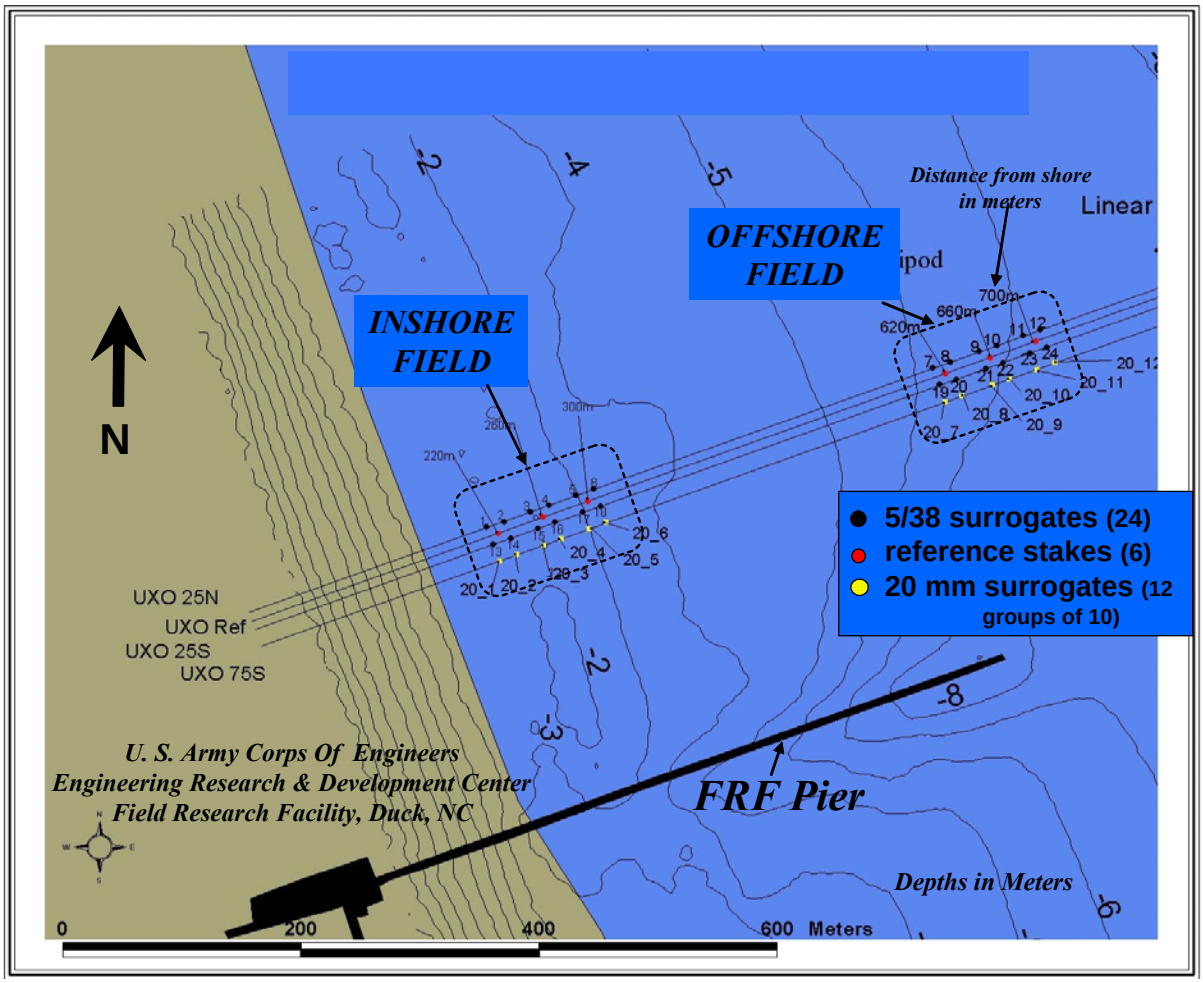

Figure 5. FRF Duck Site Overview showing the Inshore and Offshore Fields.

Figure 6 shows the head of the FRF Duck pier and the unique three-wheeled Coastal Research Amphibious Buggy (CRAB) vehicle. The CRAB is able to drive directly into the surf to provide a stable platform from which to take location measurements and install surrogates.

Figure 6. FRF Duck pier, beach, and CRAB vehicle.

2.2.2 Surrogates Used

The two ordnance sizes selected bracket the ends of the general behavior spectrum; the 20 mm rounds behave like small "sand" particles, while the 5"/38 rounds behave like larger "cobbles." The 5"/38 surrogates were built to closely mimic the design and overall physical characteristics of inert metal rounds. As such, the surrogate projectiles were approximately 5 inches in diameter at the base and 20 inches long (Figure 7). They were made of a strong, resin-type, moldable plastic that is resistant to water absorption. The HapCast plastic can be machined, has a high specific gravity (SG), and can be poured into a mold with steel core built from a standard weight lifting handle that aids in equalizing the SG. Each finished cast 5"/38 surrogate weighs 50-lbs and is approximately 5 inches in diameter at the base and 21 inches long, with a tapered point where a pinger may be inserted.

Figure 8 shows the 5"/38 surrogates in their transport rack with a white pinger inserted in the nose of several surrogates. The 20 mm steel dummy rounds are each approximately 6 .625 in. in length and less than 1 in. in diameter. Example 20 mm surrogates are shown in Figure 9.

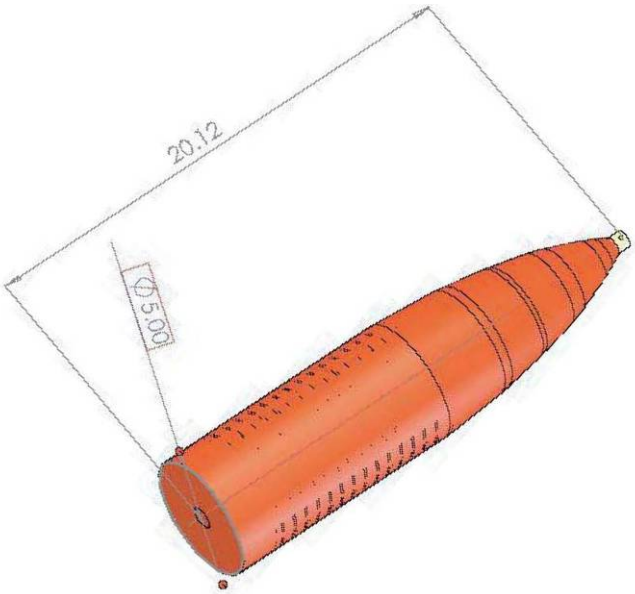

Figure 7. Surrogate projectile for 5”/38 round.

Figure 8. An assembly of 5”/38 surrogates deployed in the FRF Field Demonstration.

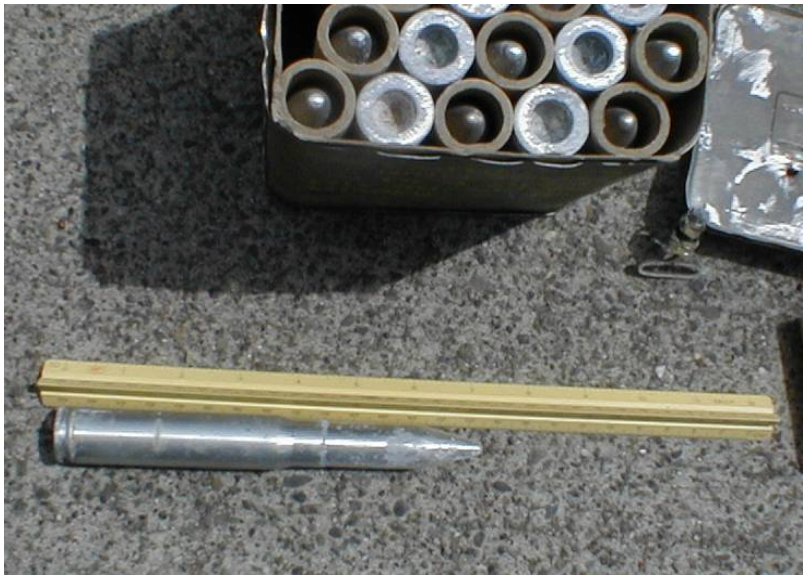

Figure 9. The 20 mm surrogates deployed are Navy standard inert shapes used in testing ammunition handling systems.

2.3 Field Validation Measurements

The validation data proved to be a slight variation on the first of the three possible observations mentioned under Sec. 1.2, Test Hypotheses. The field observations generally matched the predictions within the error bounds of the movement and environmental measurements. The demonstration results were all within an average of 24% of the predictions – but there were only "normal" storm events during the demonstration, and no "extreme" events (hurricanes). By the nature of such events, it is hard to ensure one will occur where it is wanted during a demonstration. While the movement (and non-movement periods) of the field demonstration matched the predictions well, there were no large-scale movements of the kind that might be expected with extreme weather events (hundreds of meters, in hurricanes, major storms on flat seafloors, etc.). .

The general procedures were as follows:

a. Ensure permits are in place and all personnel are briefed on the demonstration objectives and procedures.
b. Conduct the initial dive to verify seafloor conditions, test acoustic tracking devices and collect sand samples for use in Model calibration.
c. Ship surrogates, acoustic pingers, tracking devices, ADCP, tethers and stakes to site.
d. Test acoustic tracking devices, local instrumentation, and installation equipment (e.g., CRAB, LARC, etc.)
e. Move gear by truck to the dive site. Diving operations were supported by using the Lighter Amphibious Resupply Cargo (LARC) vehicle at the Duck site.

f. Install the surrogate rounds in the planned locations. At Duck, the rounds were lowered from the CRAB vehicle crawling framework.
g. Install reference stakes (metal pipes jetted into the sand). Check acoustic tracking devices to determine range of detection for each pinger.
h. Record the initial location of each surrogate. At Duck, the CRAB was used to directly survey the seafloor bottom points.
i. Record the Global Positioning System (GPS) location of each stake.

Contingencies were as follows:

a. Do not start the demonstration until surf and visibility conditions are acceptable to the divers. At least 5-6 feet of visibility is required, and the surf conditions will likely limit the ability to launch the small boat before they stop diving operations.
b. If any of the acoustic pingers fail, replace the failed pinger. Pingers may be replaced either on deck or on the seafloor.
c. If any surrogate is dropped, mark the location with a float and conduct a search to recover it.
d. Follow all required diver safety procedures. If a diving accident of any kind occurs, abort the installation.

2.3.1 Installation Notes

The installation occurred on 22 June 2005. The CRAB was so stable and the current offset so small that the survey coordinates were used as the initial measurement of surrogate as-installed position. The CRAB installation process is shown in Figure 10. The lowering line used to deploy the 5”/38 surrogates hung perpendicular to the ocean bottom, so it was also used to determine the installed location for each surrogate.

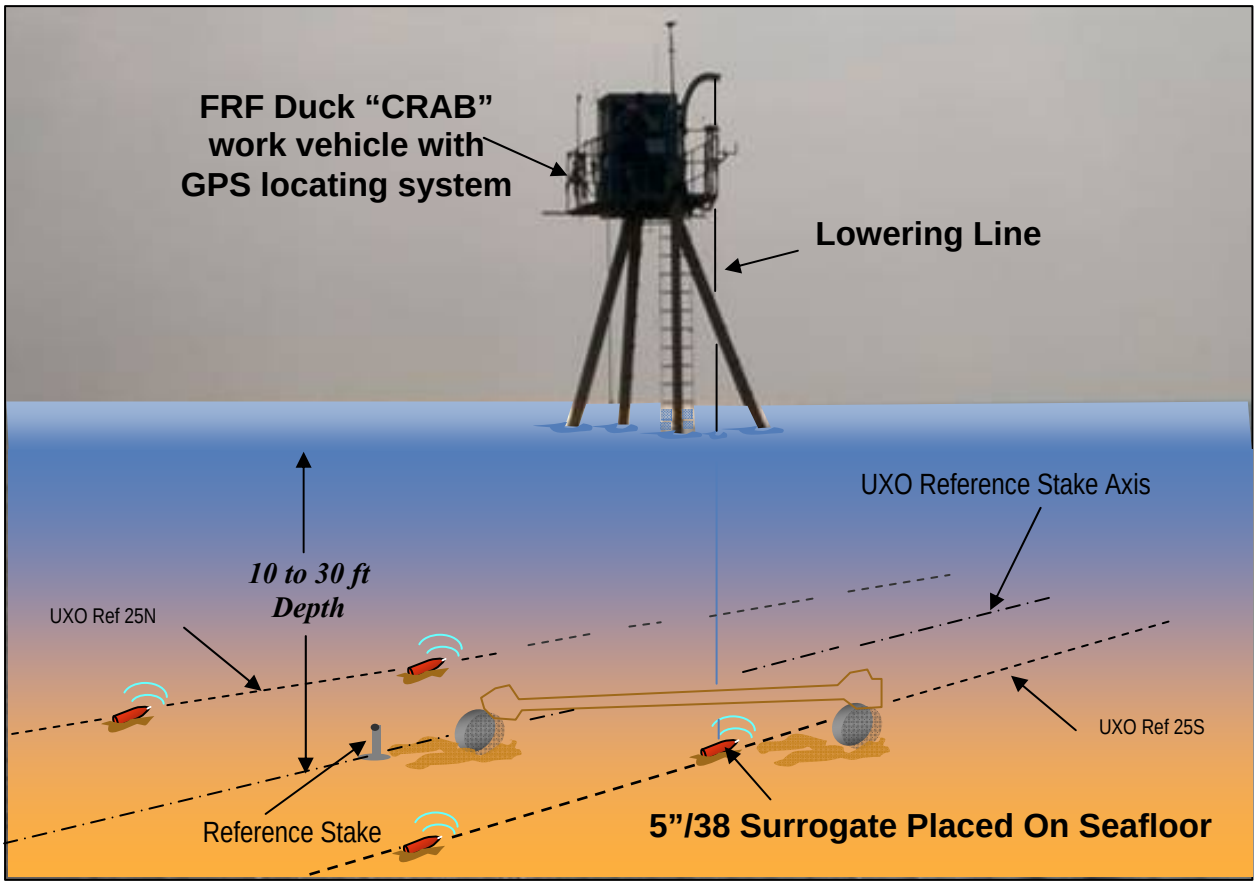

Figure 10. The FRF Duck CRAB was used to lower the 5"/38 surrogates into place.

The reference stake pipes were jetted in and their height above the bottom was recorded as a cross-check on the routine bottom surveys of bottom bathymetry that are performed weekly by the FRF Duck staff. Since the pipes were jetted in much deeper than the surface layer of sand, they provided a set of 6 direct observation points through the main axis of both surrogate fields from which to measure any accretion or erosion of the sand level, as well as the movement of the surrogates.

2.3.2 Diving Operations during Installation and First Round of Measurements

Bad weather caused the initial dive to be postponed for 5 days until 27 June 2005. The divers used that down time to learn to use the hand-held acoustic-tracking units and were able to locate all 24 surrogates during the first dive. All pingers functioned and the surrogates were trackable.

The divers were able to record the ping interval and pinger code without a problem. Close proximity frequency duplication was not an issue.

Although some of the surrogates had moved as much as several feet from their initial location and all had become buried in the 5 days since they were installed, the divers were able to

complete an initial set of movement data ("Round One") on 27 June 2005. The divers measured each surrogate's position by swimming to its location following the signal from the pinger with their hand-held acoustic tracker. Since the surrogates were buried the divers located the hand-held tracker over the surrogate burial site within a meter or so. The Benthos receiver was then used to record the distance (range) from each of two or three of the Benthos transmitters, which were located on the adjacent reference stakes; see Appendix C for hardware specifications. Although the Benthos system resolution is 0.1 m/sec of travel, the practical resolution of those ranges as derived from the statistical plots is typically a +/- meter or more because of the resolution of the hand-held diver readouts, the ability of the divers to hold the units steady, and the general complexity of the shallow water environment.

Later measurements included use of a metal detector for locating the rounds when the location using the pinger finder became unclear. When the rounds were located with the metal detector, a probe was used to make contact with the round. Then the location of the hand-held receiver was horizontally within a few inches of the actual surrogate site.

For some of the surrogates, the acoustic measurements were checked by using tape measurements of the distance from the surrogate location to the reference stakes. The tape measurement method proved to be very time consuming when compared to the Benthos transponder unit. However, the tape is much more accurate than the Benthos. Even with a 3ft bow on a 40ft measurement, the measurement will only read ~ 0.5ft further than actual. Fortunately, in each case, the tape-measured position turned out to be exactly in the middle of the estimated position using the acoustic tracking system. That suggests that the actual errors in the acoustic tracking system may be less than advertised. Because the tape measurements were more time consuming, they were not repeated.

During installation preparations, several pingers had stopped pinging well before they should have. Additionally two of the pingers were alternating from working to not working. Sufficient spares had been procured so all pingers were operational when installed and they continued to work throughout the demonstration, which extended well beyond their advertised 18-month battery life. The test layout incorporated sufficient redundancy (two surrogates at every depth) so that even if several more pingers failed there would be sufficient data recorded for a successful test.

The divers were unsuccessful when they tried to dig for Surrogate #19 by hand in the loose sandy seafloor. This noteworthy incident aided in planning future recovery or unburial efforts to confirm surrogate location. It became necessary to use a diver-held eductor system (a "gold dredge") during those operations.

The contract divers supporting FRF Duck (Chesapeake Bay Diving, Inc.) continued to handle the on-site work and took measurements when directed. That minimized the cost associated with travel. It also allowed for more timely measurements to be recorded because weather changes so rapidly on the Carolina coast.

2.4. Installation Phase Measurement Data (Round One Data)

2.4.1 Measurement Method Used

The basic approach for measuring 5”/38 surrogate locations is described below. The divers determined the surrogate locations by tracking the pingers or using metal detectors and then receiving range signals from two or more fixed Benthos transponders (
Figure 11). The sequence is as described in the discussion of diving operations in Section 2.3.2.

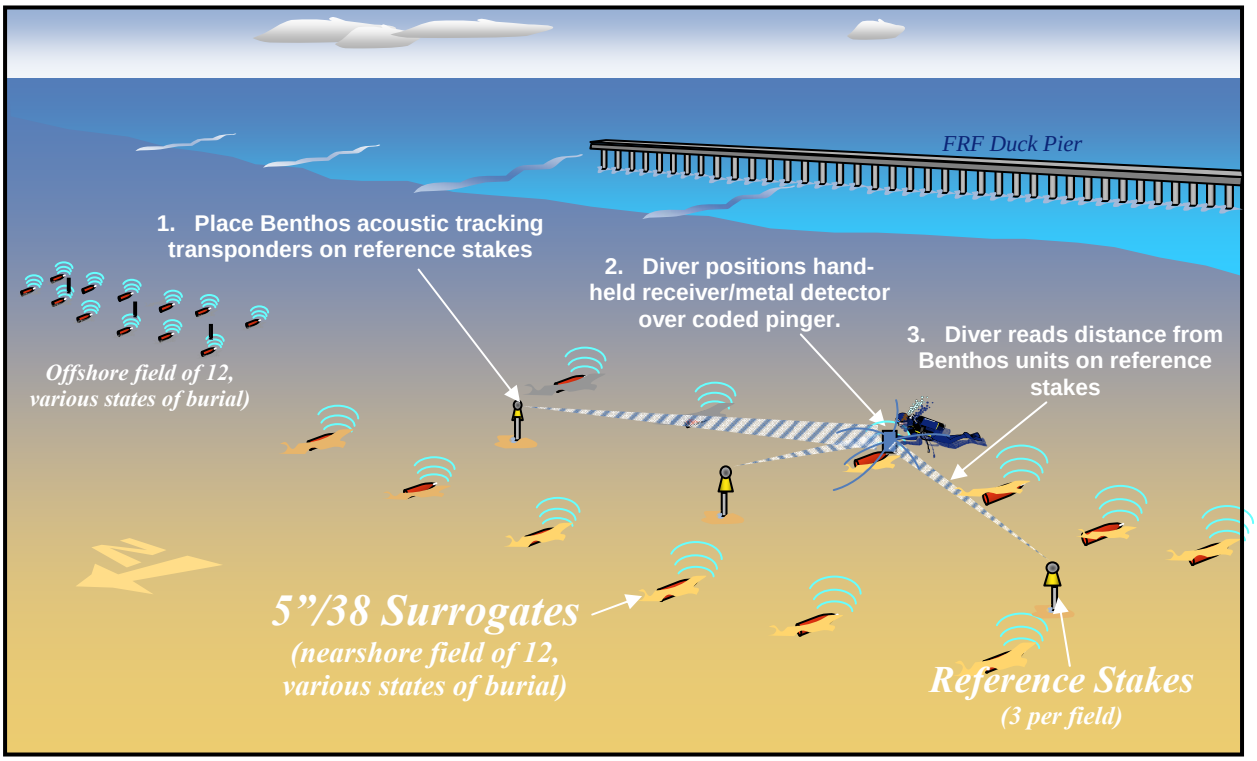

Figure 11. The FRF Duck measurement method.

The details of the conversion of the Benthos range measurements to surrogate location are given in Appendix D.

The sample size of twenty-four large surrogates provided confidence there would be at least two sets of ten data points from each measurement cycle. There is little value in having a much larger data set than ten because the accuracy of meteorological/oceanographic measurements such as waves, currents, etc., is typically not much better than 10% or so, and the standard deviation of the statistics of forcing functions (weather) is quite large. Even the *in situ* measurements of UXO surrogate movement by divers was only accurate to within a few percent. Thus, the results were sufficient for conducting a credible engineering analysis of risks.

The 5”/38 surrogates were acoustically, magnetically, or visually tracked as conditions allowed.

The 20mm surrogate rounds were allowed to move as Lagrangian drifters in hopes they might provide a useful and direct description of oceanic transport and dispersal. Their location was to be noted as they washed up on shore, or as they are visually or magnetically identified during monitoring dives for the larger surrogates. However, the 20 mm surrogates showed no movement at all during the demonstration. As a result, there were no sightings of the 20 mm rounds until samples were recovered at sea during the final stages of the demonstration. The magnetometer tests indicated the groups were exactly where they were installed, as did a limited recovery sampling.

Relative movement of the 5”/38 surrogates on the order of as little as one meter was measurable by divers. “Significant” movement occurred when the surrogates begin to move beyond the normal visibility at the site, which at Duck was on the order of a few feet. However, the movement never exceeded the range of the Benthos transponders, so the reference stakes did not need to be moved.

2.4.2 Round One Measurement Data

The first round of measurements was made 5 days after the original installation. All the 5”/38 surrogates were located and their positions measured. All were buried. The divers estimated the burial depth to be greater than approximately 12 inches because the surrogates were beyond the reach of manual probing with a dive knife.

Most of the surrogates had measurably moved from their installed location, but none had moved so far they could not be easily found with the acoustic pingers.

Figure 12 is a graphical representation of the original location and the measurement arcs for the inshore field obtained during Round One. While most of the surrogates showed measurable movement, the average migration distance was on the order of one meter.

Figure 13 shows the surrogates in the offshore field and movement of approximately 1-2 m, which is greater than that measured inshore.

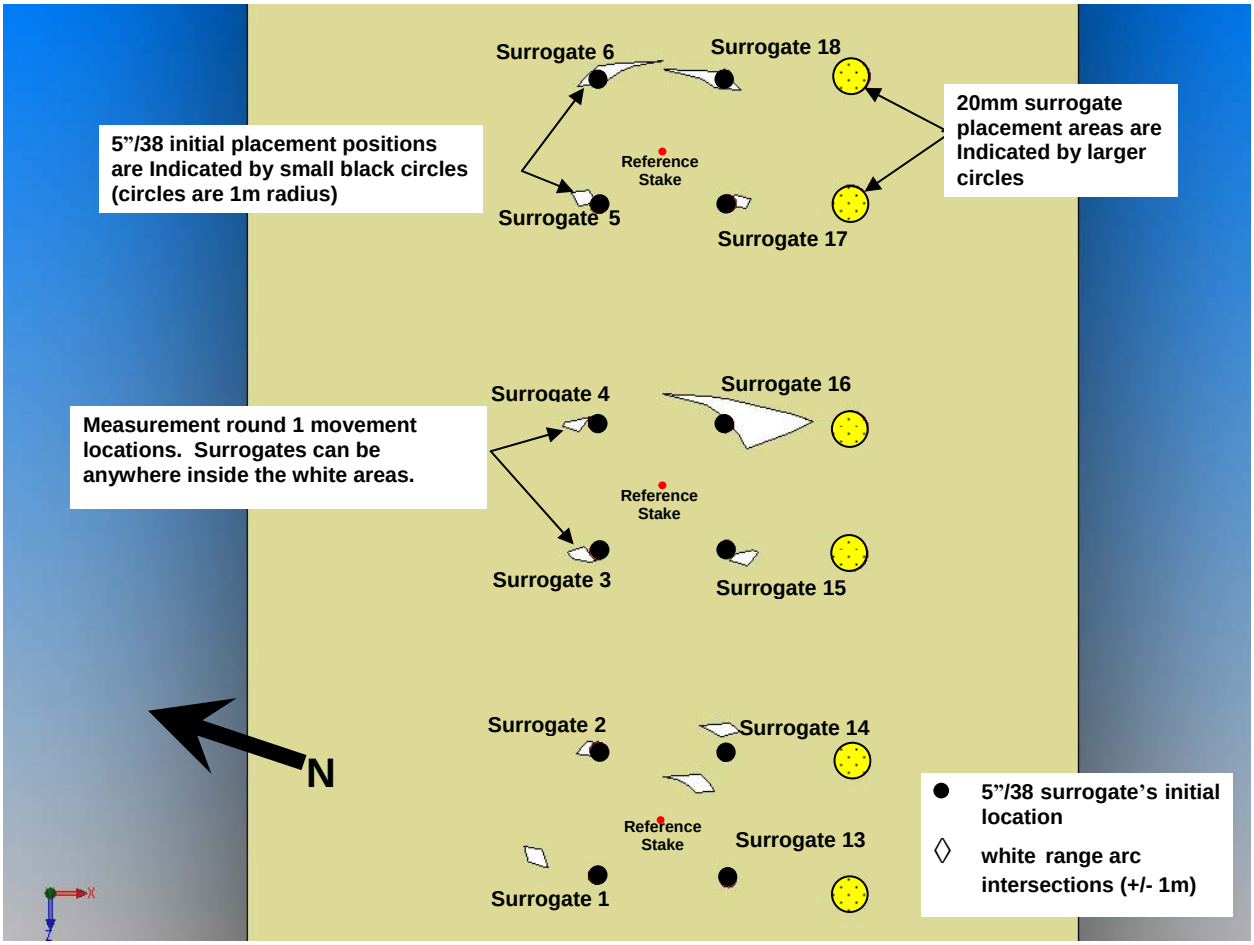

Figure 12. Inshore Field Round One measurements.

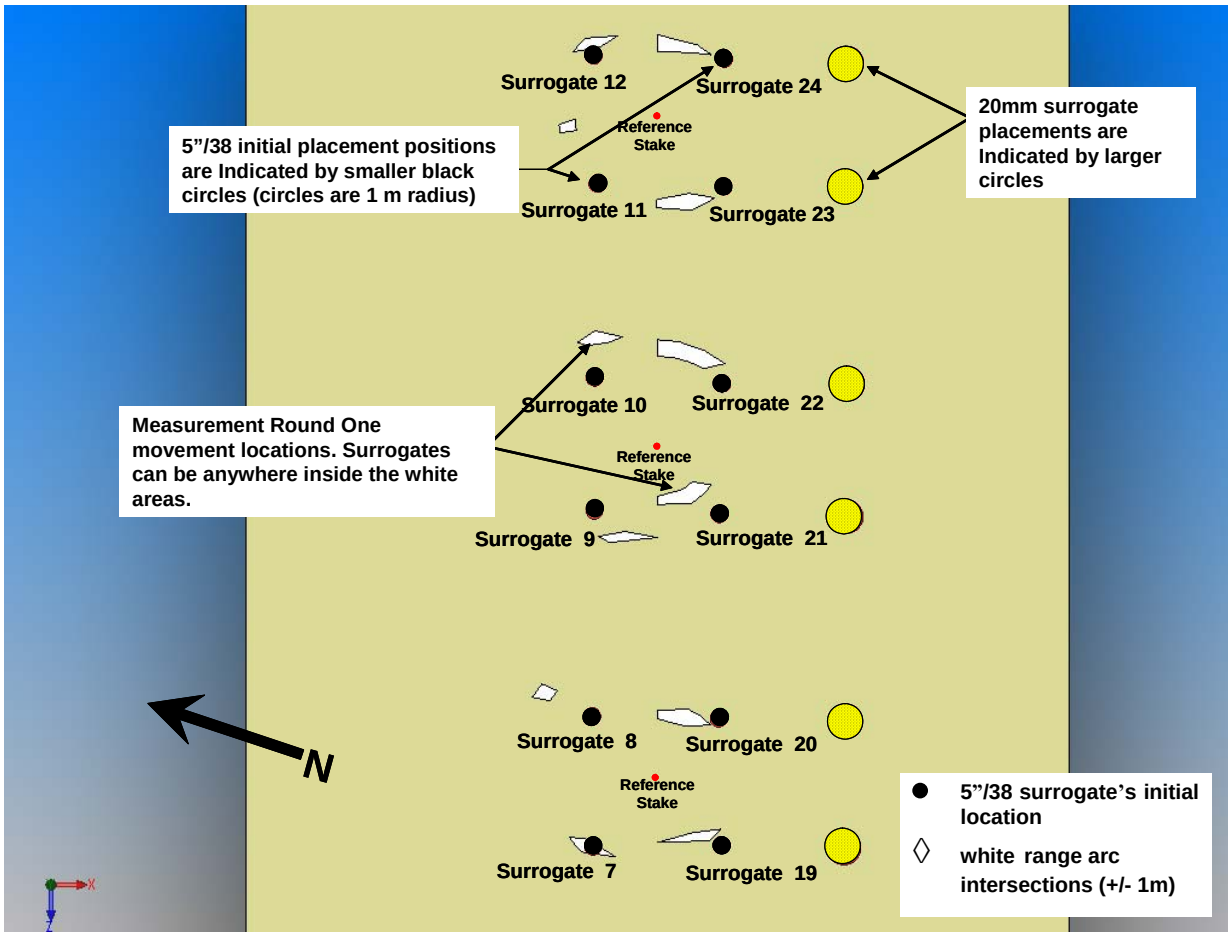

Figure 13. Offshore Field Round One measurements.

Figures 11 and 12 show detailed views of example Round One measurements. The white area of uncertainty is constructed using the three arcs showing the range to each of the three Benthos transmitter units. Each arc representing an area of uncertainty shows an accuracy range of ±1 meter range. The size and shape varies considerably from surrogate to surrogate, primarily due to the relative position of the reference stakes. Triangulating the fixes on a position is always better when the range arcs intersect at wide angles.

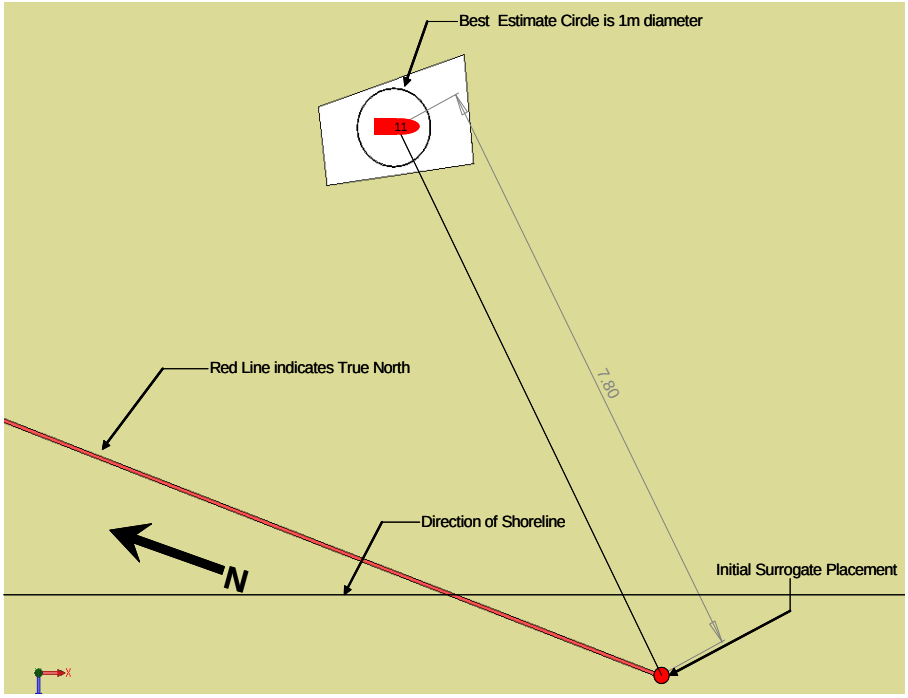

Figure 14. Round One measurement data for Surrogate #11 shows an example of the largest movement and best triangulation recorded.

Figure 14 shows a surrogate with one of the largest movements with respect to the installation point, but also one of the best acoustic fixes obtained via triangulation (smallest area of uncertainty). The surrogate moved approximately 7.8 meters in a direction of approximately 040 degrees True, which is north along the coast and slightly seaward of its original position.

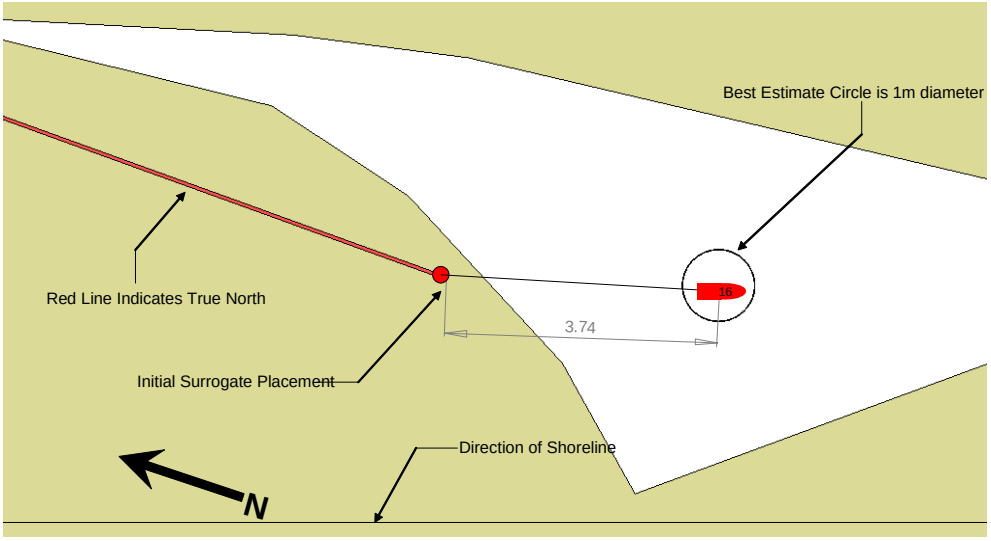

Figure 15. Round One measurement for Surrogate #16.

Figure 15 shows a surrogate with what is best described as moderate movement, but with a very large area of uncertainty and, subsequently, worst triangulation fix. The surrogate has probably moved approximately 3 to 4 meters, in a direction almost due south (parallel to the shoreline).

Table 4 shows the Round One measured movement with respect to (wrt) the initial installation location of all of the 5”/38 surrogates (distance measured in meters and direction in degrees True). The “Angle wrt True North” and “Angle wrt Shoreline” columns indicate the direction of movement. For the few surrogates that moved in a southerly direction the numbers are shown in blue.

The data plotted in
Figure 16 show the measured movement ranged from as little as 1 meter, which is in the noise of the measurements, to as much as 12 meters. The “accuracy of distance” estimate is visually derived from the size of the Area Of Uncertainty (the figure formed by the intersection of the plotted ranges from the various transponders).

Table 4. Round One Surrogate Movement (22-27 June 2005).

Surrogate	"Best Estimate" Distance (m)	Accuracy of Distance (+ / - m)	Angle wrt True North (deg)	Angle wrt Shoreline (deg)	Accuracy of Angle (+ / - deg)
1	7.7	0.2	358	18	2
2	0.9	0.3	353	13	19
3	2.0	0.4	331	-9	10
4	2.4	0.4	336	-4	10
5	2.0	0.3	7	27	7
6	0.8	0.5	125	145	34
7	0.7	0.4	348	8	29
8	6.3	0.3	6	26	3
9	4.7	0.5	201	-139	5
10	4.8	0.3	72	92	4
11	7.8	0.5	43	63	4
12	1.6	0.6	66	85	21
13	11.9	0.3	53	73	1
14	2.7	0.5	68	87	10
15	2.6	0.4	189	-151	8
16	3.7	2.2	162	182	30
17	1.4	0.4	152	182	14
18	0.7	0.3	308	-32	27
19	3.0	0.6	359	19	10
20	3.9	0.5	342	2	8
21	4.1	0.8	341	1	10
22	3.7	0.3	34	54	5
23	4.3	0.9	316	-24	12
24	5.4	0.7	357	17	7
AVERAGES	3.7	0.5	356.0	16	12
Std Dev	*2.7*	*0.4*	*90.6*		*9.5*
AVERAGE Nearshore	3.5		337.1	-2.9	
AVERAGE Offshore	4.0		14.2	34.2	

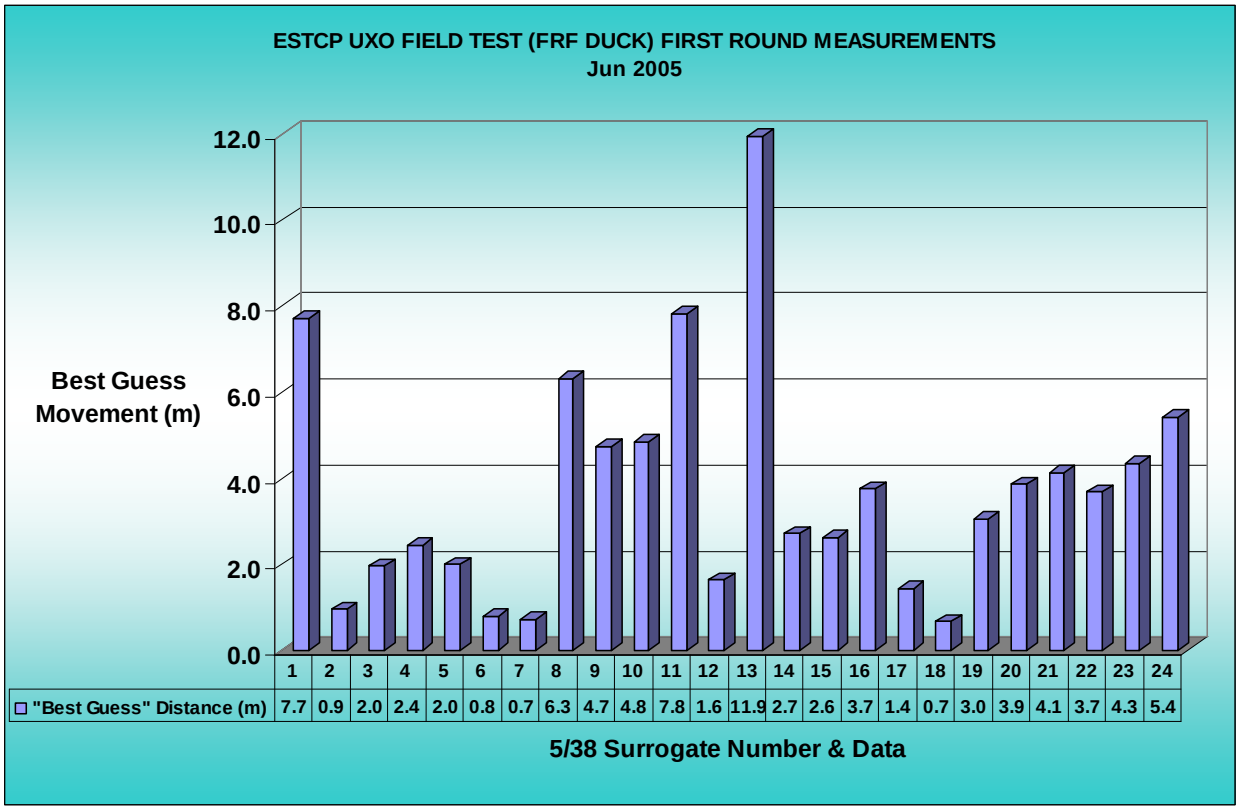

Figure 16. Round One surrogate movement measurements.

2.4.3 Round One Results

The data indicates a rather wide range of movement. Some of the surrogates rolled several meters before becoming buried, while others moved only slightly, if at all. Any movement of 1 meter or less is well inside the resolution of the measurement process. The fact that there are several cases of almost imperceptible movement also tends to confirm the accuracy of the original installation position estimates.

The average amount of measured movement was approximately 3.5-4.0 meters to the north. All but five of the surrogate measurements show net movement to the north. Surrogates 5, 15, 16, and 17 indicate movement to the south, but most of those migrations are within the noise of their particular measurements and do not substantially impact the averages.

The two largest movements were recorded for the two surrogates closest to shore (Surrogate #s 1 and 13, located in the shallowest water). However, all but one of the ten most seaward surrogates also moved substantially. Surrogate #s 8-11 and 20-24 all moved 3 to 5 meters.

There was essentially no net movement toward or away from the shore, although the inshore surrogates tended to move slightly toward shore while the offshore field tended to move slightly away from shore.

2.5 Round Two Measurement Data

On 12 August 2005, the FRF Duck team conducted the second round of measurements. Once again, all the surrogates were located acoustically and their positions measured with respect to the reference stakes.

All the surrogates were buried, at least as deeply as during the Round One measurements made about six weeks earlier. The divers used a 3-foot probe but were unable to locate them, so the surrogates must have been buried beyond that depth. The small 5-pound marker float anchors near shore were buried approximately 3 feet deep. The beach profile measurements confirmed the beach accretion.

The team checked the change in seafloor depth by inspecting the exposed length of the driven reference stakes. The reference stakes were installed with approximately 4 feet of pipe exposed above the seabed.

At the time of Round Two, the reference stake nearest to shore was completely buried, which indicates a four-foot accretion of sand. The next reference stake had only 2 feet of pipe exposed, which correlates to 2 feet of accretion, and the next pipe had 6 feet of pipe showing, which was equivalent to 2 feet of erosion at that location. The reference stakes in the offshore field exposed 4.5, 4, and 4 feet of pipe, respectively, thereby indicating that no net change in sand accretion occurred with respect to the initial installation condition. This state suggests that a degree of net accretion of sand occurred nearshore, but no net change in accretion was recorded at the locations further offshore. Long-shore sand movement likely explains this combination of conditions.

Given the minimal net change in seafloor depth and the consistently good ability to hear the surrogate pinger, it may well be that the units were not as deep as the divers believed them to be. Estimating the depth of buried objects in the seafloor can be a challenging task unless powered units are available to actually unbury the objects. Also, the Round Two data showed that some of the surrogates had moved several meters since Round One, which indicated that they did not remain buried throughout the interval between measurements – yet another point suggesting that the burial may have been less than estimated.

It is known that there are migrating sand waves in the Duck area and on most of the Continental Shelf which would explain the movement observed. The data clearly indicate that there are powerful processes affecting surrogate movement.

For this round of measurements, there were two items of interest: the incremental movement since the Round One measurement and the total movement since installation. The Round Two diver measurements only show the cumulative movement, since they are made with respect to

the same reference stakes as in Round One, so the incremental movement in terms of distance and direction is calculated by triangulation (see Appendix D, Table 1).

Table 5 shows the calculated Round Two movement (distance and direction) from initial installation and the incremental movement from the Round One positions.

Table 5. Round Two calculated movement.

Total Surrogate Movement (total sum of distance moved wrt initial placement and Rounds One and Two locations)			Measured movement between Rounds One and Two.		
Surrogate	**Movement Distance (m)**	**Movement Angle wrt True North (deg)**	**Surrogate**	**Movement Distance (m)**	**Movement Angle wrt True North (deg)**
1T	3.7	48	1	6.1	149
2T	0.7	38	2	0.7	122
3T	4.2	222	3	5.1	201
4T	1.1	22	4	1.8	129
5T*	4.5	16	5*	2.6	23
6T	2.3	241	6	2.7	256
7T	2.5	43	7	2.1	58
8T	4.2	336	8	3.4	224
9T	2.1	328	9	6.2	6
10T	1.5	419	10	5.5	266
11T	1.9	31	11	5.9	226
12T	4.3	180	12	5.2	197
13T	6.4	53	13	5.5	233
14T	3.1	248	14	5.8	248
15T	0.8	134	15	2.2	25
16T	9.4	17	16	12.6	7
17T	8.8	314	17	10.2	317
18T	3.4	255	18	3.0	245
19T	3.2	313	19	2.5	248
20T	5.8	236	20	7.8	208
21T*	2.8	133	21*	5.8	173
22T	5.3	138	22	7.2	168
23T	5.0	74	23	8.0	102
24T	3.6	41	24	3.8	136
AVERAGE	**3.8**	**162**	**AVERAGE**	**5.1**	**165**

T = total movement
* = very poor data recorded for the corresponding surrogate

The average movement was 5.1 meters just slightly east of south (parallel to the beach). Figure 17 shows the distance moved as a bar chart. The average error in the measurement was 1.5 to

1.9 meters, although some of the surrogates did show considerably larger error bands because of their location with respect to the reference stakes.

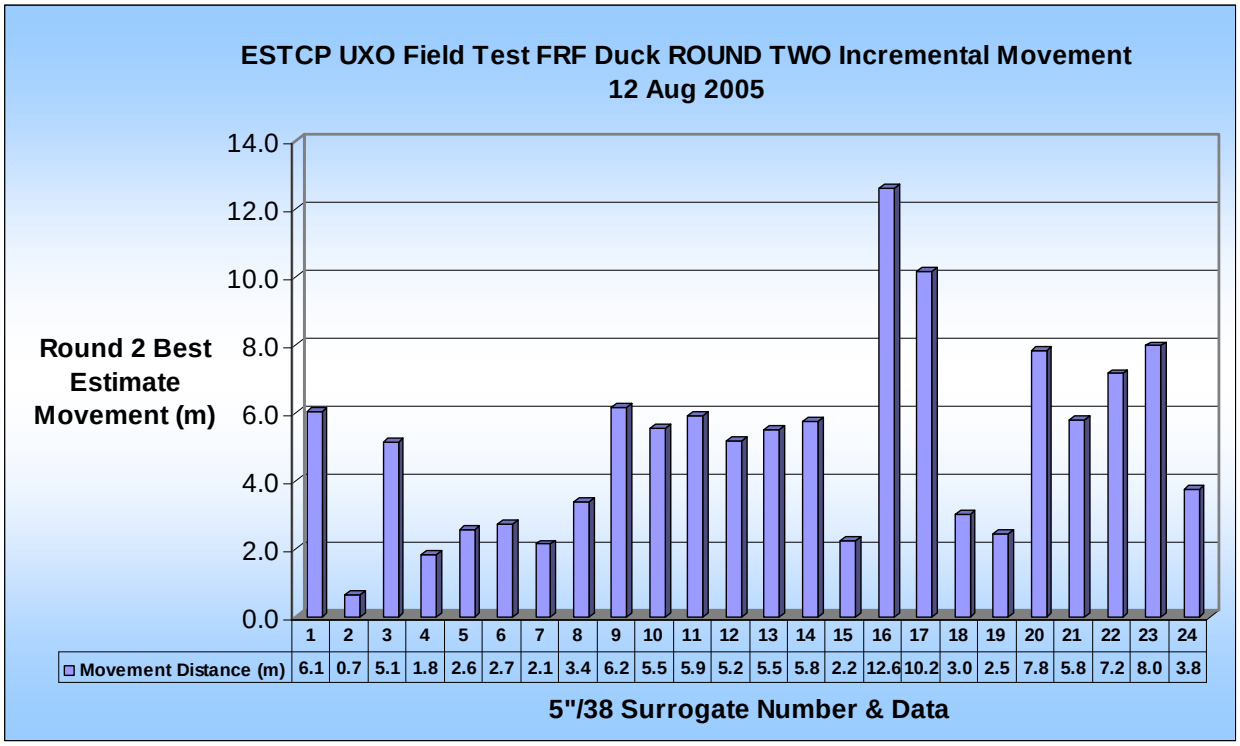

Figure 17. Incremental movement for Round Two shows the distance measured from the Round One positions over the 6-week period.

The two surrogates nearest the shore (Surrogate #s 1 and 13) moved substantially and most the seaward surrogates (#s 9-12 and 20-24) exhibited distinctive migration distances of 4 to 8 meters. This data set shows that the largest recorded movements were for two of the surrogates located on the seaward end of the inshore field (Surrogate #s 16 and 17).

The other important observation is that the average incremental movement was to the south, which was originally predicted by the general nature of the coastal currents.

Note that the Round One and Round Two "average" movements of 3.7 m north and 5.1 m to the south east do not form a closed triangle with the average cumulative vector of 3.8 m to the south east, though they are within the error of the overall measurements.

Appendix D, Figure 2, shows an example of the Round One movement plus the incremental movement derived from the Round Two measurements.

Figure 18 shows the two rounds of movement for the Inshore Field and Figure 19 shows the two rounds of movement for the Offshore Field

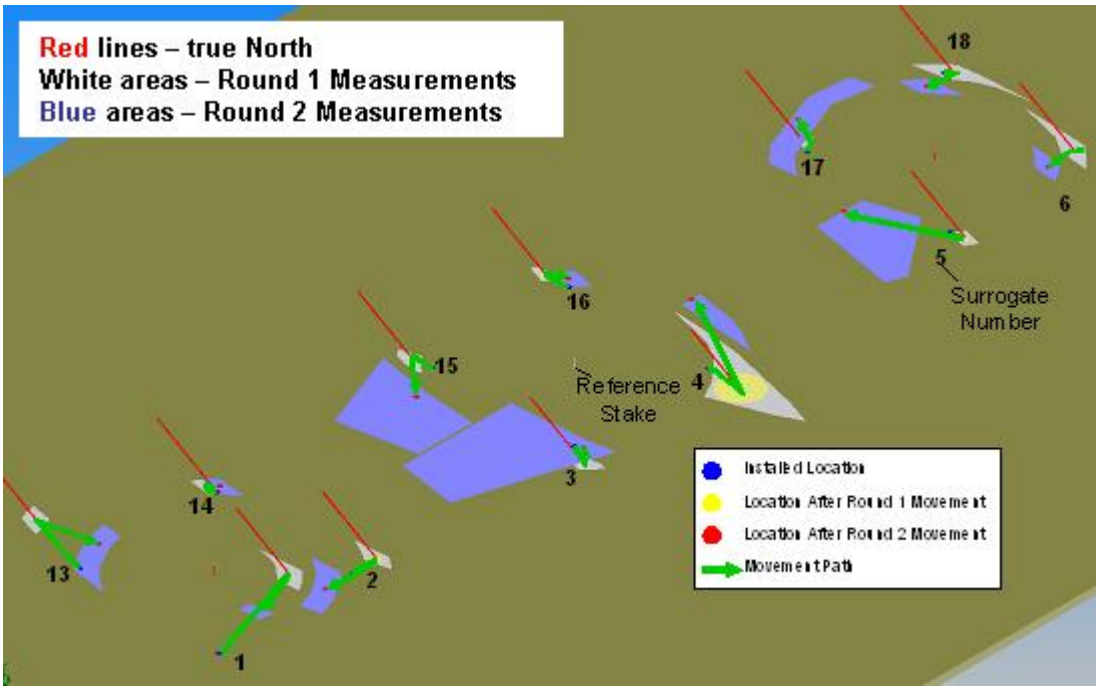

Figure 18. Inshore surrogate field, Rounds One and Two Movement.

It is noted that although most of the Round One surrogates moved north, the movement by the time of Round Two tended to be to the south.

In some instances, the Round Two data are not as consistent and accurate as the Round One data. While the average total movement was about 5.1 meters, the average error was around +/- 3.1 meters. The primary complication is that some of the rounds had moved far enough that they were no longer in a favorable position to be triangulated from the three reference stakes. That was particularly true for the surrogates that had moved close to the centerline of the fields (in line with all the reference stakes). In following rounds of measurement, additional reference stakes were used and the transponders were placed as needed to obtain better fixes on surrogate locations. This lesson was applied later in the Hawaii Field Demonstration when the reference points were placed outside the fields.

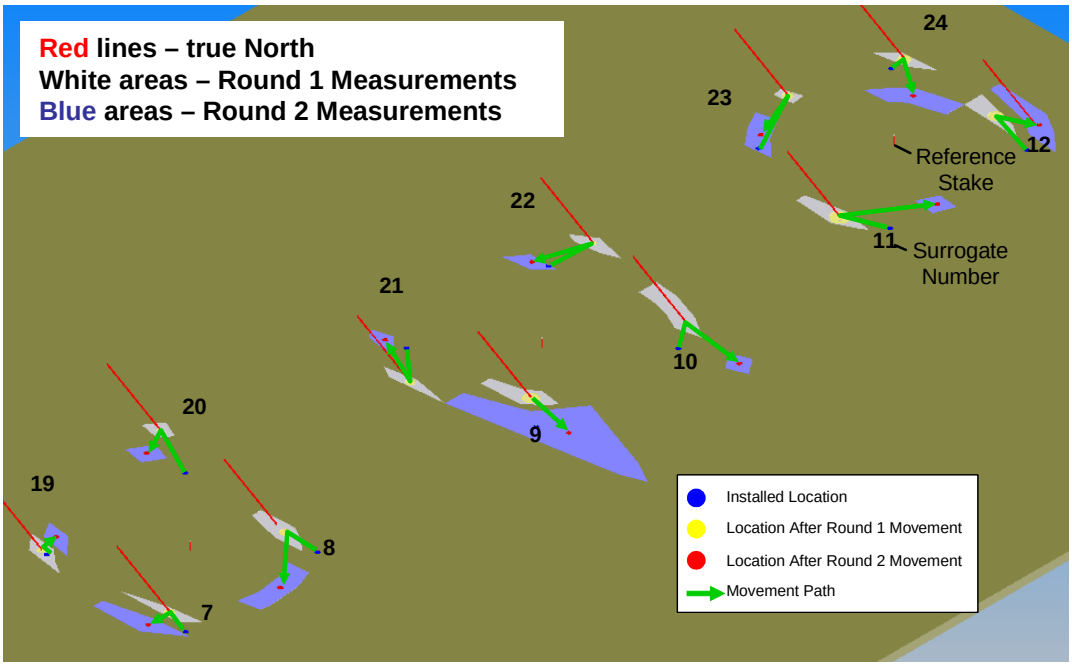

Figure 19. Offshore surrogate field, Rounds One and Two Movement.

2.6 Round Three Measurement Data

On October 20, 2005, divers from Chesapeake Bay Diving Inc. conducted diving operations in support of the UXO MM field demonstration at FRF. The magnetometer and a probe were used on rounds 6, 23, 10, and 8. The magnetometer was used in approximately a 6-foot radius and no hits were found. The probe was randomly driven in to a depth of approximately 2.5 feet and hit no solid object.

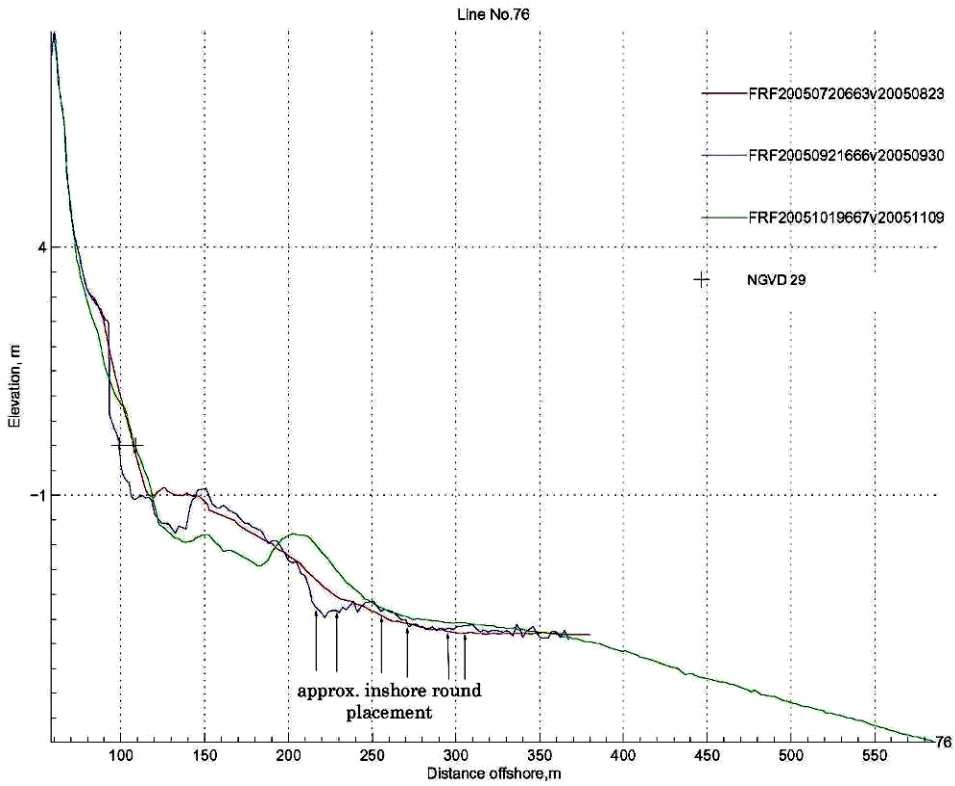

Figure 20. Survey profiles June-August 2005 indicate slight changes in seafloor level in the Inshore Field and virtually no change in the offshore field.

Figure 20 shows that through August 2005, the profiles showed little change both inshore and offshore. The wave conditions between August 12 and October 20, as documented by the FRF's 8 m directional wave array, were more active than the previous measurement periods. On occasion, waves up to 4 m in height were recorded. The profiles during this time showed formation of a bar in the area of the inshore UXO, while the offshore profile remained apparently unchanged. The FRF wave and meteorological measurements for September and October 2005 were provided separately.

On October 20th the divers were able to receive a signal from all of the 5/38 rounds, however, weaker signals, apparently from the rounds being buried, made pinpointing the inshore locations more difficult. Although there was no indication that any of the ordnance had moved, probing the sediment approximately 12 inches into the bottom at each location was unsuccessful in making contact with any of the UXO.

The 5"/38 surrogates located offshore were also buried. Although the divers did not indicate any difficulty with the signals, probing with the rod was also not successful.

At the inshore UXO sites the profile first eroded and then accreted. This is one mechanism that would result in the UXO burial. The total vertical profile change is given in Table 6.

Table 6. Total vertical profile change for inshore surrogate positions during July to October 2005.

UXO Surrogate #	Total change (meters)
1	2.75
2	2.00
3	0.75
4	0.75
5	0.75
6	0.75

The FRF dive inspector made an interesting observation that may also provide some insight into the burial mechanism. Prior to each dive, the FRF positioned small floats at the expected GPS location of the UXO. After the dive, these floats were retrieved. Because of high wave conditions at the end of the August dive, some of the floats were not retrieved. These floats consist of popcorn buoys, ¼ inch nylon cord, and 5-lb lead diver belt weights. The day before the October dive, these floats were finally removed; great effort was required to literally pull the weights out of the bottom. The inspector noticed that the lower portion of the lines did not exhibit signs of biological fouling. Since the scope of the mooring line was only a few feet more than the depth, it is hypothesized that the clean length was buried, thereby possibly providing some insight into the rate and depth of burial between August and October 2005. At the inshore location, for example at 5”/38 Surrogate #6, the bottom 0.85m (2.8ft) of the recovered marker float line was clean of biofouling. When the vertical profile change is subtracted, the depth of burial would be 0.10m. At the offshore site, the portion of the buoy line without biofouling was 0.3m. Since the profiles showed little change, the dive weight is presumed to have buried 0.3m. This may suggest a settling rate between 10 and 30cm for a 5-lb dive weight during the 39 days between the dives in August and October.

Figure 21 and Figure 22 show the measured incremental movement between Rounds Two and Three, and the wave data during that time period, respectively. The surrogates moved an average distance of 6.6m between the Round Two location and that measured in Round Three. Surrogate #16 moved the largest amount, 24m. It is noted that the measured distances for Surrogate #s 1-6, and 13 and 14 were inconsistent with the overall set of observations (i.e., unsteady acoustic tracking and large error boxes), so these outliers were subsequently eliminated from the triangulation process. Despite the absence of major storms, as shown in Figure 22, the sand wave propagation did produce movement of several meters.

Round 3 Surrogate Movement (from round 2 to round 3 movement)			
Surrogate	Movement Distance (m)	Movement Angle w/ Respect to True North	Radius of error circle (+/- m)
1*	Data Too Poor To Calculate		
2*			
3*			
4*			
5*			
6*			
7 I	10.62	192.19	1.00
8 I	8.26	181.47	2.98
9 I	1.71	295.18	2.26
10 I	4.21	219.39	1.04
11 I	3.67	241.5	1.15
12 I	0.79	309.16	1.63
13*	Data Too Poor To Calculate		
14*			
15 I	7.61	52.54	2.55
16 I*	24.48	178.21	7.59
17 I	11.58	73.05	1.72
18 I	8.72	346.25	1.58
19 I	4.52	65.93	0.88
20 I	6.12	226.96	1.55
21 I*	2.61	9.16	4.02
22 I	3.78	335.26	0.31
23 I	2.65	61.59	1.00
24 I	2.71	54.37	1.19
AVERAGE:	6.5025		

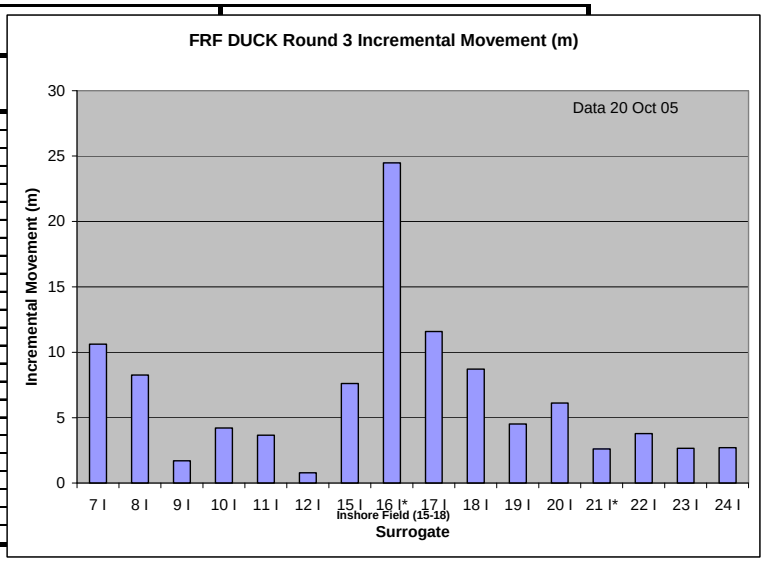

Figure 21. Round Three incremental movement as measured from the locations determined in Round Two.

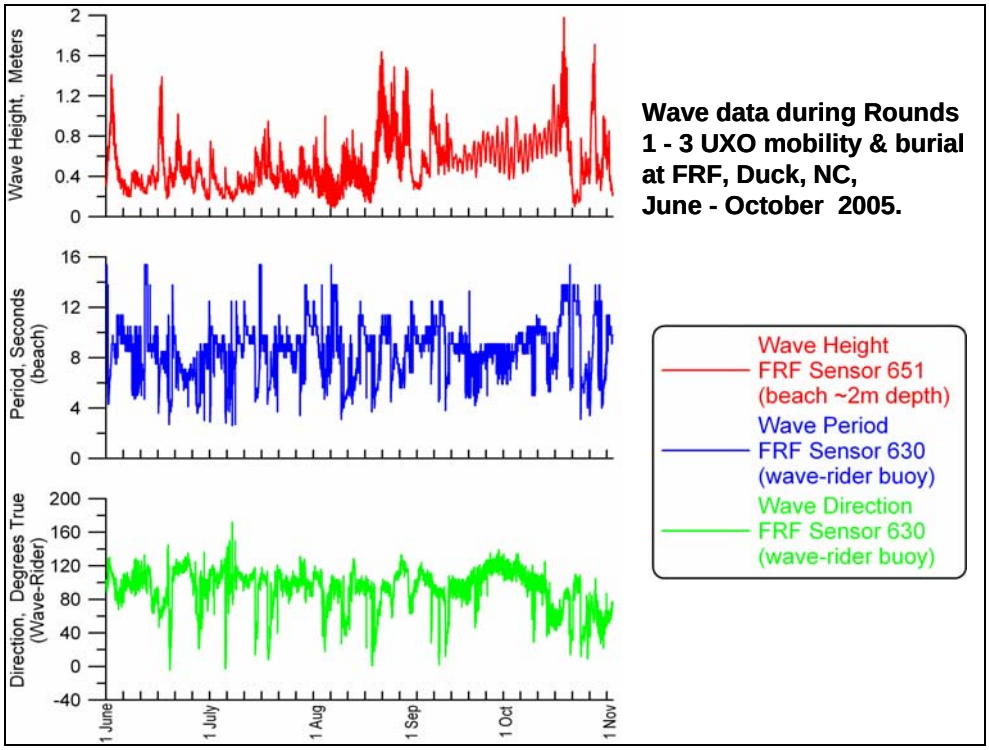

Figure 22. Wave data at FRF, Duck, for Measurement Rounds 1-3 (June-Oct 2006) indicate the absence of major storms during this period.

Figure 23 provides more detail with regard to beach profile changes; the inshore area is shown as being more active than the offshore field, with conditions that generally buried the surrogates.

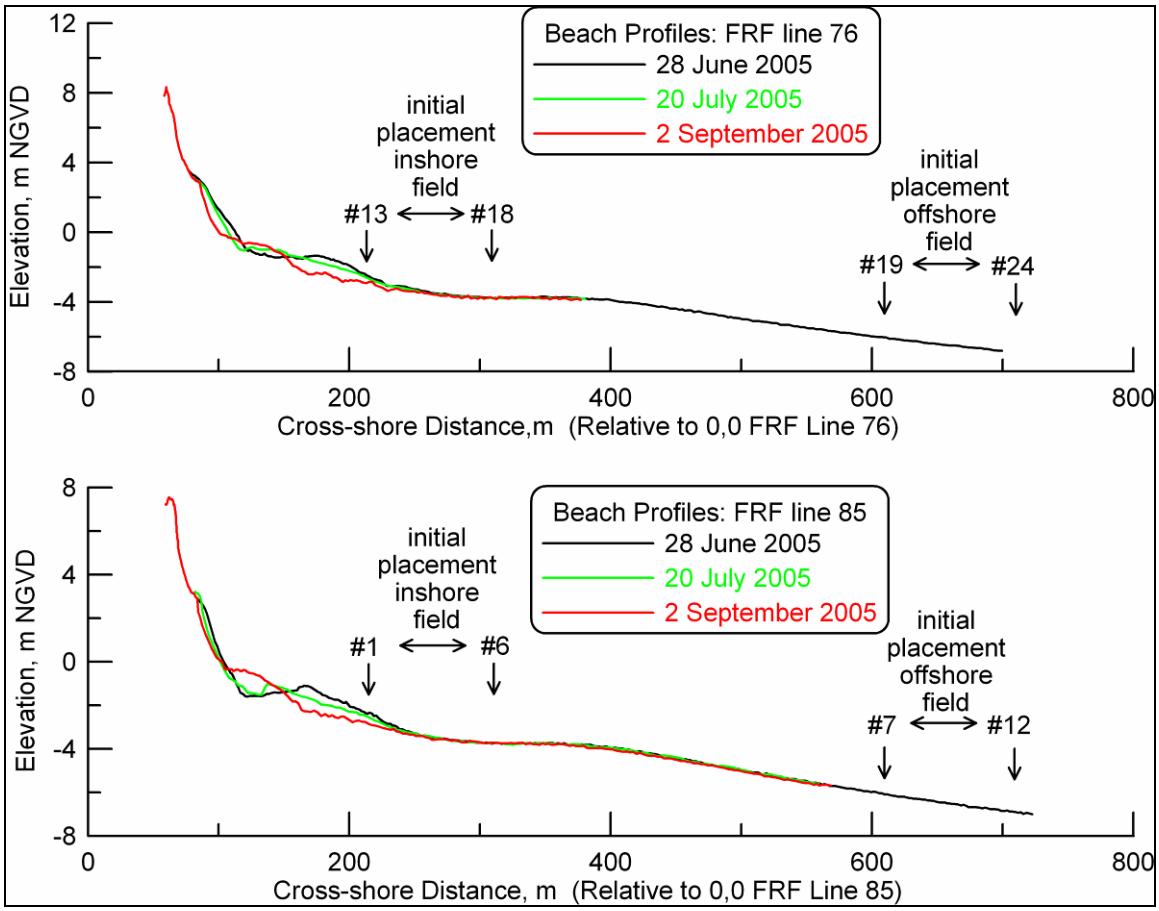

Figure 23. Shore profile changes between installation and Round Three measurements.

Figure 24 shows the measured versus predicted movement from installation through Round Three for the south line of the Inshore Field. The predictions shown by the black-dotted lines provide more detail than the few measured points, but the general trajectories and final Round Three points agree to within the accuracy of the measurements.

Figure 25 shows the comparison for the Offshore Field (north line). Although the total distances moved are generally less than identified in the Inshore Field, the model comparisons are very similar. The predictions match the general shape of the trajectories within the accuracy of the measurements. For both cases the comparison is very good.

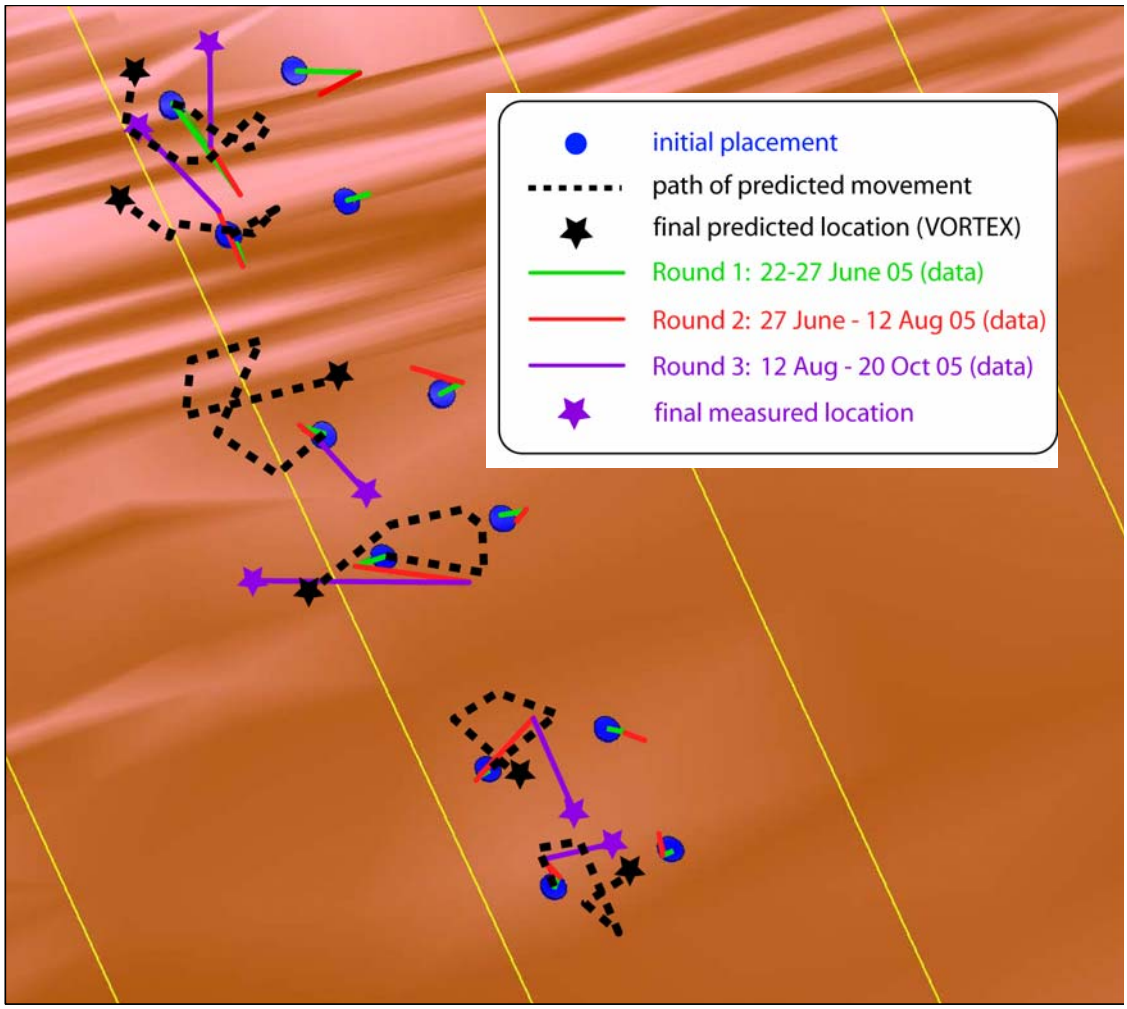

Figure 24. A comparison of predicted (MM) versus measured movement (Inshore Field, south line).

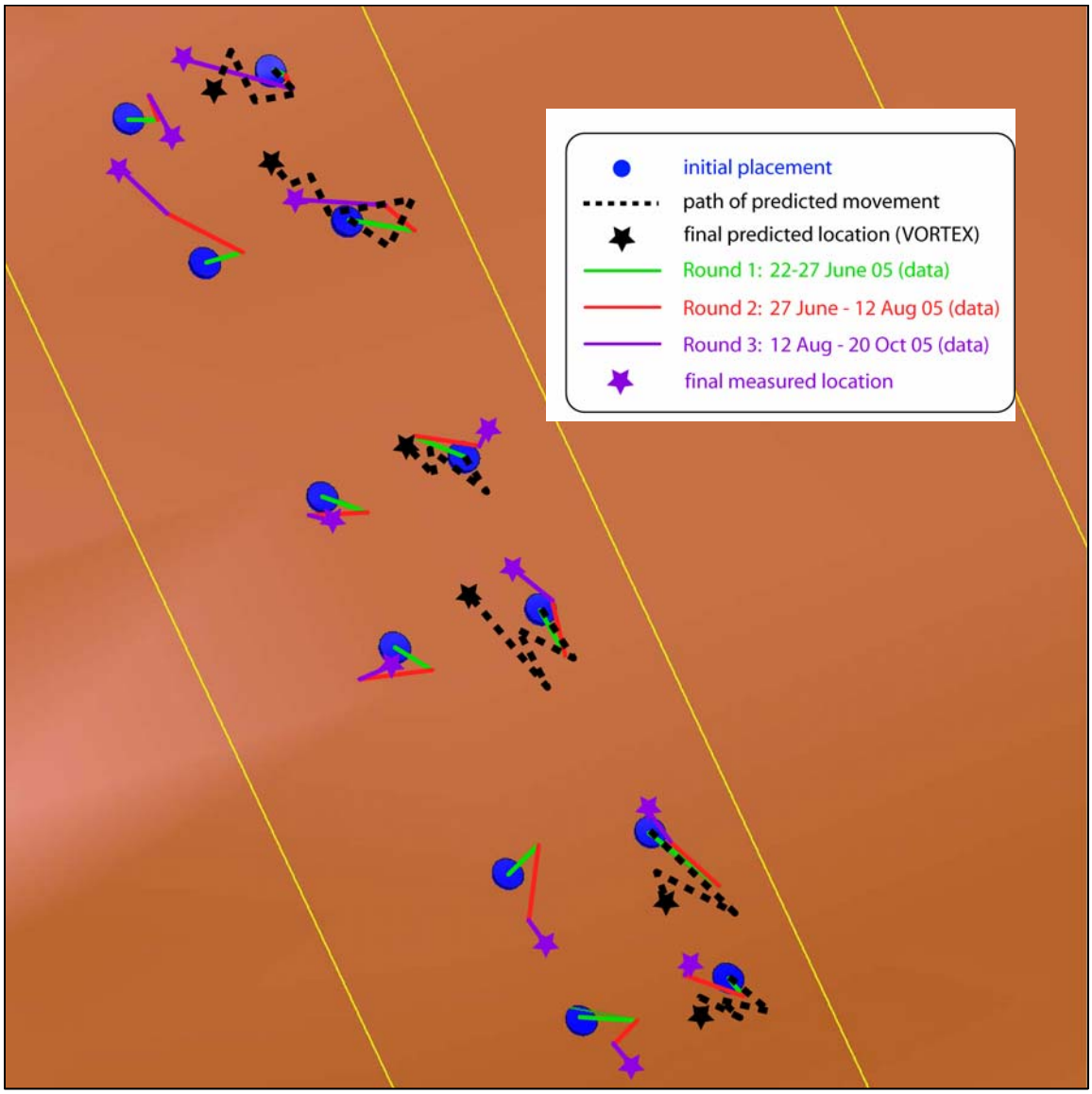

Figure 25. Comparison of predicted (MM) versus measured movement for Offshore Field (north line).

2.7 Round Four Measurement Data

The data for Round Four, recorded on 15 February 2006, were not as good as that taken in previous rounds. The insufficient data was a result of a portion of the acoustic tracking being unsteady and the fact that the associated error boxes were too large for practical measurements to be made for several of the surrogates (i.e., Surrogate #s 1-2, 8, 10, 13-14, 20, and 23). It was speculated that the rounds were more deeply buried at that time.

At the time of the Round Two and Round Three measurements in August and October of 2005, all the 5”/38 rounds were buried. A long, small-diameter rod was fabricated to document burial. Initially, the method involved probing the bottom until contact was made and then taking measurements to determine how far the bar was buried in the bottom sediment. After being unsuccessful at probing for a round during the October 2005 dive, an alternative plan was proposed. For the February 2006 dive, a “hydro lift” underwater vacuum was attached to the CRAB jet pump and used to excavate the sand to determine how deep the rounds were buried.

Surrogate #15 was the first site where the hydro lift was used. The divers excavated an approximately 30cm vertical section of sand at a time and then probed the sediment with the metal rod attempting to make contact with the surrogate. During the removal of the third section of sediment, the hydraulic pump on the CRAB failed, and contact was never made. This failure prevented any further attempts to excavate surrogates during that measurement round.

Conditions at the FRF since the last dive in October, 2005 were typical for the time of year. Waves at the FRF’s 8m directional wave array included 12 storms in which the significant wave heights exceeded 2 meters and one storm on 15 January that exceeded 3 meters. The FRF wave and meteorological measurements for November 2005 through February 2006 were provided and were used in the final calibration and validation of the UXO Mobility Model.

The storms caused the profile features to move and, consequently, the level of sand above the UXO to change as shown in Figure 26; the differences in elevation for the inshore surrogates shows that they experienced an average of more than +1 meter of burial.

To investigate how far the surrogates may have sunk into the bottom, attention was directed to the offshore UXO where the profile change was small. Initial attempts to find the UXO were hampered by a faulty pinger finder, so a backup pinger finder was used to continue the search. The backup did not contain the frequencies for Surrogate #s 8 and 10 and although there was no indication that any of the ordnance had moved, probing the sediment approximately 12 inches into the bottom at each location was unsuccessful in making contact with any of the UXO during Round Four.

Table 7 shows the measurements taken.

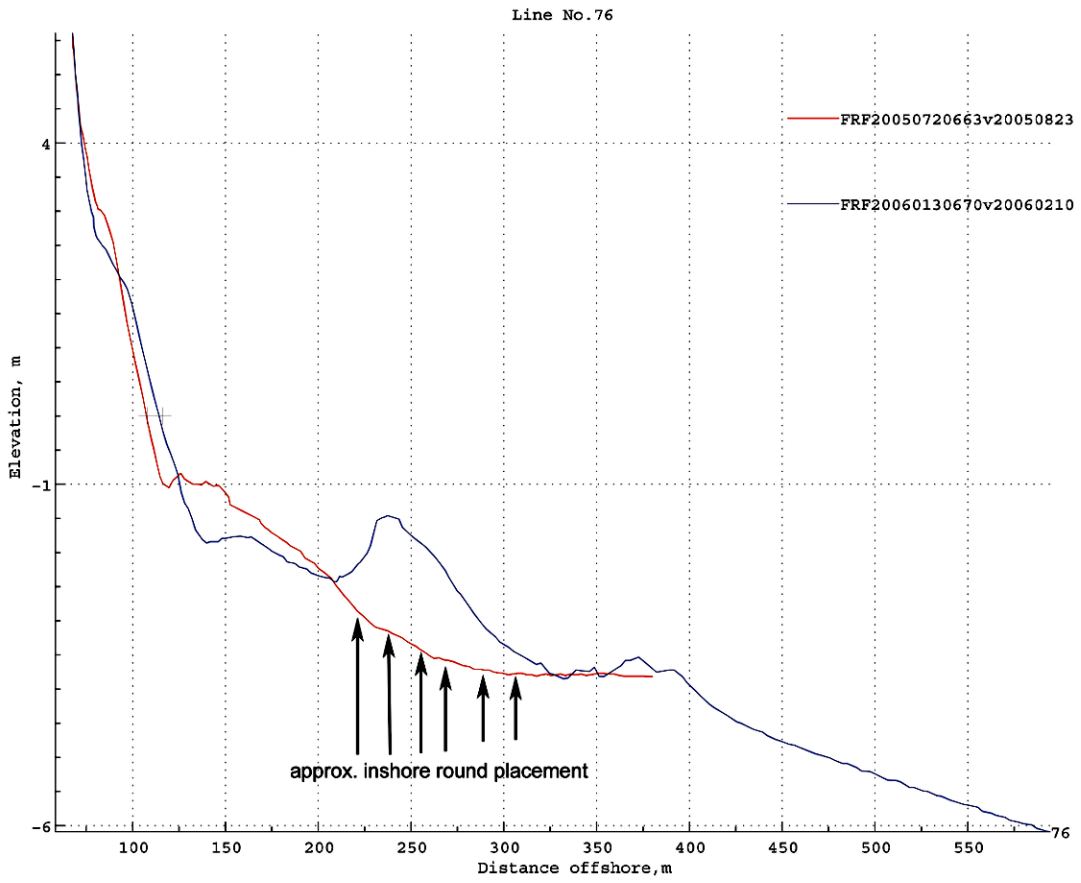

Figure 26. Inshore profile changes at FRF Duck July 2005 (red line) thru January 2006 (blue line). There was an average of more than +1 meter of sand (burial) at the inshore site.

Table 7. Round Four measurements show incremental movement since both Round Three and total movement (T).

Round 4 Surrogate Movement Data, FRF, Duck, NC (net movement from Round Three Movement, 20 Oct 2005 to Round Four, 15 Feb 2006)						
Round 4 Surrogate Movement (from Round 3 to Round 4 movement)			Total Movement (T)			
Surrogate	Movement Distance (m)	Movement Angle wrt True North	Surrogate	Movement Distance (m)	Movement Angle wrt True North	Radius of error circle (+ / - m)
1*	Insufficient Data		1T*	Insufficient Data		
2*			2T*			
3	10.4	340.7	3T	9.1	316.8	3.6
4	2.9	345.8	4T	3.8	355.8	1.8
5	2.6	270.1	5T	4.6	342.7	1.5
6	4.7	61.6	6T	2.4	61.1	1.5
7	7.3	334.5	7T	4.2	241.7	1.9
8*	Insufficient Data		8T*	Insufficient Data		
9	4.8	85.1	9T	3.6	36.7	1.5
10*	Insufficient Data		10T*	Insufficient Data		
11	5.6	53.4	11T	4.0	34.9	0.8
12	4.7	64.1	12T	3.9	116.4	0.8
13*	Insufficient Data		13T*	Insufficient Data		
14*			14T*			
15	14.6	119.7	15T	6.8	242.7	0.1
16	9.0	1.0	16T	7.4	151.0	0.4
17	5.4	257.7	17T	8.3	358.0	4.5
18	2.5	108.9	18T	7.3	336.2	0.5
19	7.2	292.2	19T	8.3	324.1	1.5
20*	Insufficient Data		20T*	Insufficient Data		
21	3.5	288.5	21T	2.0	334.9	0.2
22	3.8	304.5	22T	2.0	323.3	1.4
23*	Insufficient Data		23T*	Insufficient Data		
24	5.88	204.7	24T	3.3	114.6	0.1

		Table Key
Round Four Surrogate Movement	Surrogate	Surrogate number with respect to placement field. T = total movement * = very poor data recorded for the corresponding surrogate
	Movement Distance (m)	Distance (m) moved from the Round Three locations (20 Oct 2005) to the Round Four diver-measured locations of 15 Feb 2006.
	Movement Angle wrt True North	Angle (deg) of the movement vector with respect to True North, denotes the angle of movement between the Round Three location and the movement measurements of Round Four.
		Indicates movement from Rounds Two to Four (not Rounds Three to Four) since Round Three data were unavailable for these surrogates.

Because the total number of data points had increased, a revised method of displaying the movement (to scale) was developed. Figure 27 through Figure 33 show the sum total of movement measurements from the point of installation through Round Four. Figure 27 and Figure 28 are overviews of movement in the inshore and offshore fields while Figure 29, Figure 30, Figure 31, Figure 32, and Figure 33 are close-ups of smaller groups of surrogates.

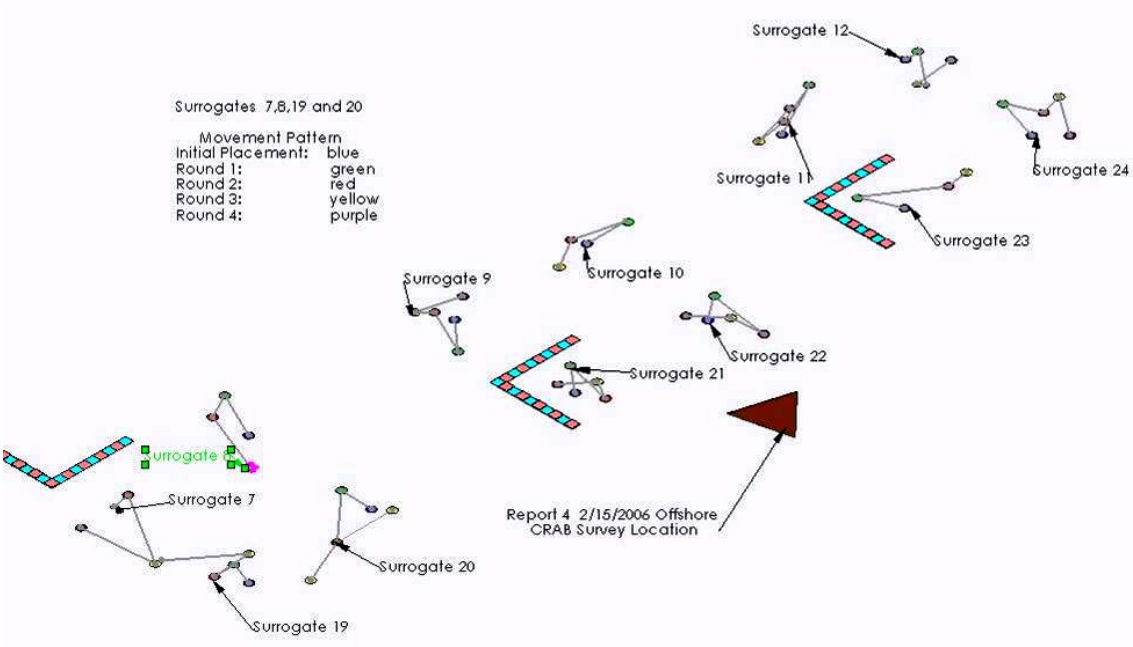

Figure 27. Summary of Inshore Field movements (installation through Round Four).

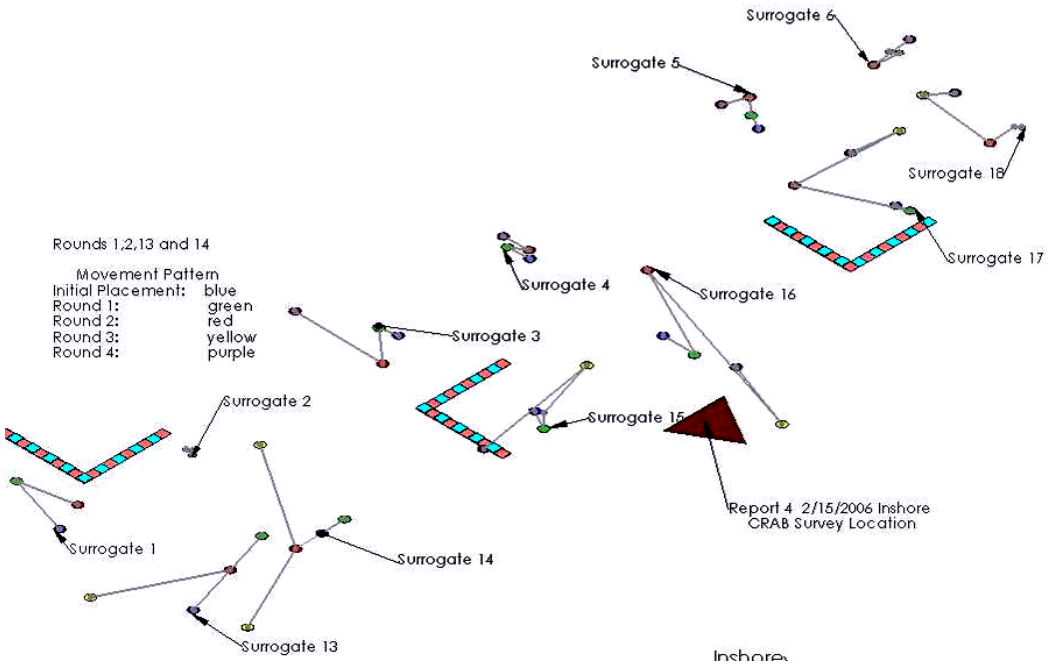

Figure 28. Summary of Offshore Field movements (installation through Round Four).

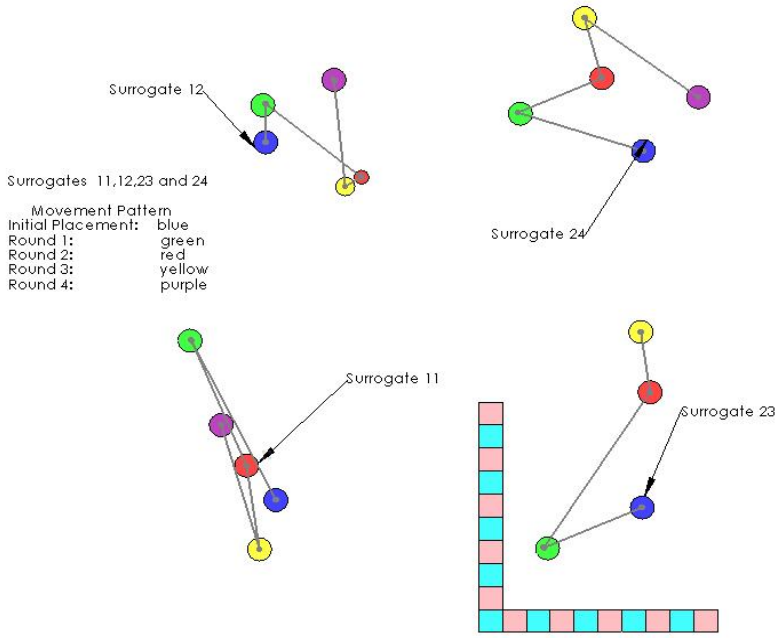

Figure 29. Surrogate #s 11, 12, 23, and 24 (Round Four).

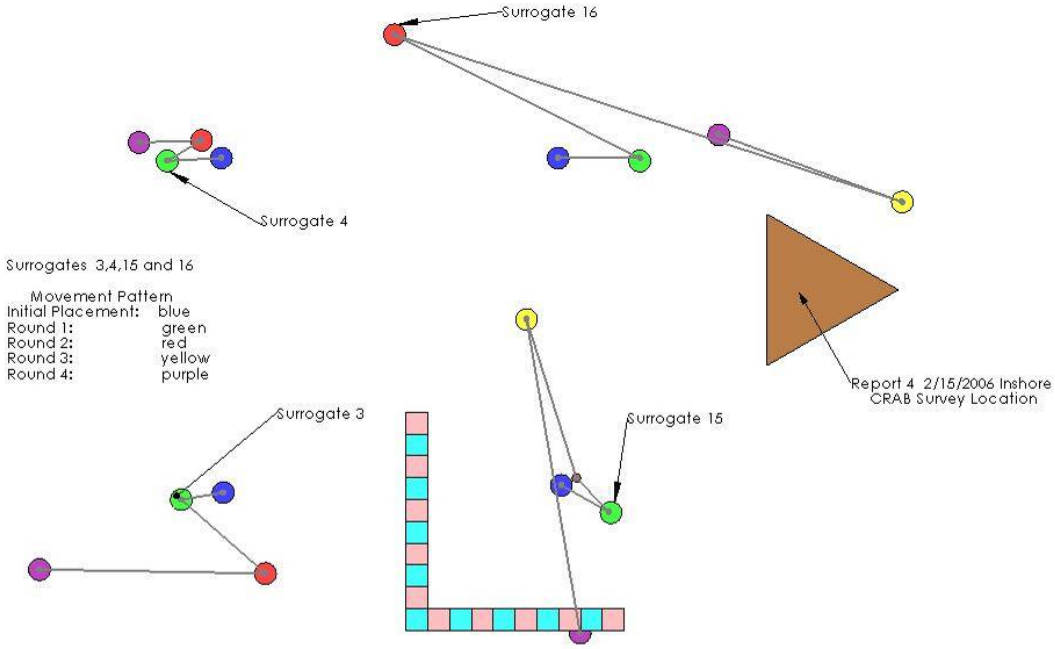

Figure 30. Surrogates 3, 4, 15, and 16 (Round Four).

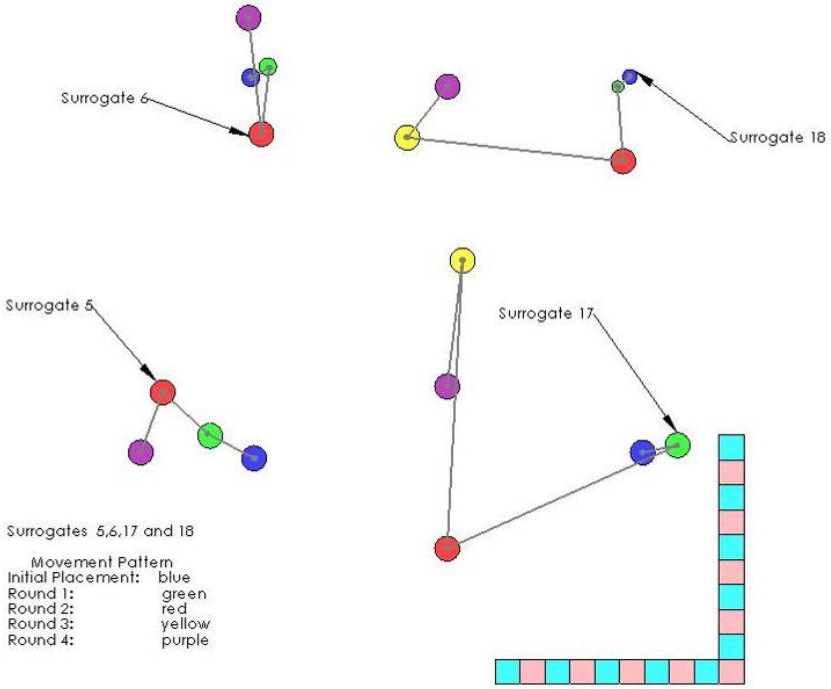

Figure 31. Surrogates 5, 6, 17, and 18 (Round Four).

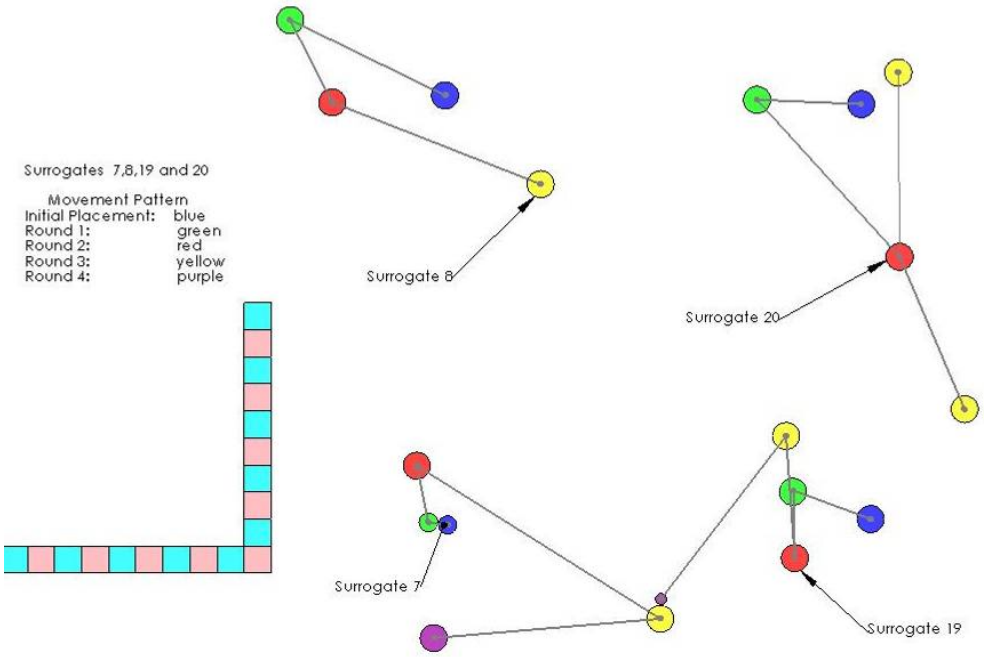

Figure 32. Surrogates 7, 8, 19, and 20 (Round Four).

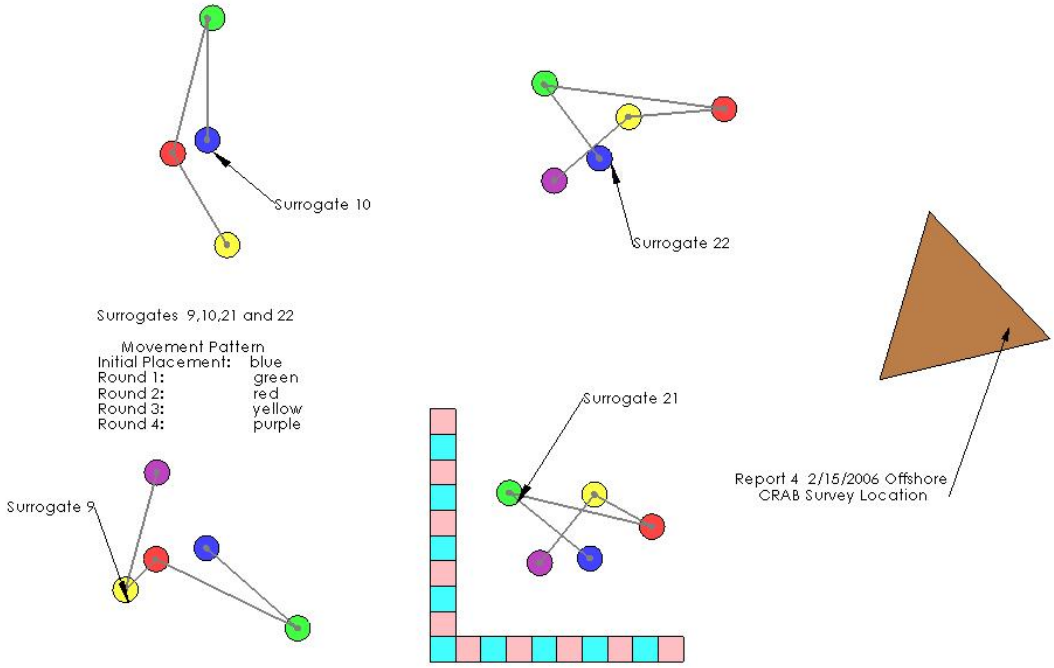

Figure 33. Surrogates 9, 10, 21, and 22 (Round Four)

In summary, Round Four did not produce as many data points as previous rounds, probably because of the increased burial depth from sand accretion in the Inshore Field, and failure of the excavation pump system. However, the data that were collected were consistent with previous data. Figure 34 and Figure 35 show comparisons between the measured and predicted horizontal movement, both in plan view and statistically.

The comparisons between the measured and predicted movement shown in Figure 34 agree to within 1.1m, the accuracy of the measurements. The statistical view of the data in Figure 35 shows the mean of the measurements to be 24% greater than those predicted by the model, which is nearly within the accuracy of the measurements.

A burial simulation comparing the predicted versus measured burial depth for Rounds 1-4 is shown in Figure 36. The significant wave height in the upper portion of the figure corresponds to the burial depth profiles given in the bottom half of the figure; the data show the model simulation results for Surrogates #1 (red) and #2 (blue) versus burial data for Surrogates #1 (cross) and #2 (diamond).

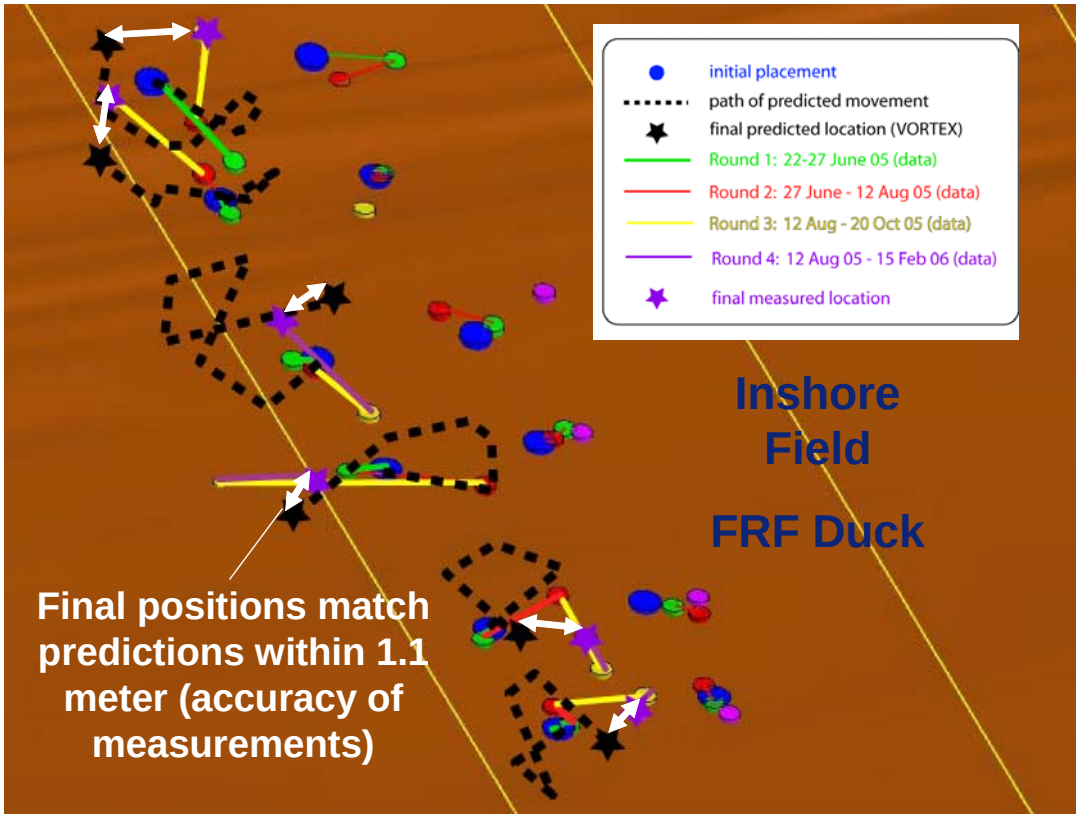

Figure 34. Comparison of measured and predicted movement (Round Four, Inshore Field, south line).

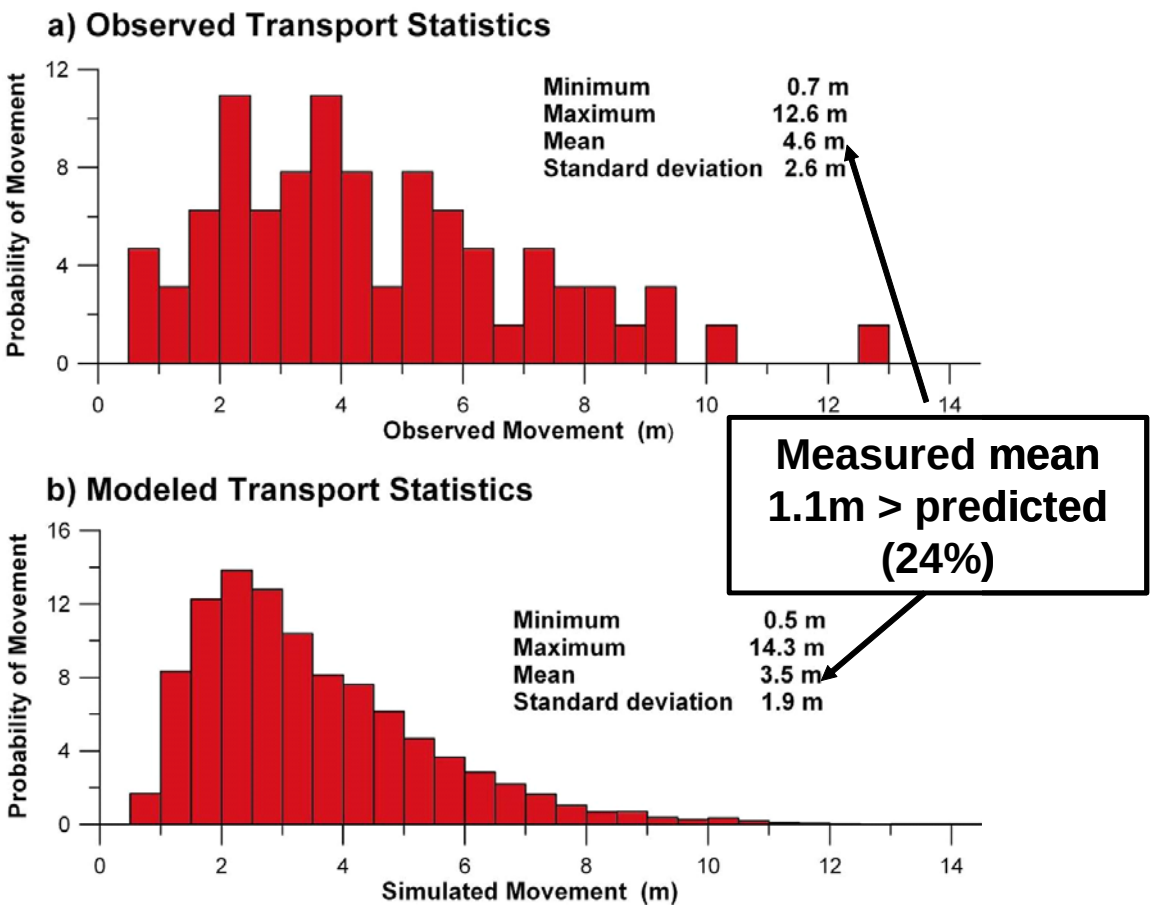

Figure 35. Statistics of measured versus modeled UXO movement (June 2005 – Feb 2006, FRF Duck Inshore Field).

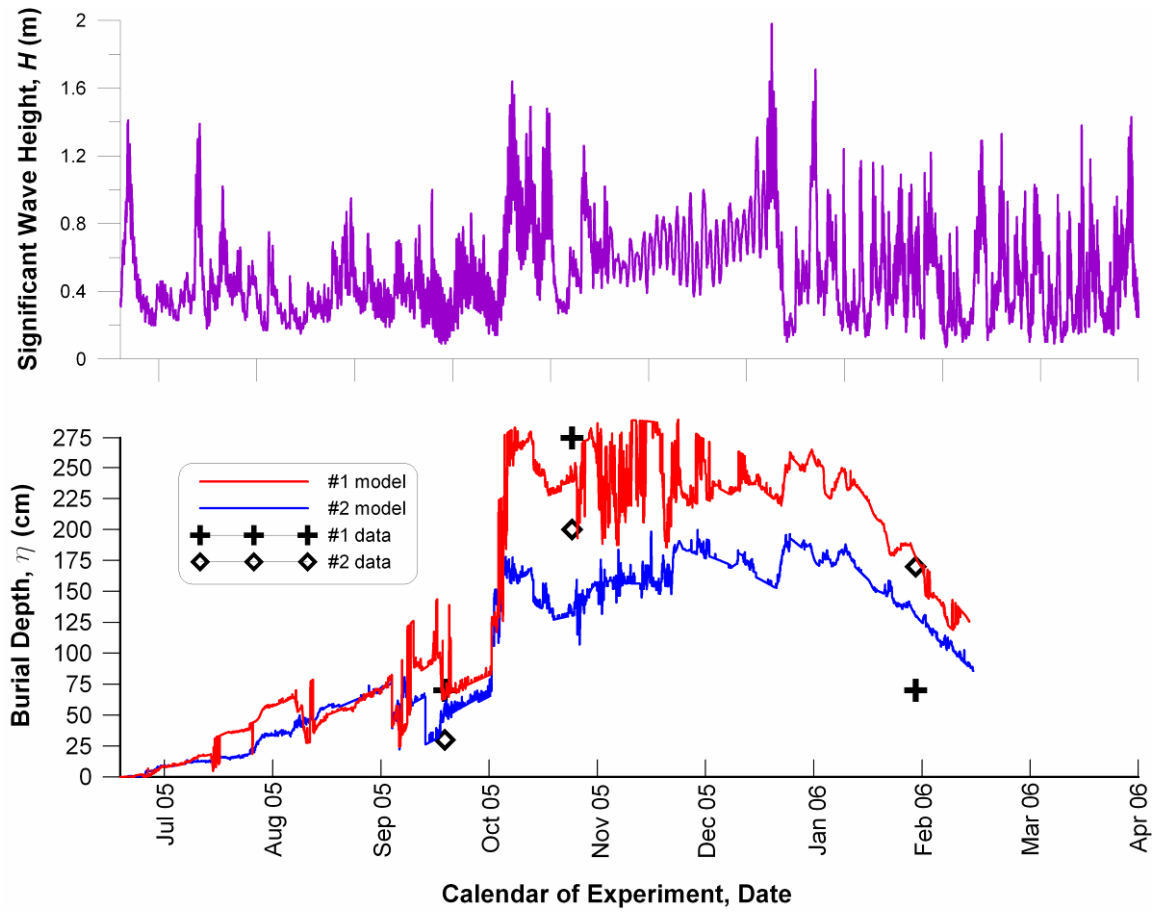

Figure 36. Burial Simulation of 5"/38 surrogates Rounds 1-4 at FRF Duck, NC, June 2005 to February 2006.

2.8 Rounds Five and Six Measurement Data

Rounds Five (July 2006) and Six (August 2006) were intended primarily to validate estimates of surrogate burial depth. An important part of that study was a review of the overall changes in beach profile between the last round of measurements (Round Four, February 2006) and the summer measurements (Round Five, July 2006).

During the time between February and July 2006, the nearshore bar moved landward as much as 75 meters in April and then moved back close to its original position in February. The July survey showed the progression landward and dispersion of the nearshore bar as shown in Figure 37. The elevation (m) profiles for February 2006 (light blue line) and April 2006 (green) show that the seaward surrogates were probably exposed at those times. In May 2006 (dark blue), the inshore surrogates were probably exposed, but in July 2006 (red), they became buried. This movement reduced the amount of sand covering the surrogates. The total vertical profile change above each of the six inshore rounds from June 2005 to July 2006 is given in Table 8 and shown in

Figure 37; little to no net bottom change occurred during February through July 2006 at the offshore surrogate locations.

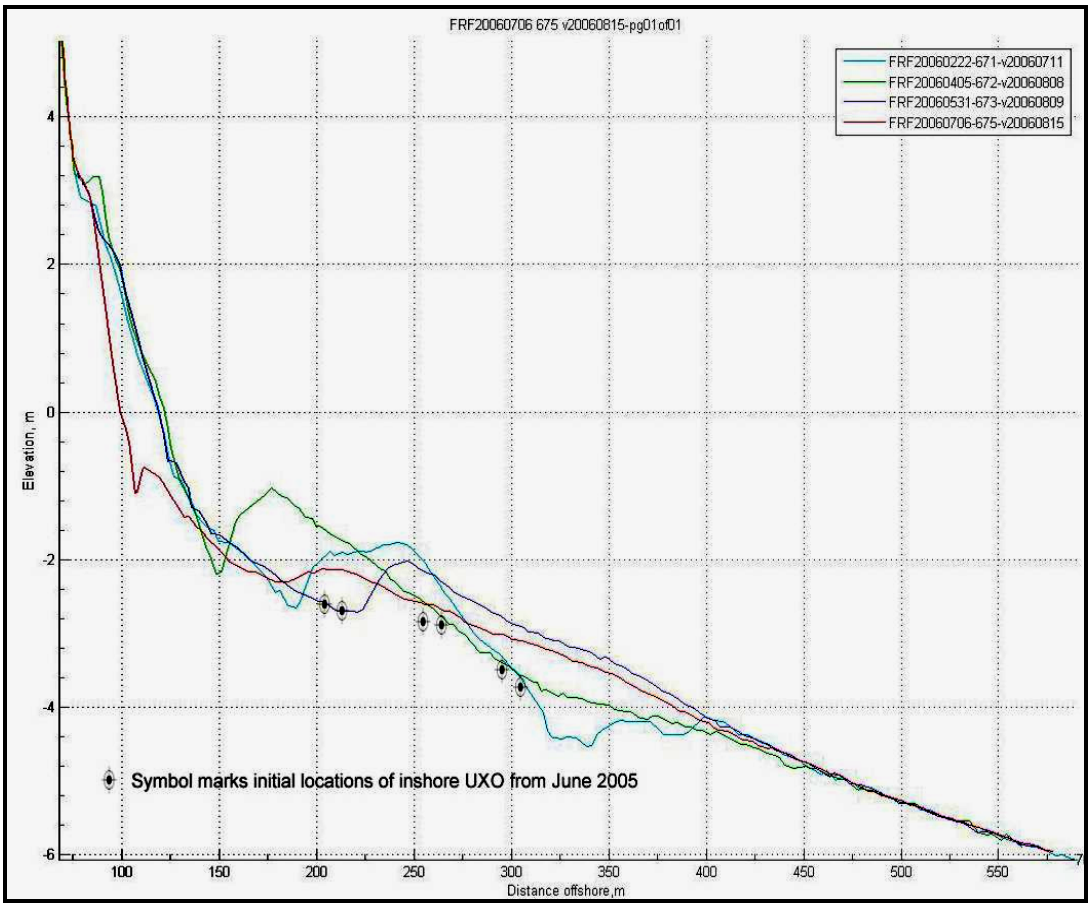

Figure 37. Survey profiles 22 Feb through 6 July 2006.

On July 27, 2006 the divers located and excavated Surrogate #23 at the offshore site. This surrogate was selected since the signal from the pinger was strong. The hydro lift was used to excavate the material above the round. After contact was made with the surrogate, the diver placed a six meter long metal rod across the hole in a shore perpendicular orientation to establish the level of the surrounding undisturbed seafloor and then measured down to the surrogate UXO. From this information the depth of burial was determined by calculating the difference from the initial sea floor elevation in June 2005 from the depth measured when the round was recovered, as shown in Table 8. The horizontal coordinates of the recovered round could not be measured with high precision but the divers stated they were less than 2m from the buoy dropped that morning which was within 1.5 meters marking the initial surrogate position. To reduce

horizontal measurement error, the CRAB was also used to make subsequent location measurements.

On August 3, 2006, the same procedure was used to uncover and measure burial depth of an inshore surrogate. Surrogate #18 was selected since its location was in an area that experienced the least amount of sediment accretion above the surrogate and exhibited a clear signal that could be heard from the surrogate's pinger. This surrogate was also found less than 2m from the buoy dropped prior to the dive on the initial coordinates of the surrogate. Table 8 contains the measured burial depths of the recovered surrogates. In both cases, it appeared that the surrogate has actually become buried deeper than their original deployment location on the sea bed.

Table 8. Surrogate burial depths as measured on 3 August 2006.

Surrogate #	Depth of burial (m) since 28 June 2005
23 (offshore group)	-0.15
18 (inshore group)	-0.51

2.9 Magnetometer Tests

In October-November 2006 an experiment was conducted to determine if a cesium magnetometer could be used to accurately locate both the 5"/38 and 20 mm surrogates. If that method proved effective it would potentially save dive costs and provide a better way to locate all the 20mm surrogates. It was also being considered as a backup method of surrogate location for the Hawaii Field Test in the event that acoustics proved unreliable in the rough seafloor environment of a biogenic reef, which is typically crossed by narrow channels or "awas".

The test was conducted by Tidewater Atlantic Research, Inc. (TAR) [7]. The experiments encountered a number of technical complications but illustrated that, with the necessary equipment and methodology, the surrogate could be located and its movement quantified.

The system was calibrated on 20 October 2006 by making in-air measurements of the surrogates in various orientations. The TAR investigator used a cesium magnetometer and one of the surrogates to conduct the in-air calibration (
Figure 38); typical detection distances were a few feet.

Figure 38. Cesium magnetometer and 5”/38 surrogate during in-air calibration testing.

Figure 39 shows the results of the calibration of the 5”/38 surrogate lying horizontally. When the surrogate was in a vertical position, the detection range increased considerably, but during the FRF Duck demonstration, all surrogates were situated horizontally and proud of the ocean floor (i.e., no impact burial). The grid is on 6 ft spacings.

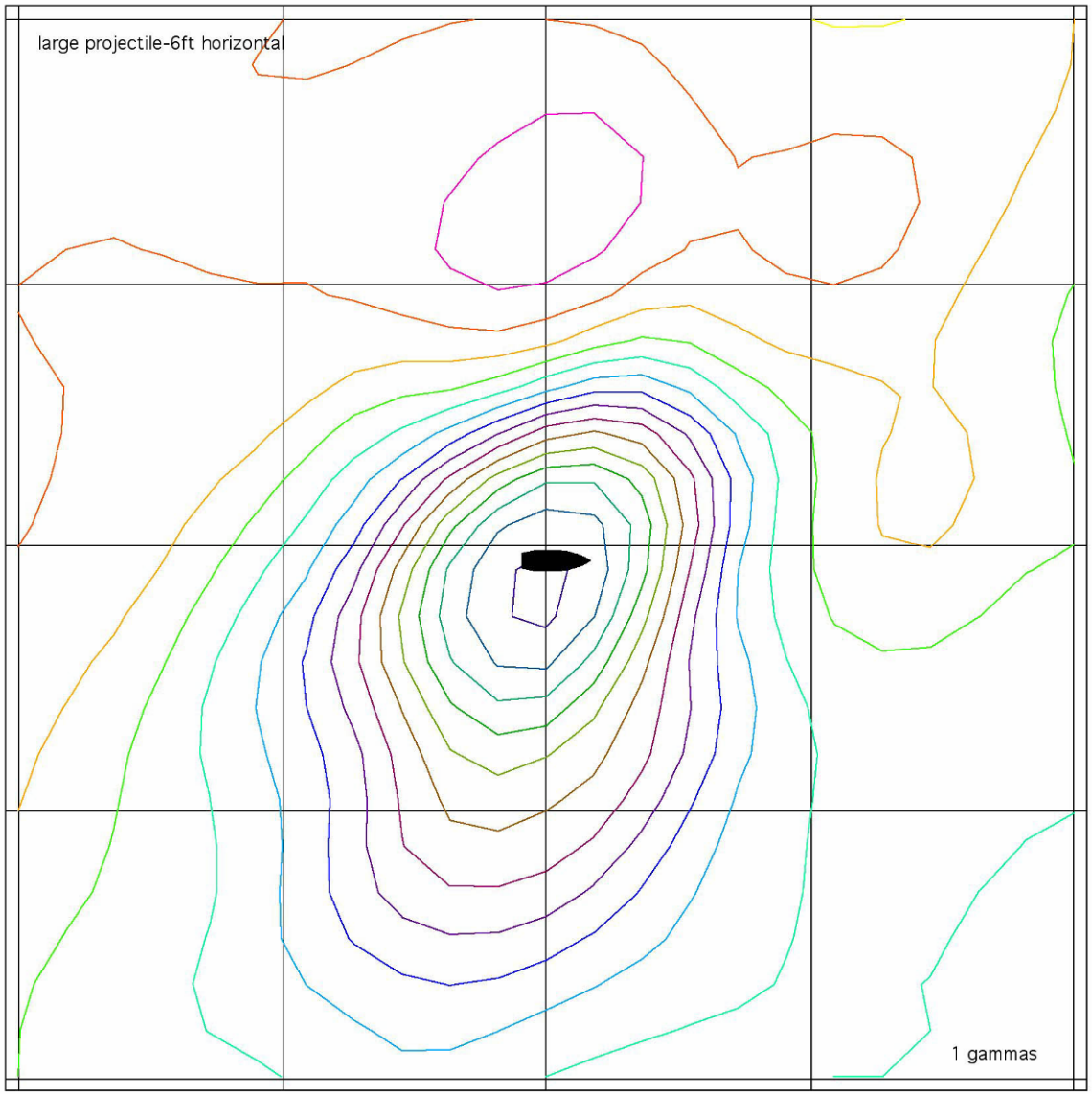

Figure 39. One gamma contour magnetic signature for horizontal 5-inch projectile generated by data collected at 6-foot elevation.

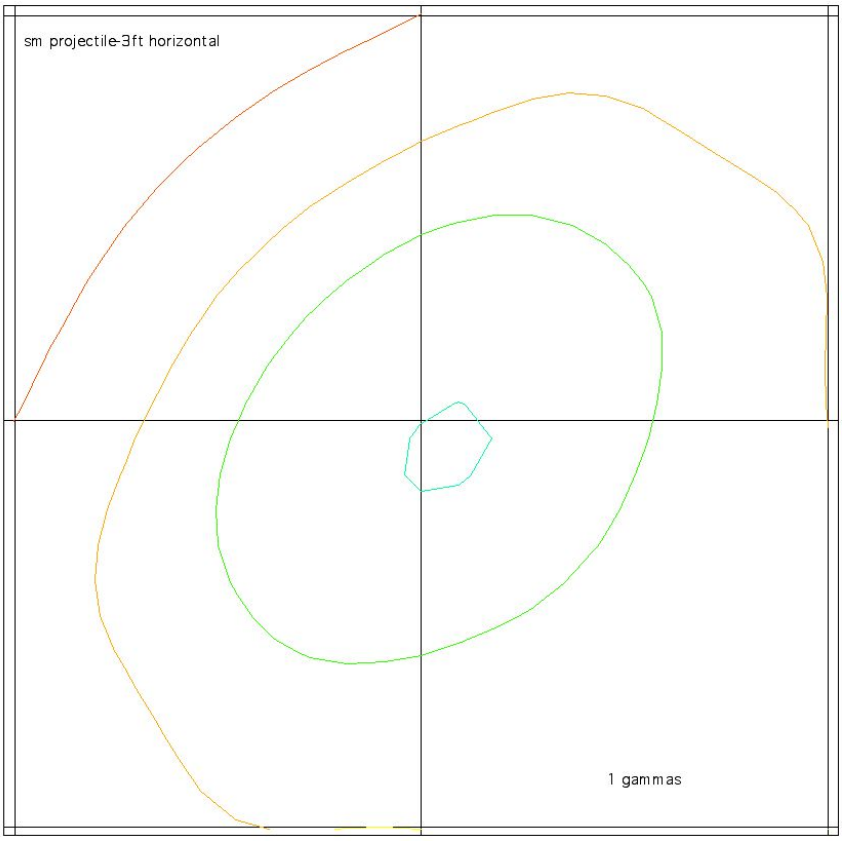

Figure 40. One gamma contour magnetic signature for horizontal 20mm projectile generated by data collected at 3-foot elevation.

Figure 40 shows that even a single 20mm round could be detected, but only at very close ranges. However, the 20mm rounds were installed in groups of 10, so it was expected that they would be detectable in the field. The grid is on 3 foot spacing.

On 1 and 2 November 2006, the weather allowed surveys of the FRF site using both the CRAB and LARC vehicles. The magnetometer was rigidly attached to a frame below the CRAB that held the magnetometer 3 ft above the seafloor. For the LARC operations the magnetometer was towed.

Although the CRAB provided a more stable platform and very accurate navigation, the CRAB hydraulics and other systems provided a considerable background magnetic noise that hampered measurements. By contrast, the LARC tow configuration was magnetically very quiet, but the system did not include an accurate means to track the location of the towed magnetometer. Appendix D provides additional information regarding the magnetic anomalies detected from the CRAB.

On 2 November 2006, the Trimble RTK/GPS system was installed on one of the FRF Duck LARC vehicles (Figure 44). The cesium vapor magnetometer was towed at a distance of 30 feet behind the LARC. HYPACK MAX was used on a laptop computer to collect data from both the positioning system and the magnetometer. The speed of the LARC was maintained at 4 knots during the survey and vessel tracks followed lanes established when the UXO was deposited. Unlike the CRAB, the LARC produced virtually no interference and anomalies were readily identified

However, the fact that the magnetometer was towed in the water column 30 feet aft of the vehicle reduced the level of geographical accuracy of positioning. While HYPACK MAX permits layback and offset to be calculated for a sensor position, its exact location can be significantly influenced by cross currents at low vessel speed. Also towing the sensor in the water column made it difficult to maintain a constant height above the bottom surface. While that condition can be improved by including depth and height above bottom sensors on the magnetometer, it cannot match positioning control achieved using the CRAB.

The shallow water depth of the inshore ordnance field made it virtually impossible to achieve a combination of sensor distance from the LARC, vehicle speed and sensor height above bottom that could have been effective. To collect comparative data, the November LARC survey focused on the offshore surrogate field.

Figure 41. FRF Duck LARC used for towing the magnetometer during the demonstration.

Initially, data from the LARC survey appeared to be more useful than that collected using the CRAB. However, more detailed analysis and high resolution contouring of the data indicated that the reference pipes installed in the UXO grid for measuring movement produced anomalies of sufficient intensity and duration to obscure anomalies produced by the test rounds. The height and position of the sensor in the water column no doubt contributed to minimize the UXO influence in the overall magnetic field. In addition, the LARC magnetic contour suggests that additional ferromagnetic material may be present at the validation site (Figure 42).

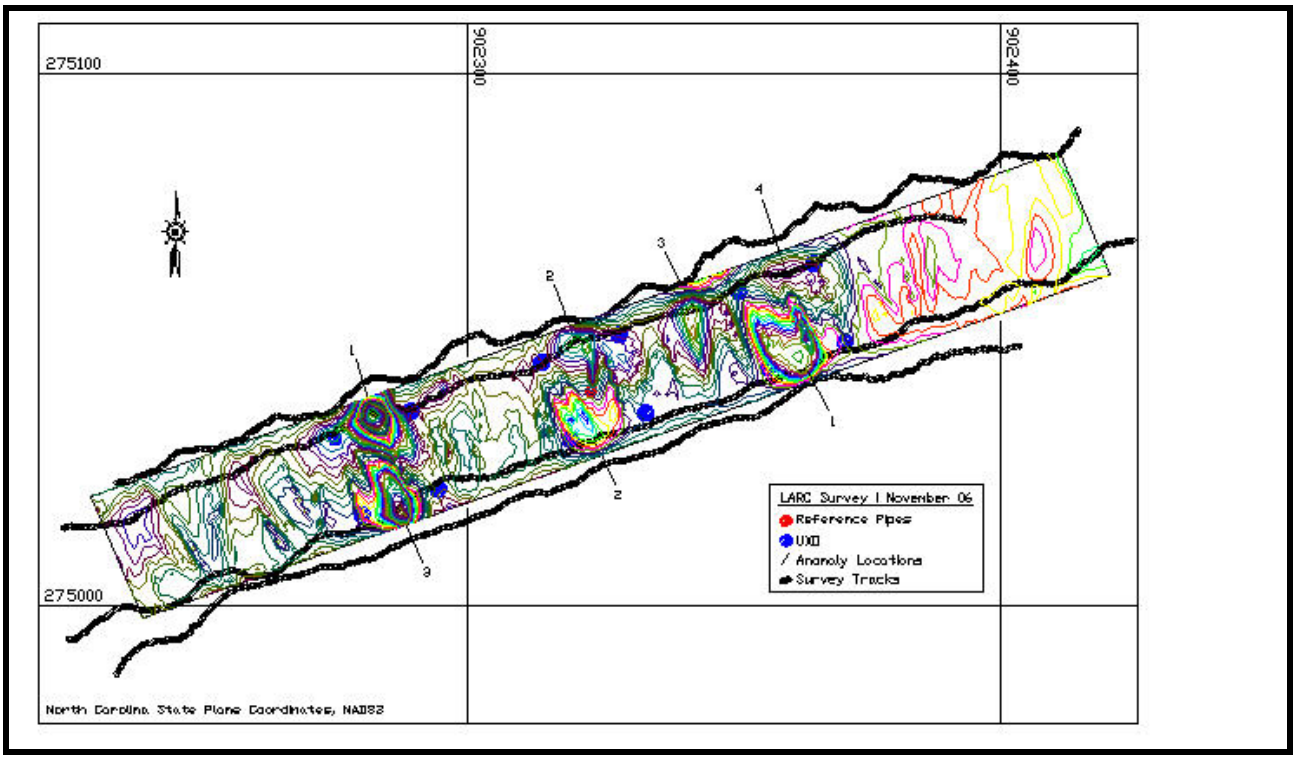

Figure 42. Magnetic data generated by CRAB underway showing UXO targets and the magnetic disturbance generated by the reference pipes.

Data generated by investigation of the deposition sites of 20mm ordnance proved to be inconclusive. The subtle nature of their signatures appeared to fall well below the threshold of detection using the validation methodology. Data would have to be collected in a much more intensive fashion with virtually no background noise for this validation to be successful.

Analysis of the data generated by the FRF Duck experiments suggest that the position of UXO can be established using a cesium vapor magnetometer using the appropriate methodology. However, there are clearly a number of issues that must be resolved to ensure the level of accuracy necessary to identify and to quantify movement of UXO. While the magnetometer detections were certainly in the same general areas and formed the same pattern as the diver

acoustic measurements, the resolution was so limited by navigation errors (towed) or background noise (CRAB) that it was not possible to derive a quantitative comparison of the two methods.

While the CRAB provided highly-accurate positioning and navigation control for data collection, the vehicle's hydraulic motors generated considerable interference while underway. While using the LARC as a survey vessel, the magnetic background data was very stable, which, in turn, enhanced the quality of the target identification. However, the survey track of the LARC was considerably less accurate that that of the CRAB. Appendix D provides some options for increasing the accuracy of the positioning and navigation control by eliminating the motor interference. Ultimately, the FRF Duck magnetometer investigations indicate that useful data can be generated using a magnetometer to identify and to determine the three-dimensional position for UXO on the seafloor. The investigation also clarified a number of technical and procedural issues that must be addressed before the desired results can be achieved. Like most initial experiments, the FRF Duck investigation results can help identify criteria for more sophisticated efforts.

2.10 Recovery

All 12 of the Offshore Field surrogates, plus two of the three reference stakes and three sample 20mm surrogates, were recovered in early April 2007. Fortunately, the Offshore Field generally saw much less net transport of the sand (and change in overall water depth) than the Inshore Field. The average burial depth at the time of recovery was only 3-7 inches.

In each case, the CRAB helped to place the divers down on top of the as-installed location and they found they were able to immediately locate the surrogates there. This was not an unexpected outcome, because as shown in the Round Four analysis, the surrogates tended to move back and forth around the original installation locations, which is consistent with the mechanics of infrequent unburial during sand wave passage. While occasional movement of as much as 10 to 20 feet from the original location was recorded, no net transport was measured.

One very important part of the initial recovery analysis was the discovery of substantial biofouling on the recovered 5"/38 surrogates, an example of which is shown for Surrogate #22 (Figure 43). It is not possible to calculate the exact duration of exposure from the size and nature of the biofouling alone. The growth depends on temperature, water velocity, amounts removed by scouring, etc. However, the mere presence of the biofouling validates that the surrogates were exposed at least several days, and probably considerably more. This noteworthy occurrence is important because none of the measurements happened to coincide with a time of exposure – the divers never saw the surrogates between the installation and the recovery. The fact that the biofouling covers a substantial part of the surface confirms that the surrogates were in fact exposed sufficiently for them to have participated in the scour/roll process predicted by the MM. In short, the MM predicted exposure and movement; the biofouling confirms the exposure and the location measurements confirm the movement.

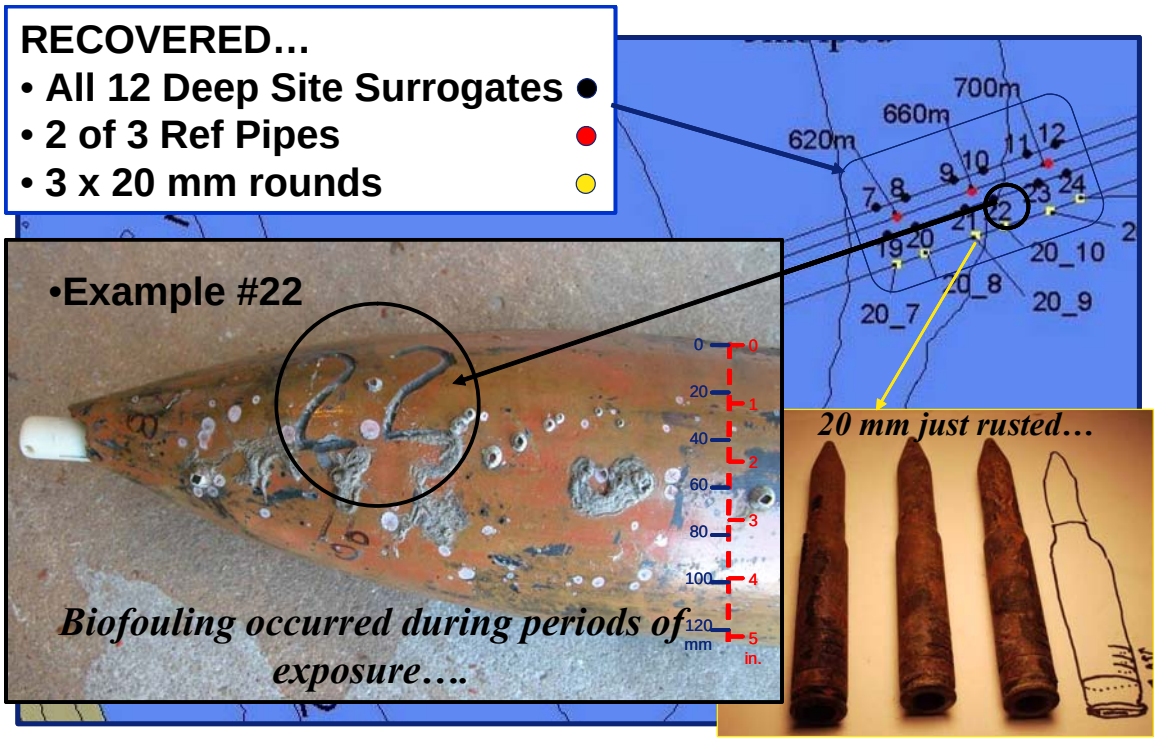

Figure 43. Evidence of biofouling confirms that 5”/38 rounds were at times unburied, which is consistent with Model predictions (Offshore Field recovery, 3-13 April 2007).

The recovered surrogates are in storage at FRF Duck. Recovery of the Inshore Field surrogates was planned – and actually attempted – on several occasions throughout the summer of 2007. Plans remain to retrieve the remaining surrogates; specific retrieval actions are planned for FY08.

3.0 Future Plans

3.1 Demobilization

Divers removed all but twelve (Inshore Field) 5”/38 surrogates. It is likely that they have become entombed several feet below the seafloor. While they pose no further risk to the environment or personnel, especially since the surrogates are inert, the FRF staff will attempt to recover the remaining 12 surrogates when weather permits or until funds are expended. The recovery operation will likely require approximately 1-2 dive days.

There are no restoration steps required for the seafloor area because it is a high-energy coastal zone. Any disturbances of the seafloor have already been erased by wave action.

The recovered surrogates will be stored at FRF Duck pending final recycling of the materials.

3.2 ESTCP UXO Mobility Model Final Report

The data from this Field Test have been combined with the data from the Hawaii Field Test, which was completed in June 2007 [1], and used in a final calibration and validation of the UXO Mobility Model for those two coastal environments. The ESTCP Final Report [6] is in preparation and will contain a summary of the results of the two field tests.

4.0 UXO Mobility Model Validation on FRF Duck Data

4.1 Technical Approach

The *Vortex Lattice (VORTEX) Scour and Burial Model* is the basic module within the MM used to predict migration and burial behavior of UXO surrogates. The trailing edge coastal environment selected for this experiment was the U.S. Army Corps of Engineers Field Research Facility (FRF) located on the Atlantic Ocean near the town of Duck, North Carolina.

4.1.1 Process Model Architecture

Migration and burial processes consist of two distinct types: nearfield and farfield. These operate on significantly different length and time scales. Nearfield processes occur over length scales on the order of the body dimensions and on time scales of a wave period (a few seconds to hours), and are primarily governed by scour mechanics. In contrast, farfield processes involve changes in the elevation of the seabed with cross-shore distances of hundreds of meters that may extend along the coast for kilometers. Farfield time scales are typically seasonal in nature and are characterized by longer periods due to variations in climate and travel time of longshore sediment fluxes associated with accretion/erosion waves. These processes are coupled together with the component code modules in an architecture diagrammed by the flow chart shown in Figure 44 and referred to as the *Vortex Lattice (VORTEX) Scour and Burial Model* [2]. The farfield processes and inputs are found above the orange line in Figure 44 while the nearfield processes and inputs are below the green line.

As with any boundary value problem, the solution follows from specifying initial conditions, forcing functions and the boundary conditions, from which the response is computed using a set of process-based algorithms. This computational sequence proceeds in Figure 44 from the top of the diagram down, with the set of forcing functions and initial conditions bundled together in a *module* shown by the pink shaded box at the top of the flow chart, while boundary conditions (beige box) and response (blue box) modules of the farfield are found in the pathways below that. The farfield response modules are upstream of the nearfield modules in the computational flow chart because the farfield processes determine the fluid forcing and elevation of the sand bed around the object, which is essential to specifying the nearfield boundary value problem.

The forcing function module (shown in the pink box) provides time series of waves (code module #2), currents (code module #3) and sediment flux (code module #4). Waves and currents are derived from direct observations by means of the directional wave arrays and Acoustic Doppler Current Profilers (ADCP) maintained by the Field Research Facility at Duck Pier.

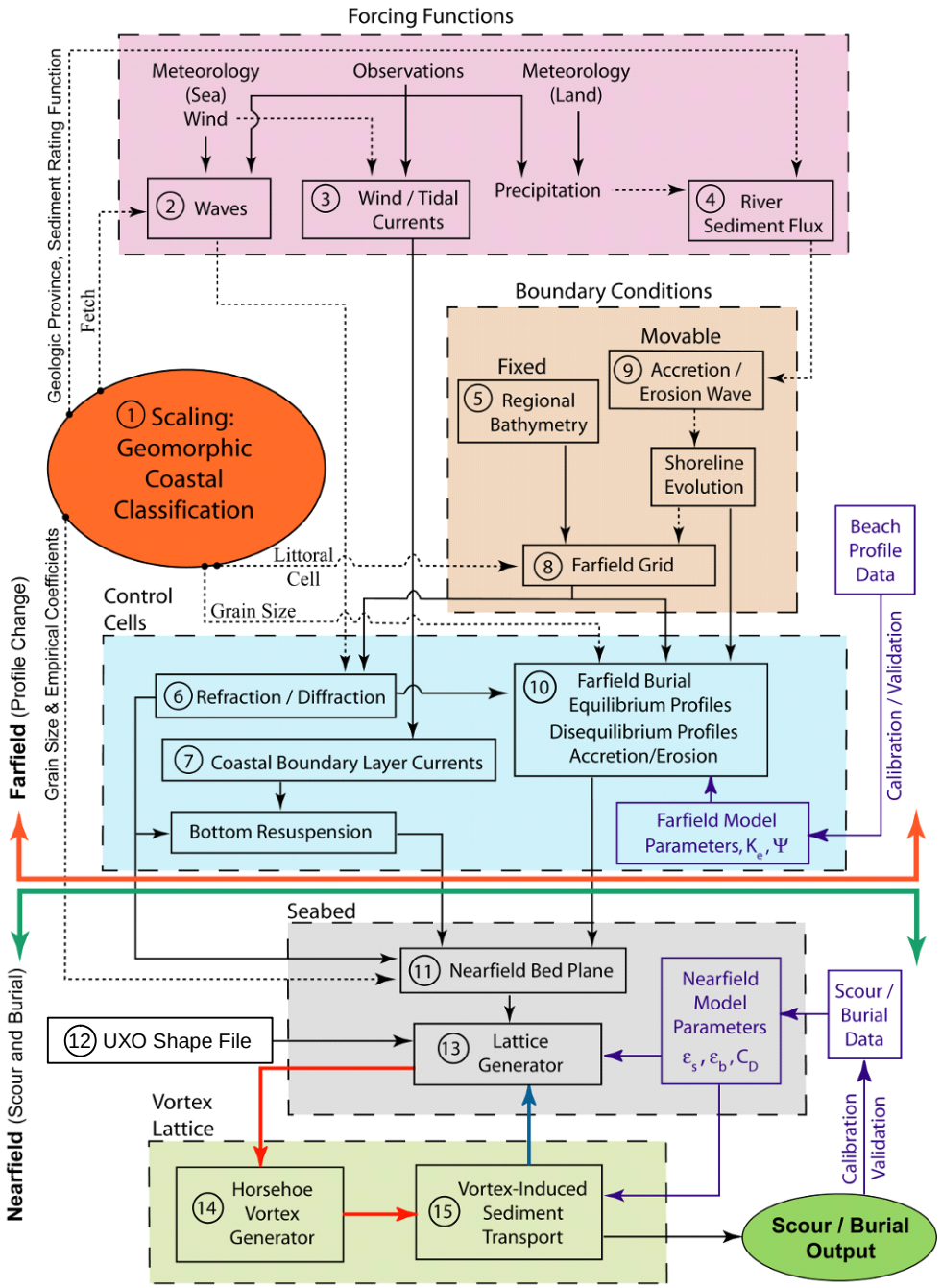

Figure 44. Vortex Lattice Scour Burial Model after [2].

Fluxes of river sediment are neglected as explicit boundary conditions, but the sediments are accounted for in the grain size distributions of the offshore sediments. The wave and current forcing provides excitation applied to the deep water boundary of the farfield computational

domain. These boundaries are specified in the boundary conditions module (beige box) in Figure 44, where the farfield computational domain is assembled from a series of boundary-conforming control cells (Figure 45), using a combination of bathymetric data obtained from National Ocean Survey (NOS) and United States Geological Survey (USGS) [8] as compiled by the National Geophysical Data Center [9]. From these data bases, the gross morphology of the barrier sand spits and continental shelf along the Outer Banks (Figure 45) were assembled.

With these forcing functions and boundary conditions, the farfield response module (blue box) computes the spatial and temporal evolution of the fluid forcing and bottom elevation along the two littoral cells that comprise the Outer Banks (Figure 45). At the FRF site, these littoral cells are bounded in the cross shore by Cape Henry to the north, Cape Hatteras in the mid-reach where the angle of the coastline makes a dog-leg departure toward the southwest, and Cape Lookout to the south. FRF Duck is located just east of Albemarle Sound, in the center of Figure 45.

Predominately quartz sediments of glacial origin produce cross shore bottom gradients having one of three matching profile segments:

1) stationary profile that extends from deep water in the mid-continental shelf region, inshore to closure depth h_c, where profile changes become vanishingly small,
2) shorerise profile that continues from closure depth to the wave break point; and,
3) bar-berm profile that begins at the break point and ends at the berm crest.

The stationary profile is invariant with time and is given by the regional bathymetry. Bottom elevation changes along the non-stationary profiles of the shorerise and bar-berm (
Figure 46a) are computed by (code module #10) in the farfield response module (blue box) using equilibrium profile algorithms after [10], [11], [12], [13], [14]. The stationary and non-stationary profiles are interpolated to create a Cartesian depth grid within each littoral cell on which simultaneous refraction and diffraction patterns are computed by (code module #6) using algorithms from [15], [16] to specify fluid forcing by shoaling waves.

Fluid forcing by currents in the farfield are computed in (code module #7) where wave induced streaming and mass transport are based on algorithms after [17], [18], [19] and shallow water tidal currents follow from algorithms after [20]. Fluid forcing time series and bottom elevations computed in the farfield response module are through-put to the nearfield response modules shown below the green line in Figure 44. The farfield throughput is applied to the local seabed boundary conditions module (gray box). These local boundary conditions include two types: 1) the slope and elevation of the seabed plane around the object base derived by (code module #11) from location in the farfield control cell; and 2) the shape file of the body in question (code module #12). These two local boundary conditions are used to generate lattice panels by (code module #13) that define the object and bedform of the surrounding seabed (
Figure 46a). This lattice is the computational domain of the nearfield scour-burial processes in which the method of embedded vortex singularities (vortex lattice method) is applied in (code module #14) using algorithms after [21], [22], [23]. This method employs horseshoe vortices embedded in the near-bottom potential wave oscillation to drive local sediment transport in (code

module #15) based on ideal granular bed load and suspended load equations after [24], [25], [26], [27]. A horseshoe vortex is specified by code module #14 for each lattice panel during every half-cycle of the wave oscillation; the image method for vortex induced velocity at any point near the bed is depicted in Figure 47. The horseshoe vortices release trailing pairs of vortex filaments into the local potential flow field that induce downwash on the neighboring seabed (Figure 47b), causing scour with associated bed and suspended load transport as computed by (code module #15). This scour action by trailing vortex filaments can be seen occurring in nature in Figure 48.

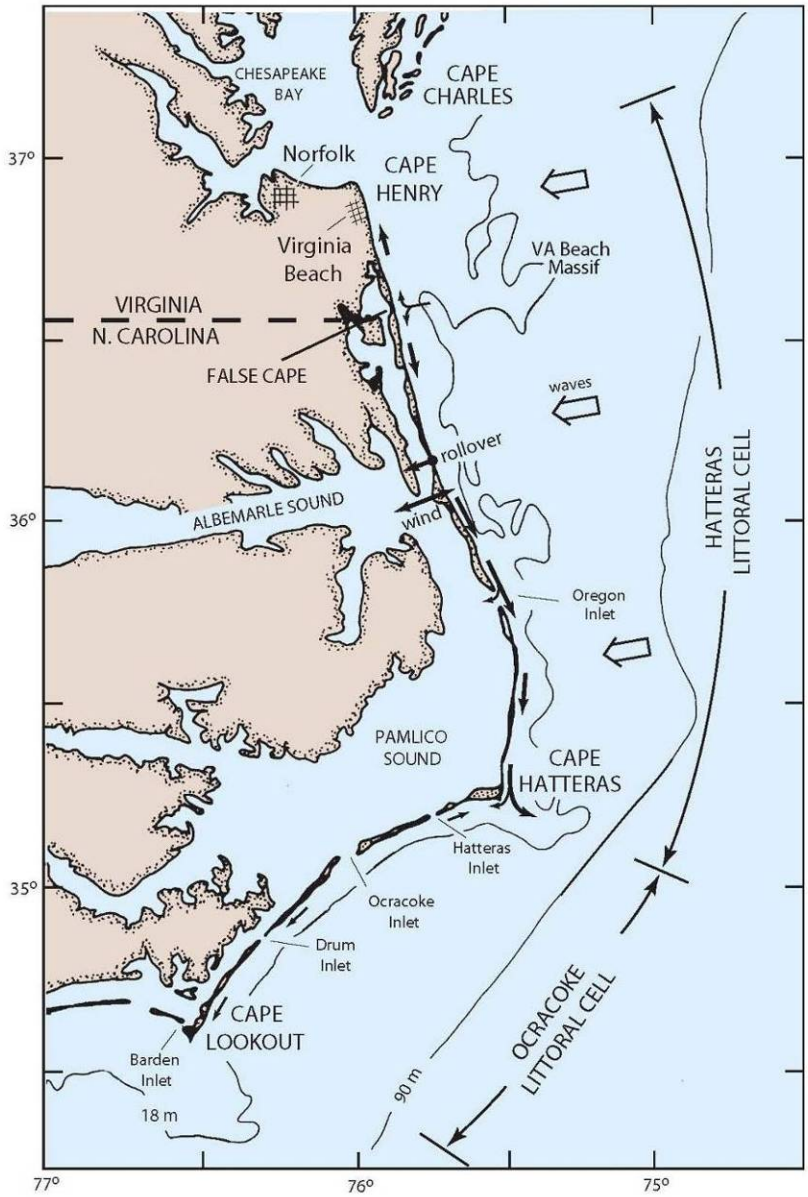

Figure 45. Hatteras and Ocracoke littoral cells along the outer banks of North Carolina.

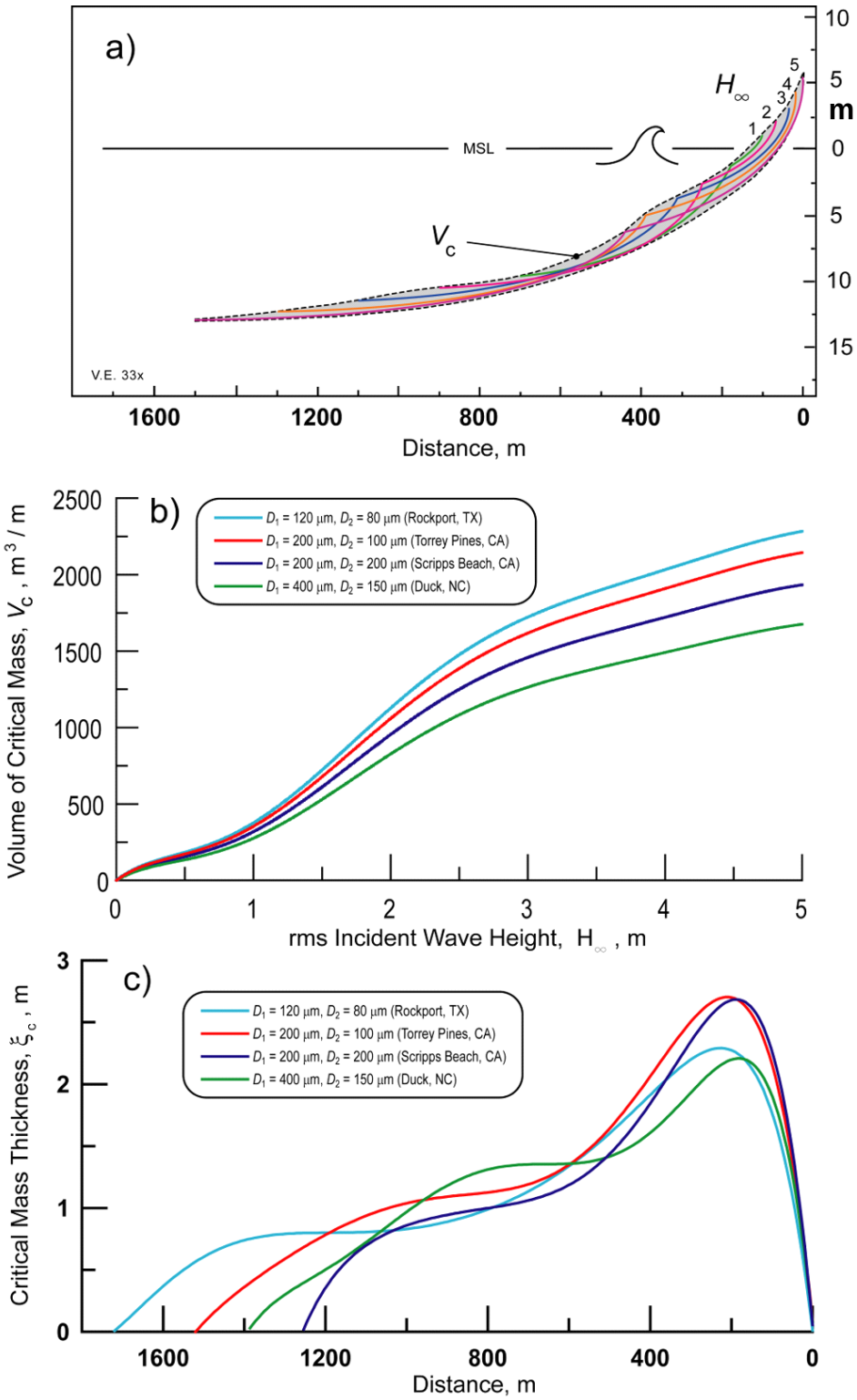

Figure 46. Critical mass cross-section (a), volume (b), and thickness versus distance (c).

The lattice generation in (code module #13), horseshoe vortex generation in (code module #14) and sediment transport computations in (code module #15) are implemented as leap-frog iterations in a time-stepped loop shown by the red and blue pathway arrows at the bottom of Figure 44. The leading time step (delineated by the red arrow pointing from code modules #13 to #14) computes the strength of the horseshoe vortex filaments generated by the pressure gradients and shear setup over the lattice panels of the combined body-bedform geometry of the previous (lagging) time step. The bed and suspended load transport induced by these filaments results in an erosion flux from certain neighboring lattice panels on the seabed and a deposition flux on others, based on image lifting line theory (Figure 47a) as first applied in Jenkins and Wasyl [28] to a mobile sedimentary boundary. The erosion and deposition fluxes of the leading time step are returned in the computational loop to the lattice generator (blue arrow) where those fluxes are superimposed on the lattice geometry of the lagging time step. That superposition produces a new lattice geometry for implementing the next leading time step. With this leap-frog iterative technique, an interactive bedform response is achieved whereby the flow field of the leading time step modifies the bedform of the lagging time step; and that modified bedform in turn alters the flow field of the next leading time step. This lead and lag arrangement is based on the fact that the inertial forces of granular bed near incipient motion are large compared to those of the fluid [24], hence the flow field responds faster to a change in bedform than the bedform can respond to a change in flow field. The codes for (code module #1) through (code module #15) have been linked end-to-end in the latest generation of the MM found in Appendix A.

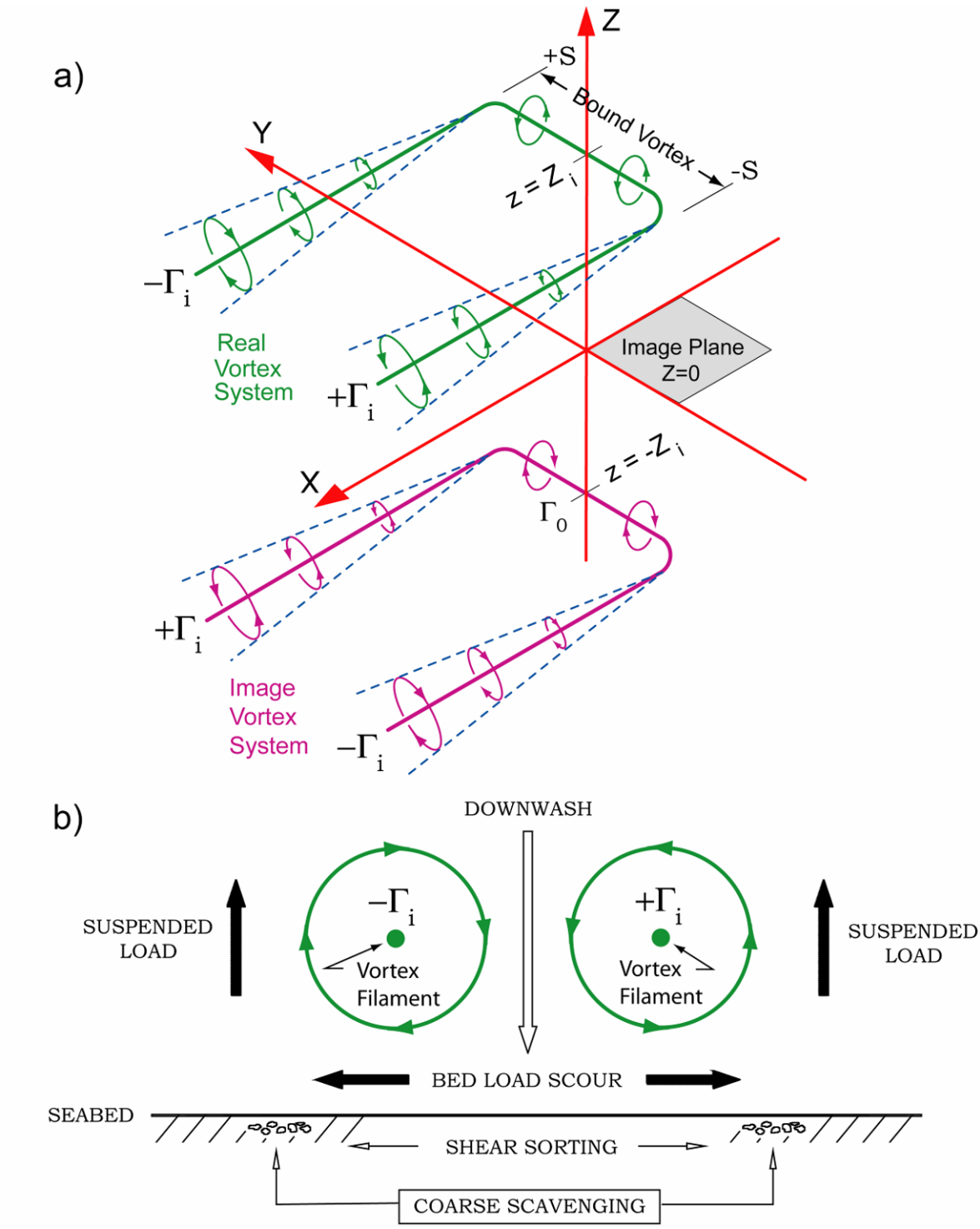

Figure 47. Vortex induced velocity at any point near the bed: (a) image plane due to the horseshoe vortex system of an imaginary lattice plane, (b) schematic in the vertical plane.

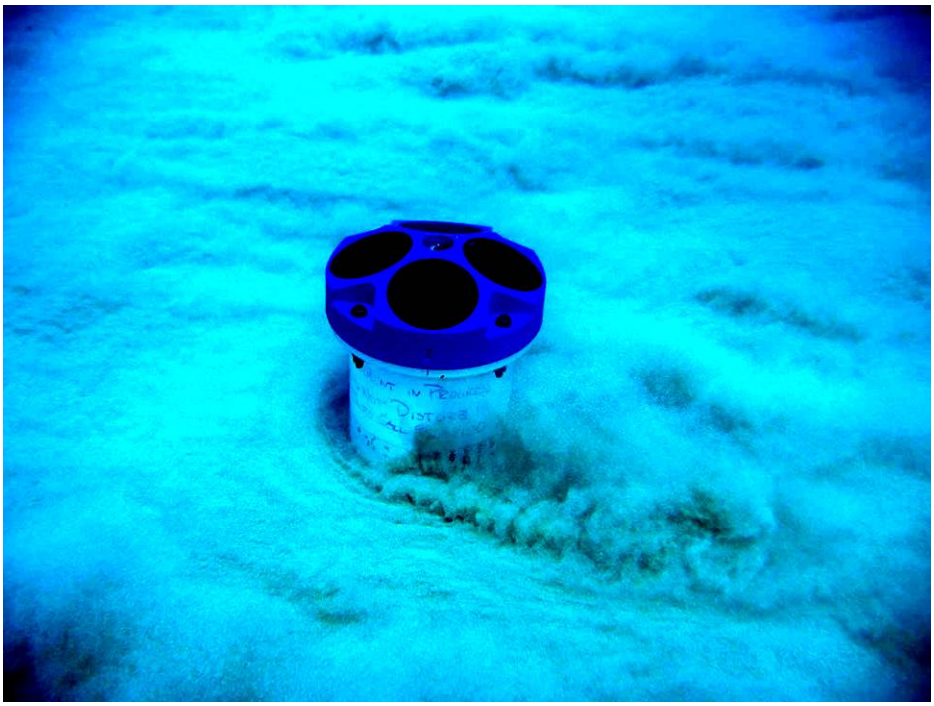

Figure 48. Vortex shedding around the ADCP, a vertical cylinder.

4.2 Model Initialization

4.2.1 Farfield Initialization

Farfield initialization involves data base constructions and model parameterizations for model inputs above the orange line in Figure 48. A detailed listing of these inputs can be found in [3]. They are reviewed here in context specific or unique to the FRF site.

4.2.1.1 Bathymetry and Construction of Farfield Grid

The stationary farfield bathymetry was derived from the NOS digital database compiled by the National Geophysical Data Center [8], [9], and was subsequently assembled in a far field grid as contoured by the white lines in
Figure 49. Depth contours are labeled in yellow based on meters below the 0 m mean sea level (MSL) contour. This coarse-scale bathymetry defines the basic shelf and nearshore morphology of the Outer Banks littoral system, including the Hatteras Littoral Cell and the Ocracoke Littoral Cell, where FRF is located in the Hatteras Littoral Cell north of Oregon Inlet (cf. Figure 45) at the place designated by the green star in Figure 49. The system of barrier islands and sand spits that control the beach and shoreline dynamics of this highly variable littoral system are defined by the 0 m MSL contour, evident in the satellite photo in the inset at the lower right hand corner of
Figure 49. The far field grid is assembled from a 2,401 x 2,401 point array (5,764,801 grid points) formatted by latitude and longitude using 3 x 3 arc second grid cell resolution and yielding a computational domain of 168.1 km along the x-axis (longitude) and 222.3 km along the y-axis (latitude). This is the largest grid on which the MM has computed UXO transport and burial to date, and was necessitated by the broad-scale longshore fluxes of sediment and mass exchange occurring between the Hatteras and Ocracoke Littoral Cells.

The small amount of grid distortion between x- and y- length scales in the farfield grid is compensated internally during a transformation to Cartesian coordinates using a Mercator projection centered on FRF. For the non-stationary bathymetry data inshore of closure depth (less than -12 m MSL) we use the equilibrium beach algorithms from Jenkins and Inman [16]. Depth contours generated from these algorithms vary with wave height, period and grain size and are contoured in
Figure 49 for the range of wave parameters measured at the FRF site (at the locations shown in Figure 50) for the two largest storms occurring during the UXO experiment (Figure 51 and Figure 52).

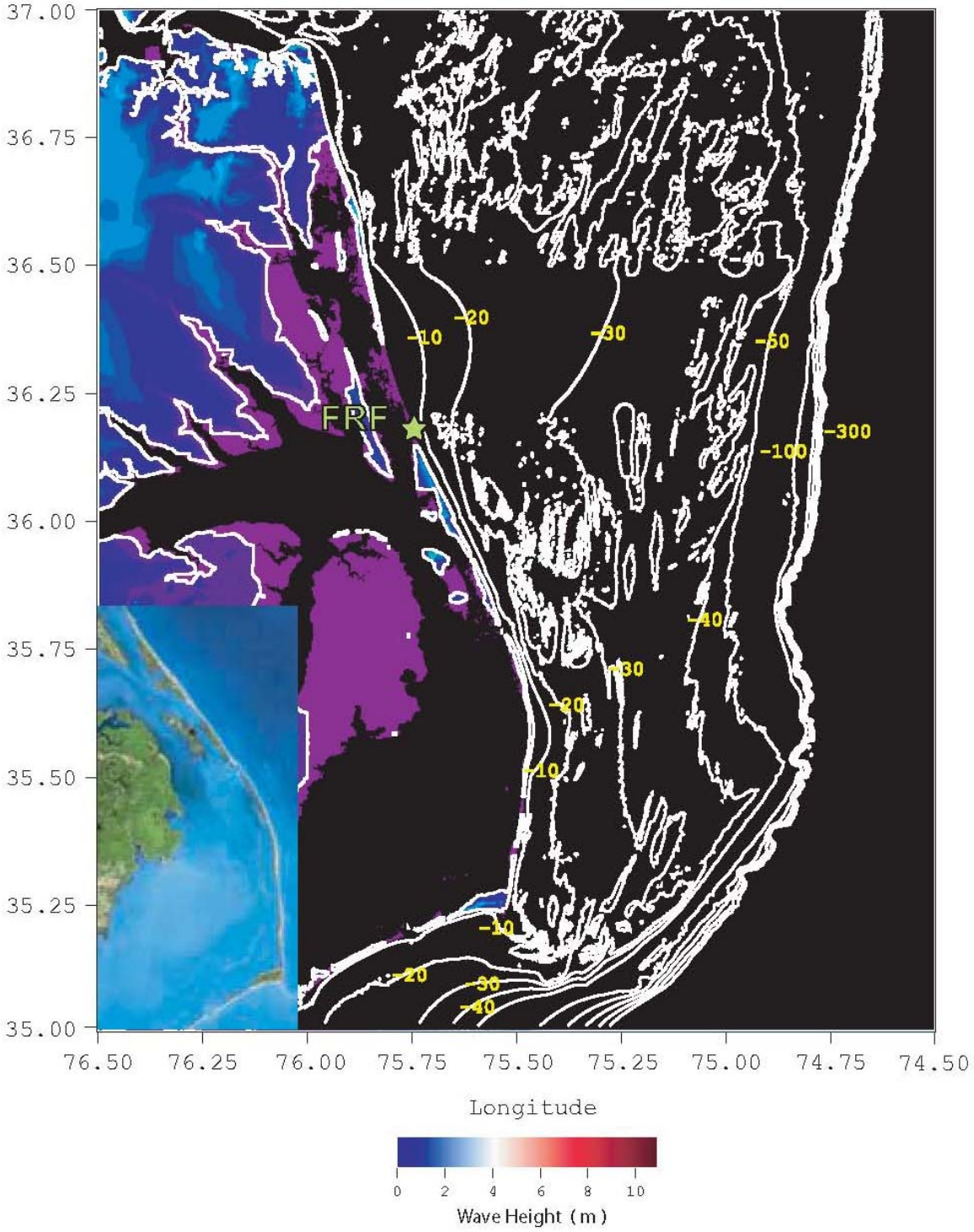

Figure 49. Regional bathymetry off of the Field Research Facility (FRF), Duck, NC, used for the littoral cell and refraction/diffraction analysis.

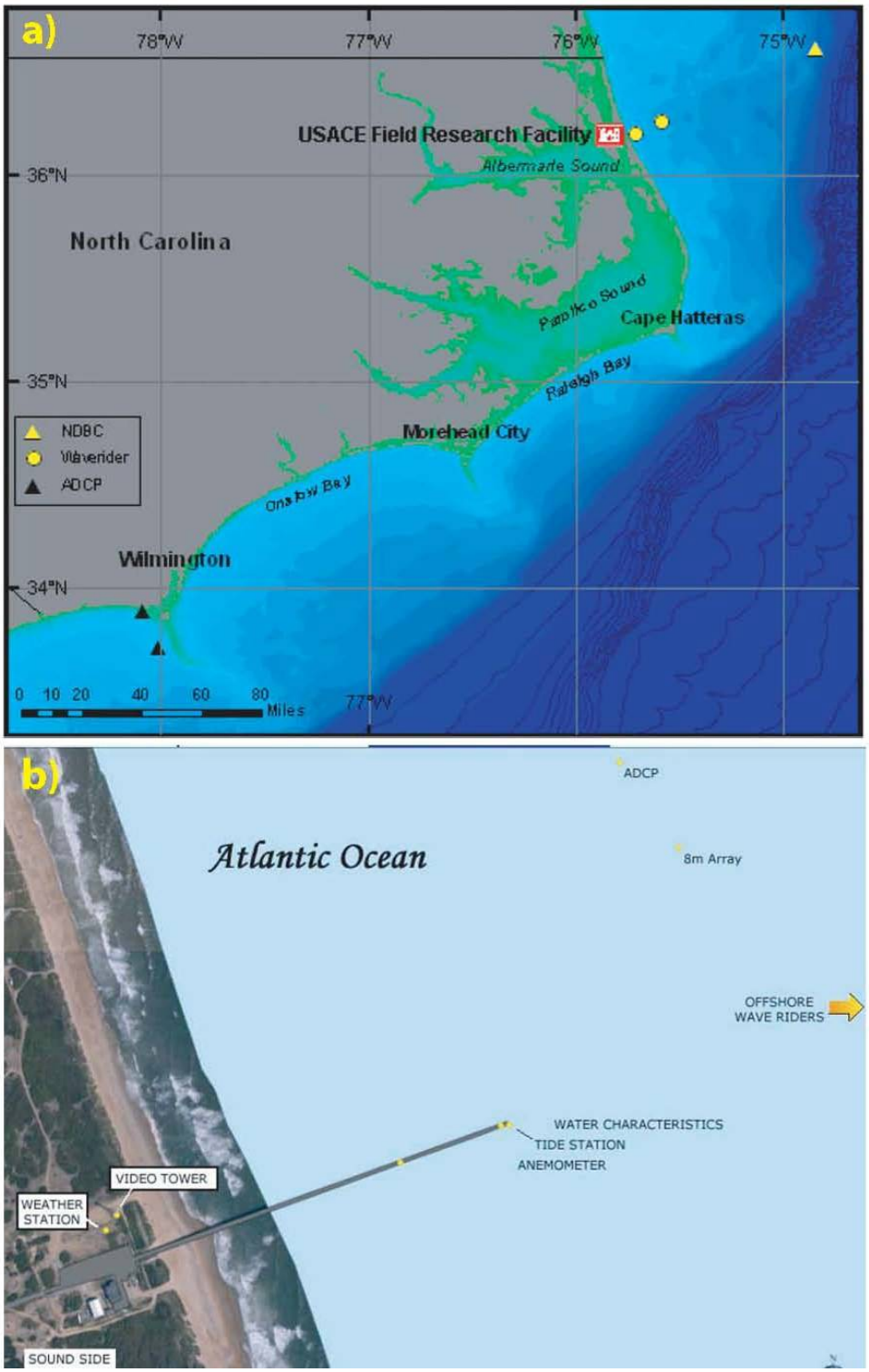

Figure 50. Wave measurement buoys and other instrumentation locations offshore of FRF.

While Figure 49 defines the broad-scale morphology of the shelf and barrier island system of the Outer Banks, the micro-bathymetry of the near-shore bar system in which the UXO were placed was resolved with high resolution survey data taken monthly by the routine beach monitoring program maintained by FRF using their CRAB. These surveys were used to calibrate the elliptic cycloid algorithms of the model to predict profile evolution over the duration of the simulation, 22 June 2005 to 16 February 2006.

The UXO surrogates were placed in two groups (inshore group and offshore group) along two cross-shore parallel lines next to FRF profile range lines # 76 and # 85. During the first two months of the deployment, (July and August 05) there were only small profile changes along these two range lines (
Figure 53) as the wave climate was dominated by benign short period summer wind waves (Figure 52). During the September through November 2005 time frame, several moderate early winter storms brought waves up to 3m height (Figure 51 and Figure 52), resulting in the development of complex longshore bar and trough bed forms (
Figure 54). The type-b cycloid algorithms in the MM were found to give the best fit to the profiles having these bar-trough bed forms. The type-b cycloid has been built into the G-95/ FRF version of the VORTEX code (Appendix-A) using the general solution algorithm:

$$h = \frac{\pi\varepsilon\, x}{2I_e^{(1)}}\left(\frac{1-\cos\theta}{\theta-\sin\theta}\right) = r\left(1-\cos\theta\right) \qquad (1)$$

Here h is the local depth; x is the on-off shore position; r is the radius vector measured from the center of the cycloid ellipse whose semi-major and semi-minor axes are a, b; e is the eccentricity of the cycloid ellipse given by $e = \sqrt{1-b^2/a^2}$; $I_e^{(1)}$ is the elliptic integral of the first kind; and θ is the angle of rotation of the cycloid, (see Jenkins and Inman, 2006, [16] for more details). The cycloids are given by the trajectory of a point on the circumference of an ellipse that rolls seaward in the cross-shore direction under the plane of $h = 0$. This trajectory defines the elliptic cycloid and the segment traced by the first half of a rotation cycle ($0 < \theta < \pi$) of the rolling ellipse is the equilibrium beach profile.

The depth of water at the seaward end of the profile ($\theta = \pi$) is $h = 2b$ for the type-b cycloid. The length of the profile X is equal to the semi-circumference of the ellipse:

$$X = \frac{2bI_e^{(1)}}{\varepsilon} \cong \frac{\pi\, b}{\varepsilon}\sqrt{\frac{2-e^2}{2(1-e^2)}} \qquad \text{at } \theta = \pi \qquad \text{(type-b cycloid)} \qquad (2)$$

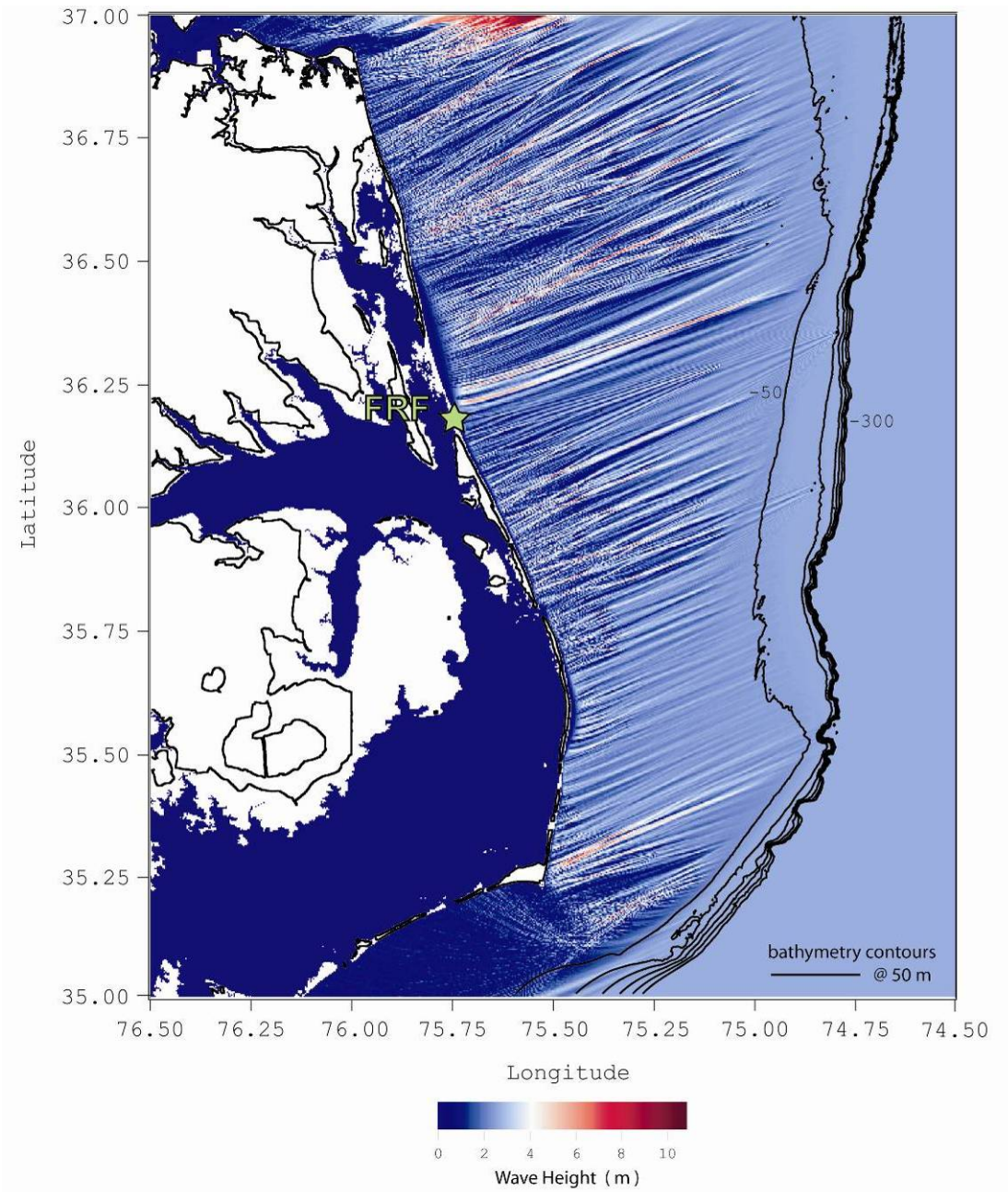

Figure 51. Refraction/diffraction pattern for storm of 25 October 2005, during UXO mobility experiment at FRF Duck, NC, where H = 3.12m, T = 10.5 sec, and α = 52deg.

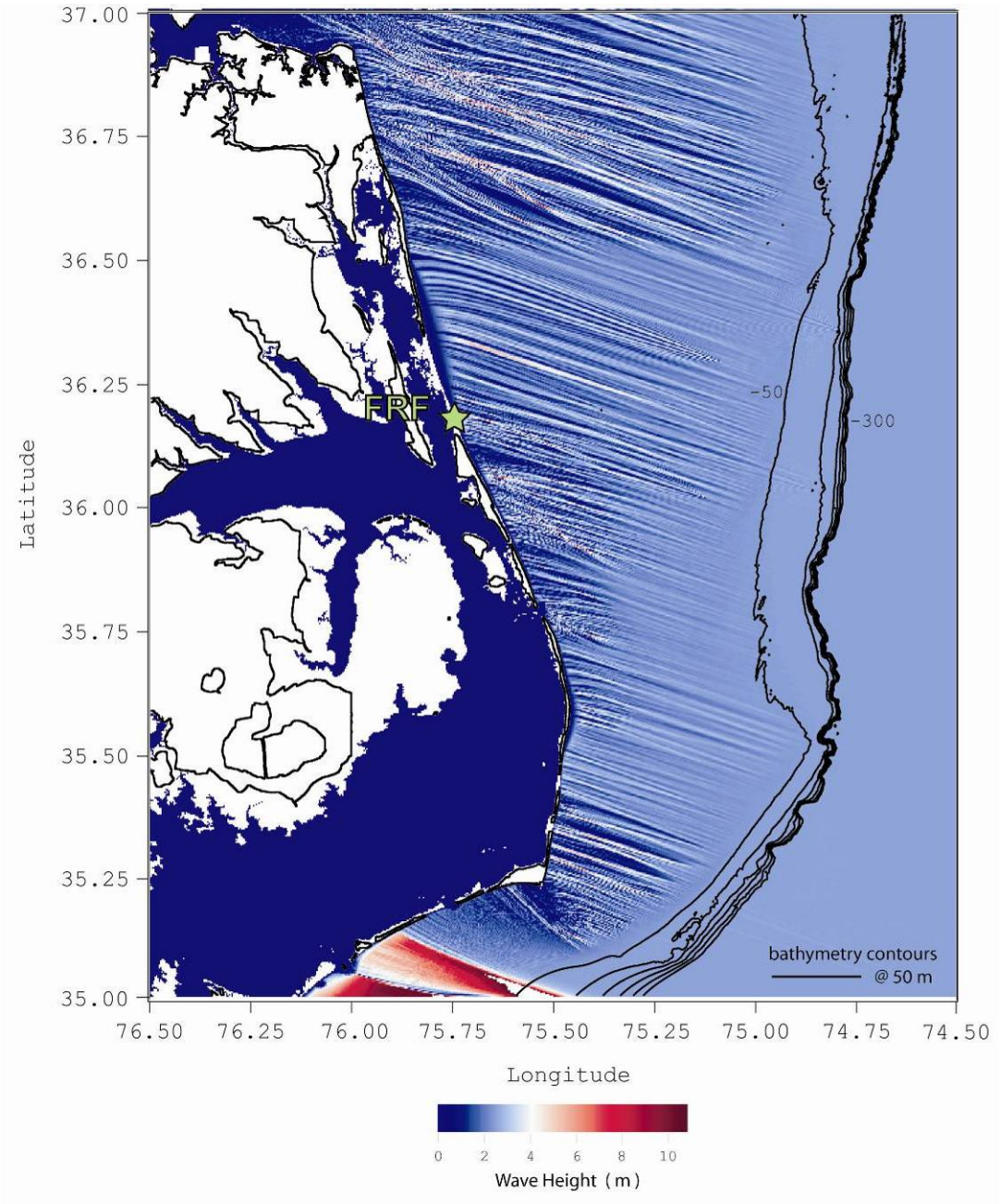

Figure 52. Refraction/diffraction pattern for storm of 16 September 2005 during UXO mobility experiment at FRF Duck, NC, where H = 2.96m, T = 9.1 sec, α = 11.6 deg.

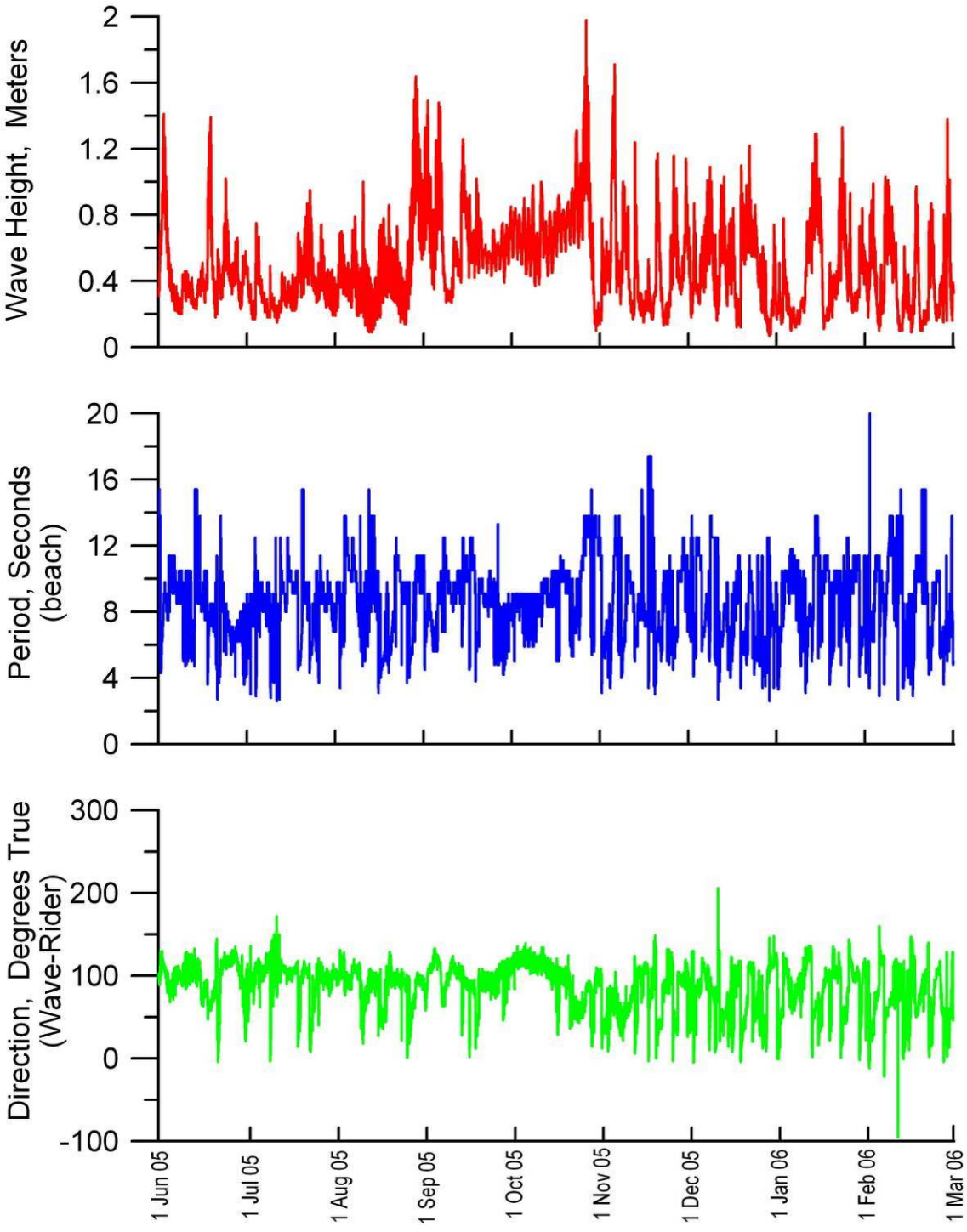

Figure 53. Wave data for Rounds 1-4, Field Demonstration, FRF, Duck, NC: (a) wave height in surf zone, (b) wave period, and (c) wave direction (1 June 2005- 1 March 2006).

The measured FRF surveys along FRF ranges lines #76 and #85 were used to calibrate the parameters (*e, b*) in equations (1) and (2) using a best fitting process that minimizes the mean squared error between the type-b cycloid and the measured profile.

An interesting feature of these calibrated cycloid profiles using the supporting survey data is that the closure depth was only $h_c \cong$ 6 m to 7m when normally it is about twice that value. The explanation for this beach profile anomaly was the unusually benign wave forcing that persisted throughout the experiment.

4.2.1.2 Wave and Current Forcing

Spatial variation in wave forcing over the barrier island system of the Outer Banks is derived from refraction/diffraction analysis over the far field grid as shown in Figure 51 and Figure 52, based on directional wave measurements from instrumentation maintained by FRF. This instrumentation includes a directional wave buoy in 17m water depth (Sensor #630), pier-mounted pressure sensors at 2m depth, (Sensor # 651) and an ADCP/ pressure sensor array installed at 8m depth (Figure 50). Figure 51 and Figure 52 use the directional wave buoy data as deep water boundary conditions in the calculation of the regional variation in the shoaling wave field based on refraction/diffraction analysis. Figure 51 provides spatial detail of the shoaling waves from an early northeaster storm occurring 25 October 2005, showing how the shelf bathymetry breaks up the incoming northerly waves into a series of directional beams along the Outer Banks.

Figure 52 shows the corresponding shoaling response to southerly waves generated along the leading edge of a trailing cold front that passed over the region on 16 September 2005. In either case, directional beams induced by the shelf bathymetry produced pronounced patterns in the nearshore of shadows (regions of locally smaller waves) and bright spots (regions of locally higher waves). Wave-driven nearshore currents flow away from bright spots and converge on shadows. The northerly waves in Figure 51 are found to produce considerable banding between shadows and bright spots immediately to the north of Duck Pier (where the UXO fields are placed between range lines # 76 and #85). The along shore variation in wave height between these shadows and bright spots produces considerable divergence of drift with associated rip cells and complex bar formations of the type shown in Figure 54.

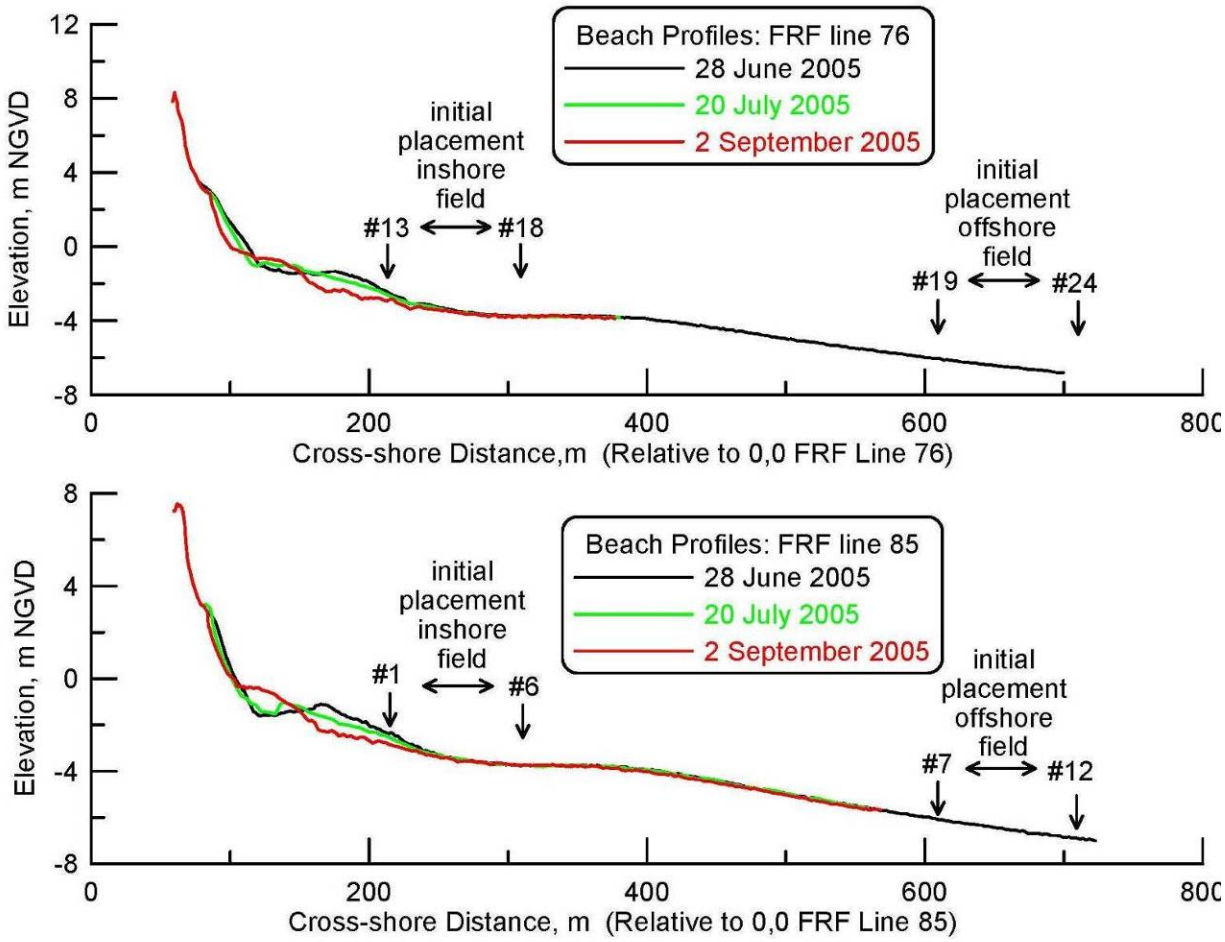

Figure 54. Beach profile variation during Field Demonstration, FRF Duck, NC, 28 June – 2 September 2005.

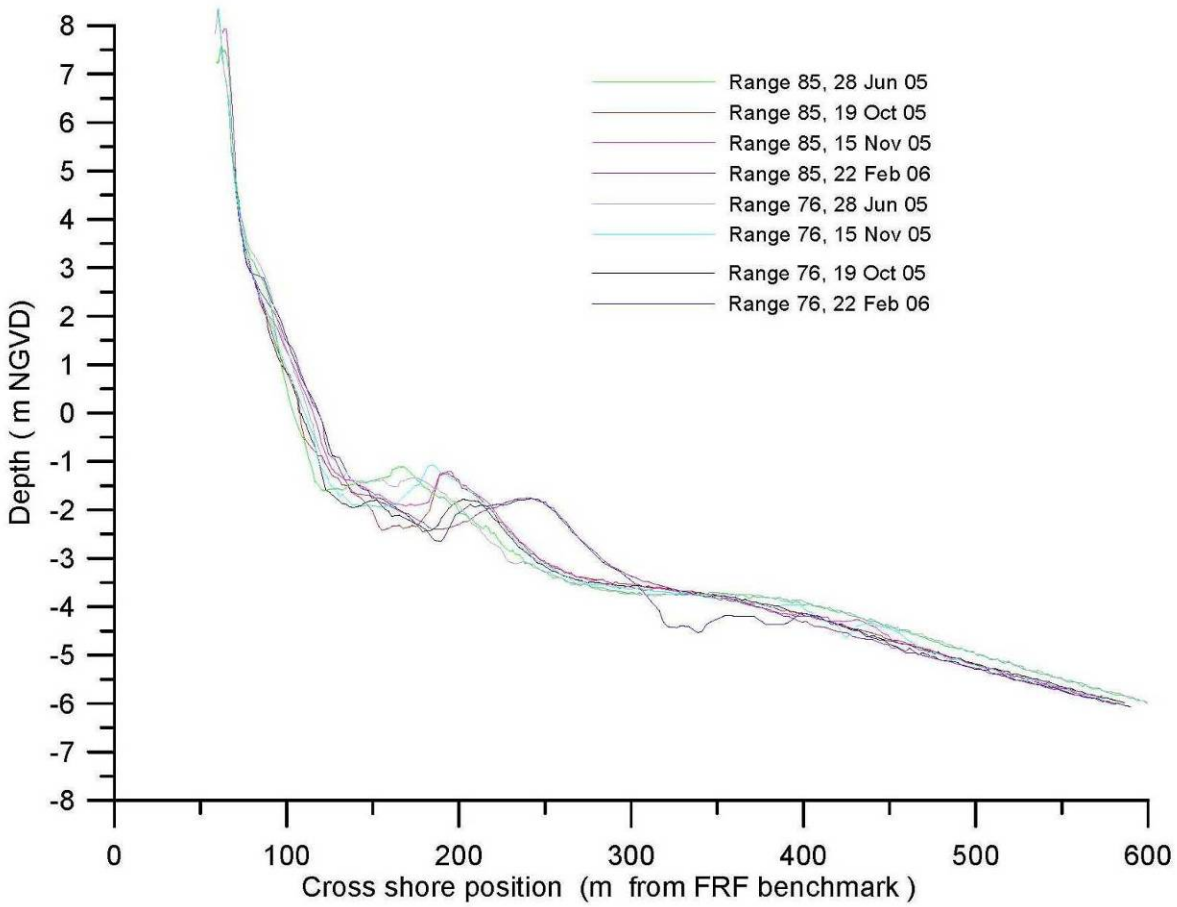

Figure 55. Beach profile variation during Field Demonstration, FRF, Duck, NC, 28 June 2005 – 22 February 2006.

Repeated wave shoaling computations with the buoy data (sensor #630) of the kind shown in Figure 51 and Figure 52, combined with the wave pressure measurements from Duck Pier (Sensor #651) allowed us to assembl an unbroken time series of wave height, period and direction (Figure 53) that spanned the full nine month deployment of the UXO experiment (Rounds 1-4). The most notable feature of this record was the occurrence of unusually small wave heights (Figure 53a) during the fall and winter months. Normally wave heights of 5 m – 8m are quite common along the outer Banks during this time of year. The benign wave climate encountered during the Rounds 1-4 of the UXO experiment was the essential environmental feature determining the nature of the outcome, an outcome that for the most part showed only modest movement of the UXO with deep burial.

4.2.2 Nearfield Initialization

Nearfield initialization involves data base constructions and model parameterizations for model inputs below the green line in Figure 44. A detailed listing of these inputs can be found in [3]. They are reviewed hereafter in specific context and with respect to the FRF site.

4.2.2.1 Sediment Parameters

The nearfield of the model was gridded as described in Section 1.1 for a fine to medium coarse sand bottom that was parameterized by 20 grain size bins according to the grain size distribution shown in
Figure 56. The cumulative distribution in this figure (blue line) reveals that the Duck sand is well sorted by the wave action, and mineral analysis indicates it is predominately quartz of glacial origin [29]. The median grain size is 565 microns, and 70 % of the sediment is comprised of medium-coarse sand between 450 microns and 750 microns. These sediment characteristics are well suited for the ideal granular relations used in the VORTEX Lattice Model, [2]. Based on these sediment grain sizes (
Figure 56), wave heights (Figure 53), and UXO placements on the active beach profile (
Figure 55), The thickness of the critical mass (depth of permanent entombment) is $\xi_c = 220$ cm for the inshore UXO group; $\xi_c = 140$ cm for the offshore group; and the critical mass of sand (volume of sand that must be removed to expose buried UXO) is $V_c = 600$ m^3 to 1200 m^3 per meter of shoreline (Figure 47).

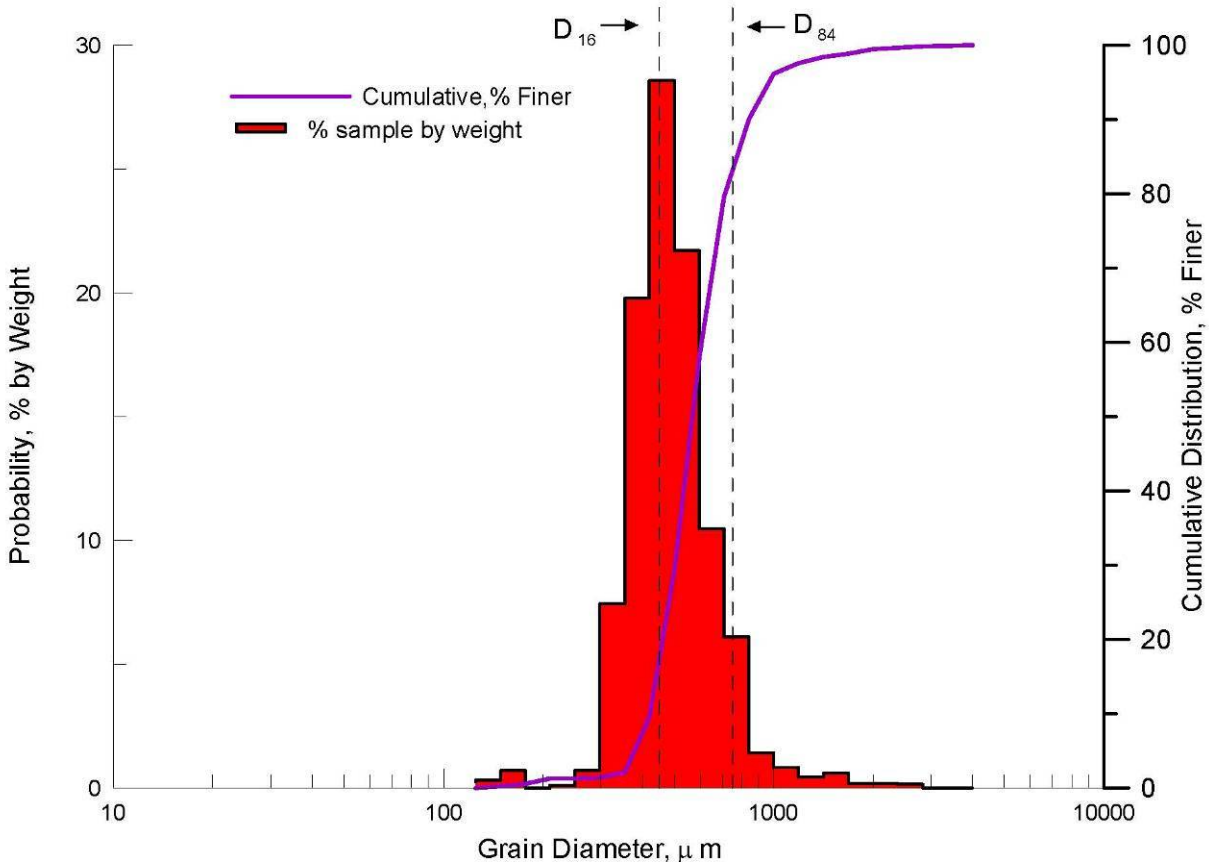

Figure 56. Grain size distribution of sediment, FRF Duck, #B6-S1, 1 September 2005.

4.2.2.2 UXO Shape Lattice

To provide a systematic and manageable set of inputs for shape specific calibration parameters we concentrated our model simulations on the 5”/38 Naval projectile shown in Figure 43. These rounds were approximated by an elliptic frustrum revolved about the major axis of the round, say the *y*-axis, taken for example as the transverse axis to the mean flow as shown in Figure 49. For this orientation the generalized shape of the round can be represented by the analytic expression:

$$R(y) = a - a\left(\frac{y}{S}\right)^{\beta} \qquad (3)$$

where $a = D/2$ is the basal radius and D is the basal diameter of the round; $R(y)$ is the local radius at any arbitrary location y along the major axis of the round; S is the total length of the round as measured along the y-axis; and β is a constant that adjusts the pointedness of the round. A best fit of equation (1) to the 5”/38 round using the dimensions shown in Figure 7

found that β =3.5. To accommodate these dimensions and the small radius curves of the shape, the MM shape lattice file was gridded for 3mm grid cells. The dry bulk mass of the 5”/38 surrogate rounds was nominally $\rho_s V_0 g = 22.8$ kg.

4.2.2.3 Burial and Migration from Mode 1 Analysis

Prior to considering the influence of the local bathymetry and forcing history on the burial migration response of the UXO, we test the model in Mode 1 using the UXO shape lattice files on the Duck grain size distribution for a flat planar bed with constant wave forcing. Figure 57 presents the modeled instantaneous vortex and scour field produced from a 5”/38 UXO resting proud on the bed with the major axis aligned transverse to a train of monochromatic waves with 12 sec period propagating from right to left. The wave oscillatory velocity amplitude at the top of the bottom boundary layer is 100 cm/sec. This velocity amplitude corresponds to the super-critical transport regime [2] for the grain size distribution in Figure 56. In this regime, flow separation with a basal vortex is observed on the down-wave (shoreward) side of the UXO, inducing formation of a scour hole. As the scour hole deepens, the round slips or rolls into the hole, resulting in migration and burial through what is known either as a *scour and slip* or *scour and roll* burial sequence [2], [11], [13], [14], [21]. At the instant the flow field in Figure 57 was calculated, the burial/ migration progression of the UXO had advanced to a state of 64% burial in a medium-coarse sand bottom.

At an advanced stage in the burial/migration progression referred to as *lock-down,* burial becomes sufficiently extensive that migration is no longer possible [28], [29], [30]. Note that full entombment occurs only after the UXO is fully buried to a depth that precludes further movement except in extreme conditions. For excitation by monochromatic waves of various periods and heights, the distance a UXO migrates before lock-down occurs has a monotonic dependence on a parameter of dynamic similitude referred to as the Shield’s parameter. This parameter, which combined with the grain Reynolds number, is now recognized as a reliable predictor of whether or not a grain will erode, is a measure of the flow inertia relative to the inertia of the UXO. Explicitly, the Shields parameter, Θ , or dimensionless shear stress, represents a ratio between the hydrodynamic forces (drag and lift) acting to move the UXO and the gravitational forces acting to restrain and bury the UXO, where

$$\Theta = \frac{u^2}{g'D} \qquad (4)$$

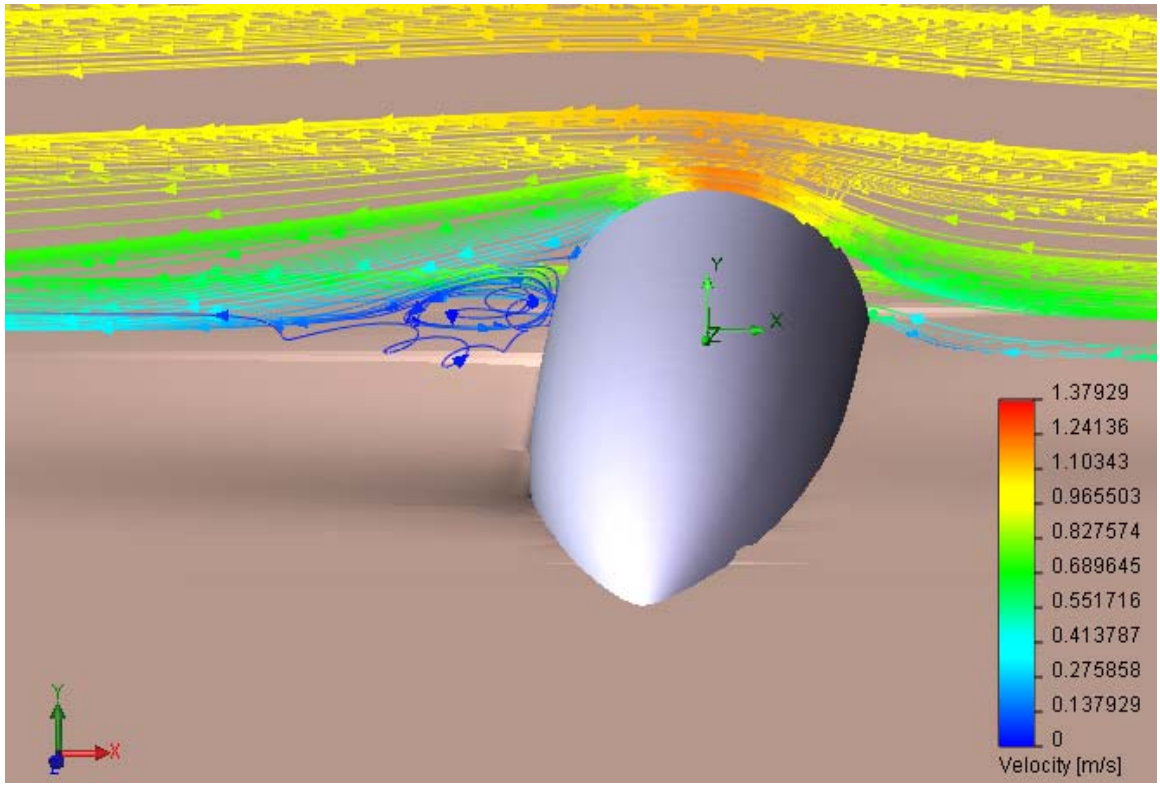

Figure 57. Vortex and scour field from a Mode 1 simulation of the 5”/38 UXO surrogate.

In equation (4), u is the oscillatory wave velocity amplitude at the top of the bottom boundary layer; D is the basal diameter of the UXO; g is the acceleration of gravity; $g' = g(\Delta\rho / \rho)$ is the reduced gravity; and $\Delta\rho = \rho_s - \rho$ is the density difference between the UXO and seawater density, ρ. Flat bed simulations of the type shown in Figure 57 show that UXO mobility increases with increasing wave velocity (proportional to wave height and inversely proportional to wave period); with decreasing caliber of the UXO; or with decreasing density (specific gravity) of the UXO.

For shallow water waves in the typical Outer Banks period band of 9 sec to 12 sec, Mode 1 analysis shows there is little burial or migration of the 5”/38 UXO for wave heights less than 0.4 m (sub-critical regime), see [28], [29], [30], [31] for more details on sub- and super-critical transport regimes. Once wave height exceed 1.2 m, migration and burial proceed rapidly (super-critical regime) until burial lock-down arrests further migration. At that point, further migration is only possible if broad scale bed erosion of the bed reduces the degree of burial. Recurrence analysis of the wave height time series in Figure 53 indicates that wave heights were sub-critical 48.8% of the duration of the deployment during Rounds 1-4 of the UXO experiment at FRF, Duck NC, and that super-critical conditions persisted only 5.4% of that deployment due to the benign nature of the wave climate. Thus, the observed migration was the result of relatively rare super-critical wave events, and only some of those events would actually move the UXO because super-critical waves had to occur concurrently with beach profile shifts in order to re-expose the UXO and release them from burial lock-down. These kinds of temporal interplay can not be resolved by the simple Mode 1 analysis in Figure 57; but rather depend on the history of the wave forcing and burial/migration response. We investigate those temporal relationships and their statistics of recurrence in the following section.

4.3 UXO Migration/Burial Model Performance at FRF Demonstration

The model performance in Mode 3 is tested against data from two separate UXO sites deployed at FRF, Duck, NC, between 22 June 05 and 15 February 06. Figure 62 gives the details of the lay-down pattern in relation to the FRF Research Pier and the local bathymetric features. Twelve UXO surrogates of a 5”/38 naval round were deployed at each of the two test sites for a total of 24 surrogates. The in-shore field (surrogate #s1-6 and #s13-18) was located on the north side of the FRF Pier in a nominal depth of 2m to 3m MSL, while the off-shore field (surrogate #s 7-12 and #s 19-24) was laid at depths between 6 m and 7 m MSL. At both the offshore and inshore sites, surrogates were laid in two along-channel rows parallel to FRF survey range lines #76 to the north and #85 to the south (
Figure 59). The surrogates were set at nominally 20m spacing in the cross-shore direction, with six surrogates in each row. The surrogates were laid on 22 June 07 and thereafter the position and burial depths of each surrogate was measured at six intervals referred to as “Rounds”. Round One measurements were made on 27 June 2005; Round Two on 12 August 2005, Round Three on 20 October 2005, Round Four on 15 February 2006, Round Five on 26 July 2006, and Round Six on 3 August 2006. Both burial and migration were measured during Rounds One through Four. Thereafter, only burial was measured for a few selected surrogates. Since burial and migration are coupled phenomena, we focus our analysis and modeling validation on Rounds One through Four.

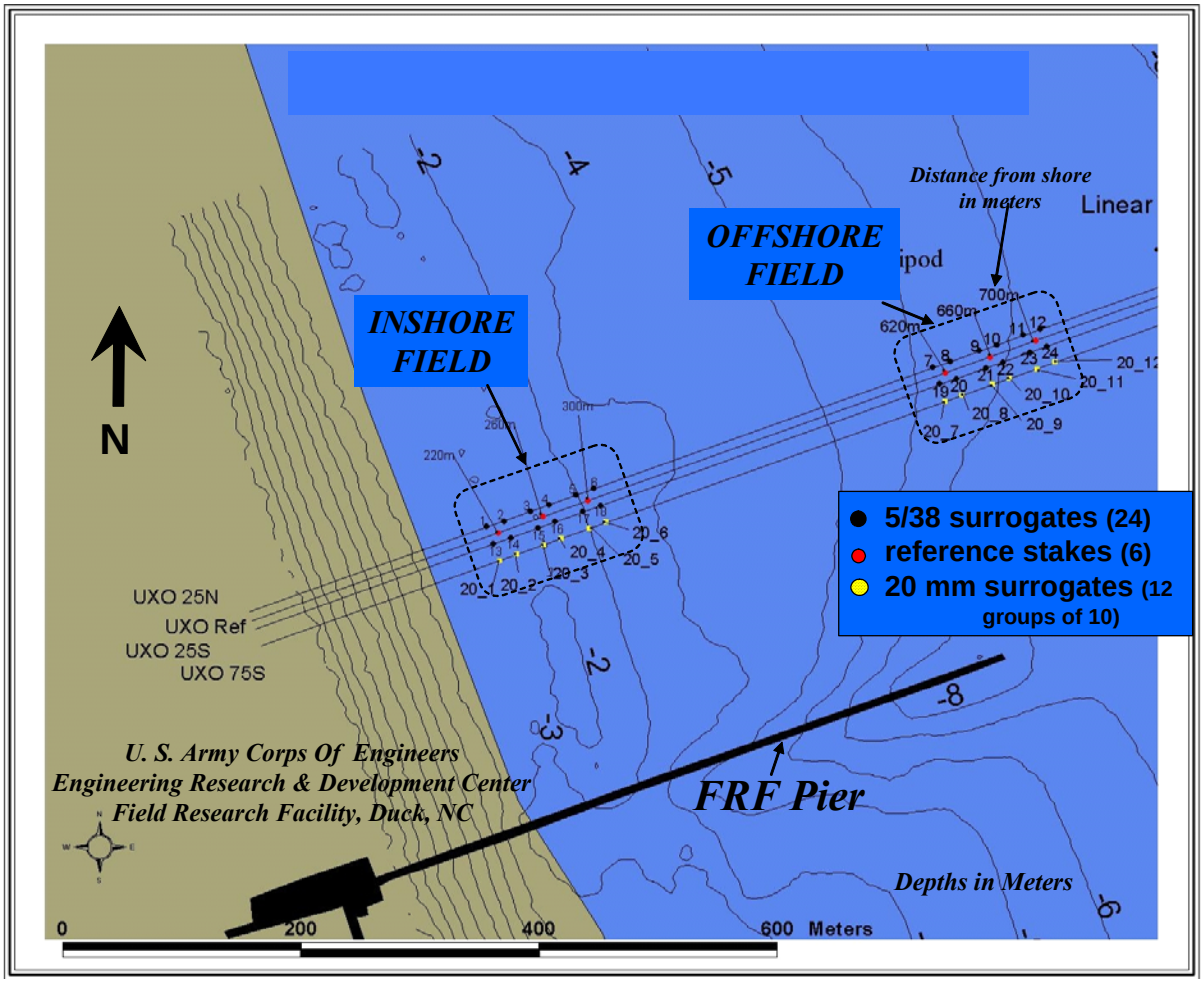

Figure 58. The lay-down pattern of the inshore and offshore fields (black dots signify 5”/38 surrogates, red dots denote reference stakes, and yellow dots are 20 mm surrogates).

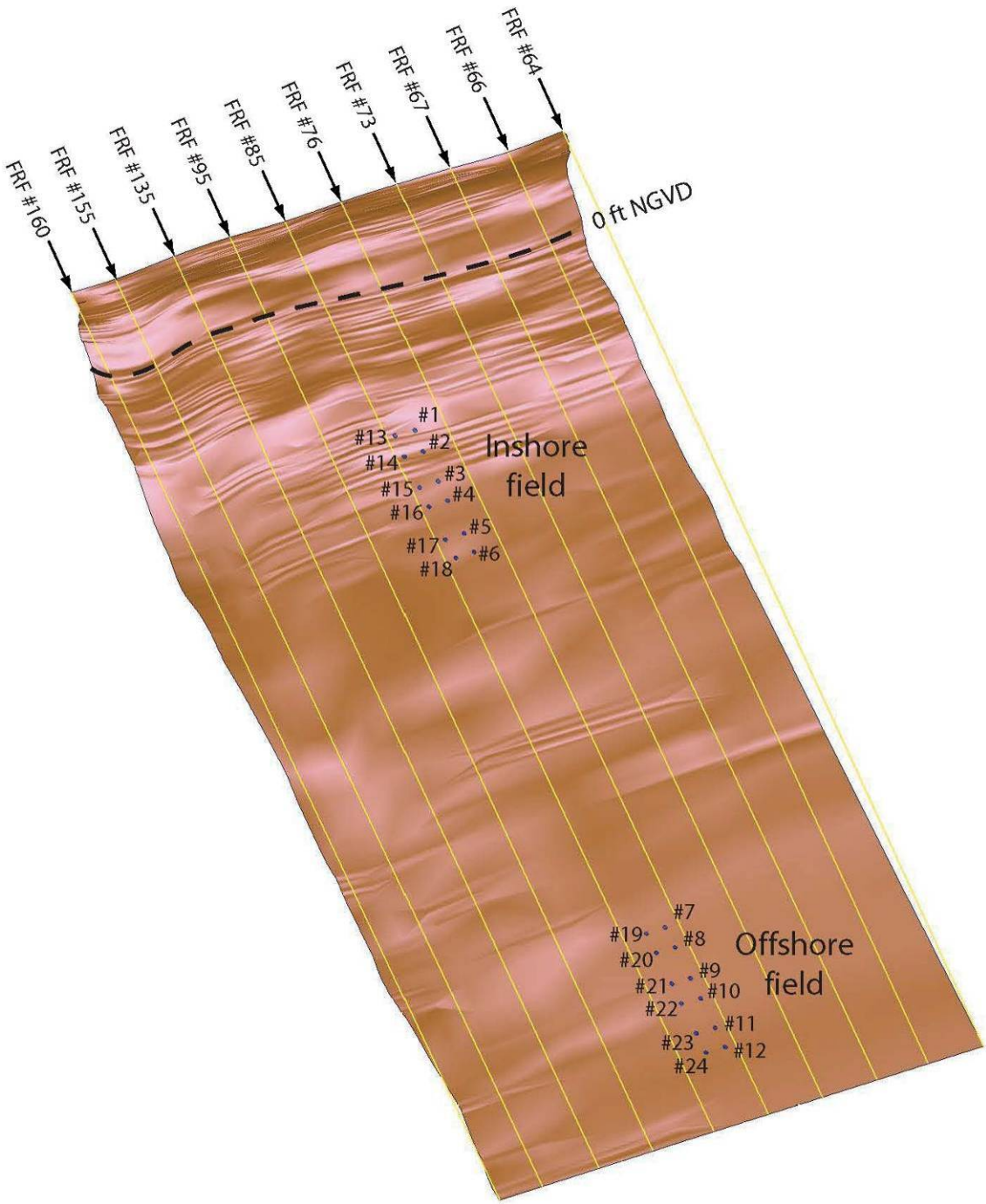

Figure 59. A 3D rendering of the surrogate deployment, FRF, Duck, NC, June 2005, shows the longshore expanse of bar systems from on-range profiles.

Because the surrogates all became buried during the experiment, the primary method for locating the surrogates was an acoustic ranging technique utilizing embedded pingers in the surrogates, each with a unique code for identification. Once the surrogate was located by its pinger, position was triangulated from distances measured to three reference stakes implanted in the seabed along the cross-shore axis of each group, as shown schematically in
Figure 60. Two distance measurement techniques were used, 1) tape measurements, and 2) acoustic ranging using a Benthos Model DRI-267A directional range finder. The accuracy of the acoustic ranging measurements were found to be within 5% of tape measurements of distances of 20m to 40m, or an uncertainty of typically less than 1m. Acoustic ranging was the predominant technique used to ascertain surrogate position throughout Rounds One through Four because it was faster to implement, while tape measurements were particularly difficult in the shallow inshore group where the tape would tend to stream out over curved paths in the wave surge.

Burial depths were measured manually by divers by probing into the bottom with a small diameter bar until refusal depth was reached. When this technique failed to obtain refusal depth once the surrogate became buried 1m or more, burial was calculated from elevation changes in the surveyed profiles at the location of the surrogate along FRF ranges #76 and #85 (cf. Figure 54). The largest profile changes that caused the deepest degree of burial were associated with the continuously evolving parallel bar systems that are ubiquitous in the near shore of the Outer Banks. Figure 59 shows the extent of the parallel bar system in the neighborhood of the surrogate fields based on a three dimensional reconstruction of the shore rise and bar berm from FRF beach profile surveys taken along FRF Ranges #64 - #160 at the time of the Round One measurements, 5 days after the initial installation. These bar systems migrated continuously throughout the remaining measurement cycles taken during Rounds Two through Four of the experiment, as evidenced by the profile variations in Figure 54, particularly in the neighborhood of the inshore group. The migration of these sand bars lead to episodic re-exposure of buried surrogates, leading to additional short periods of migration between the various measurements between Rounds One and Four.

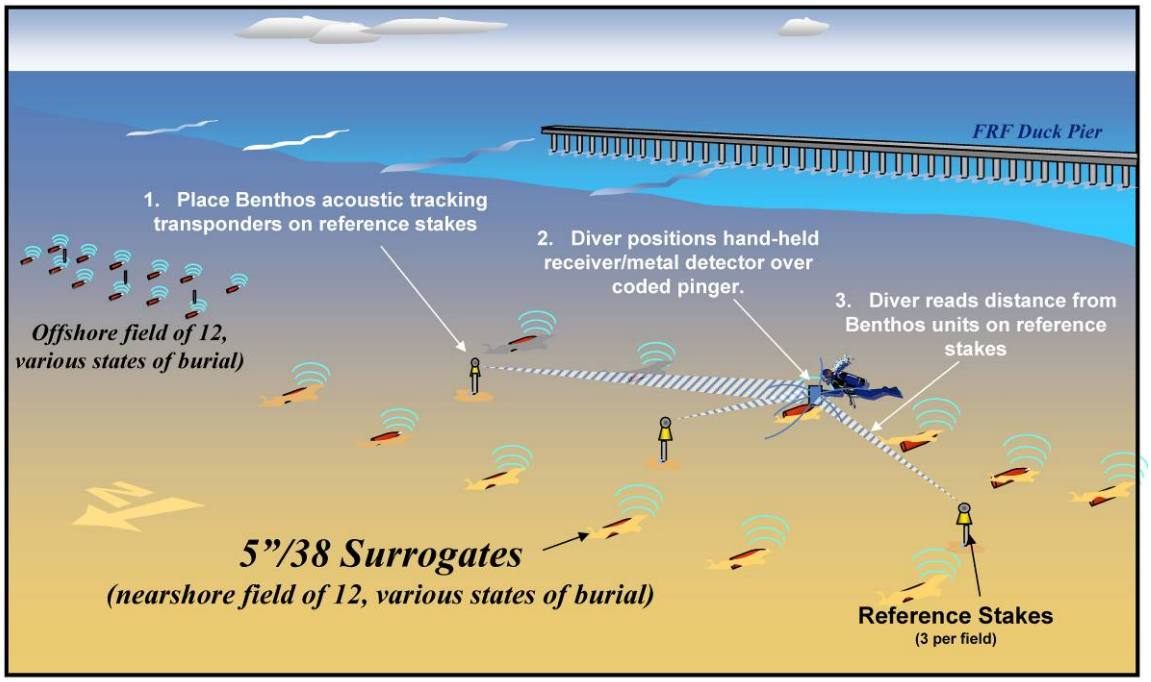

Figure 60. Schematic of acoustic directional ranging technique for locating surrogate positions during the FRF Field Demonstration.

4.3.1 Model Predictions of UXO Migration and Burial Rates

Migration and burial of each of the 24 UXO in the inshore and offshore test sites at FRF (Figure 59) were simulated by the MM in Mode 3 configuration using wave forcing from Figure 53, fine-scale bathymetry from Figure 54, Figure 55, and Figure 59 and the grain size distribution in Figure 56. The model computed burial and migration at time step intervals of $\Delta t = 20$ minutes.

Figure 61 and Figure 62 give the MM simulations of time evolutions of burial and migration for two of the most active 5"/38 UXO surrogates, #3 in the Inshore Group and #11 in the Offshore Group (cf. Figure 59). Figure 61 and Figure 62 show the time evolutions for these two surrogates during Round 1, 22-27 June 2005; Figure 63 and Figure 64 show the time evolutions during Round 2, 27 June-12 August 2005; Figure 65 and Figure 66 show the time evolutions during Round 3, 12 August - 20 October 2005; and Figure 66 and Figure 67 show the time evolutions during Round 4; 20 October 2005 - 15 February 2006. In each of these plots, migration distance (blue) and burial depth (red) are predictions of changes (in scalar lengths) relative to horizontal position and burial depth at the start of each round. For the start of Round One, the initial position and burial depth are taken as zero; thereafter, the starting horizontal position and burial depth are the end points of the preceding round. In each panel of Figure 61, the migration distance is read from the outer left-hand vertical axis; burial depth is read from the outer right-hand vertical axis; and wave height is plotted in gray according to the inner left-hand vertical axis. For the Inshore Group (Figure 61, Figure 63, Figure 65, and Figure 67), migration

was primarily along shore towards the north and south with the convention that transport to the south (in the direction of predominant littoral drift) is taken as positive, while movement toward the north is negative.

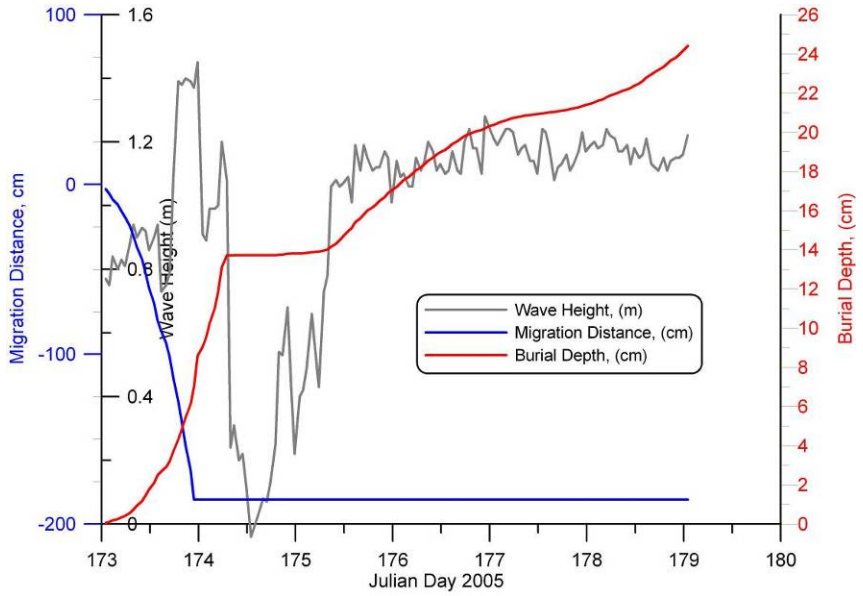

Figure 61. MM simulation of migration and burial sequence of 5”/38 surrogate #3, Inshore Group, Round One, FRF Duck, 22-27 June 2005.

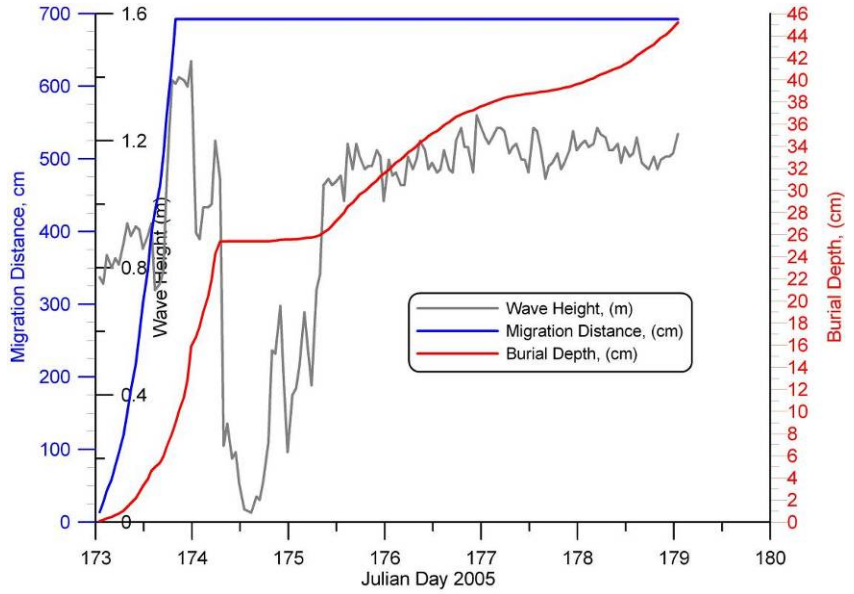

Figure 62. MM simulation of migration and burial sequence of 5”/38 surrogate #11, Offshore Group, Round One, FRF Duck, 22-27 June 2005.

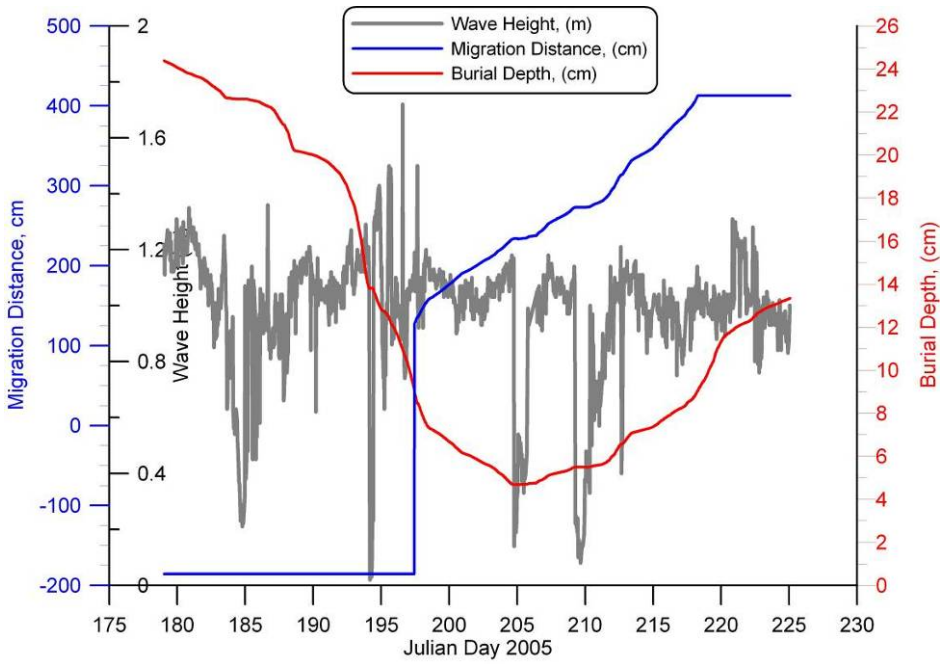

Figure 63. MM simulation of migration and burial sequence of 5”/38 surrogate #3, Inshore Group, Round Two, FRF Duck, 27 June – 12 August 2005.

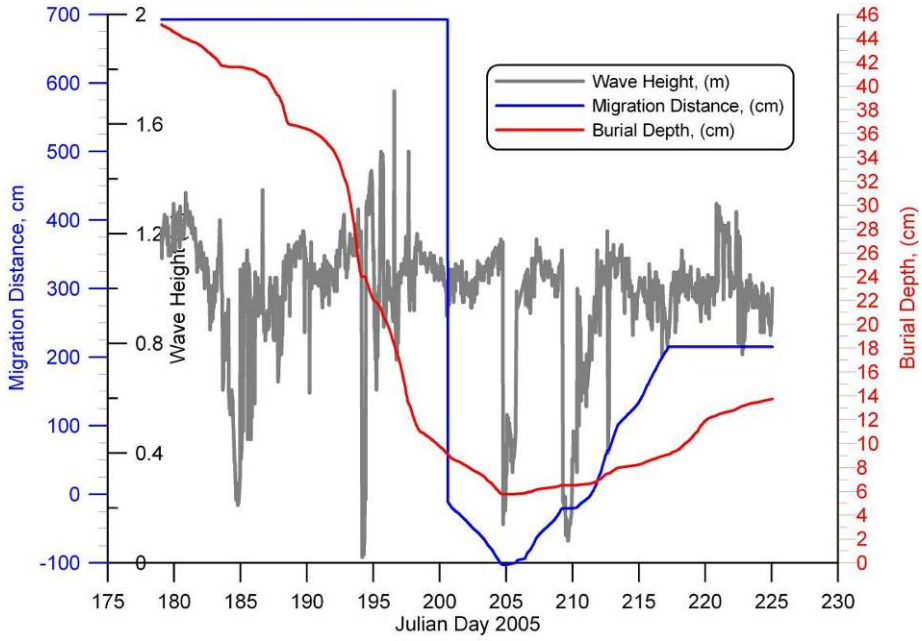

Figure 64. MM simulation of migration and burial sequence of 5”/38 surrogate #11, Offshore Group, Round Two, FRF Duck, 27 June – 12 August 2005.

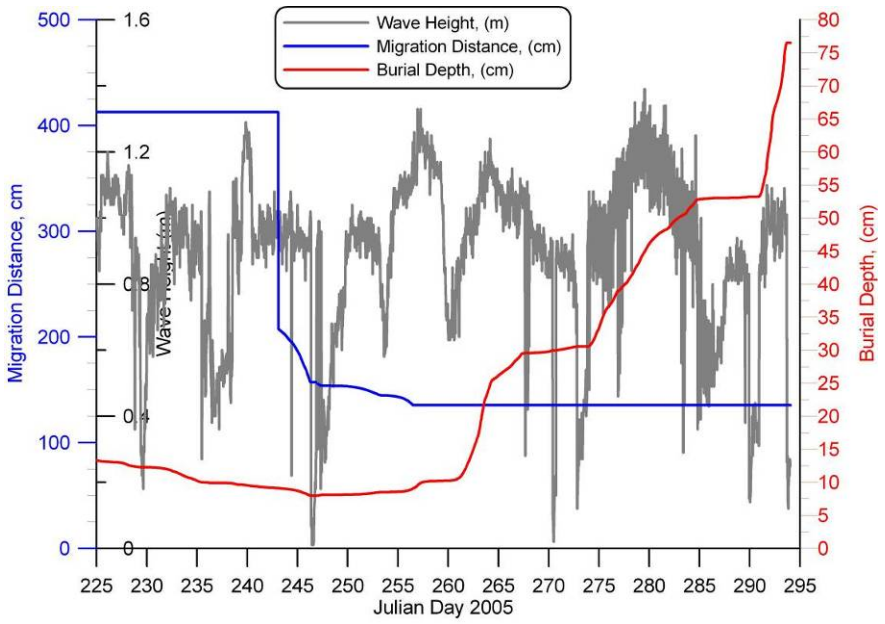

Figure 65. MM simulation of migration and burial sequence of 5”/38 surrogate #3, Inshore Group, Round Three, FRF Duck, 12 August – 20 October 2005.

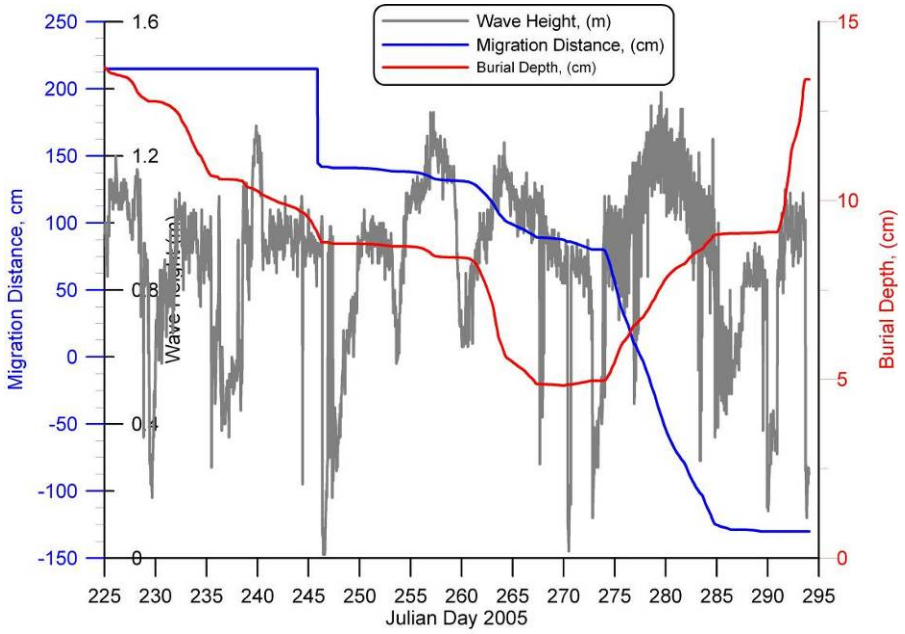

Figure 66. MM simulation of migration and burial sequence of 5”/38 surrogate #11, Offshore Group, Round Three, FRF Duck, 12 August – 20 October 2005.

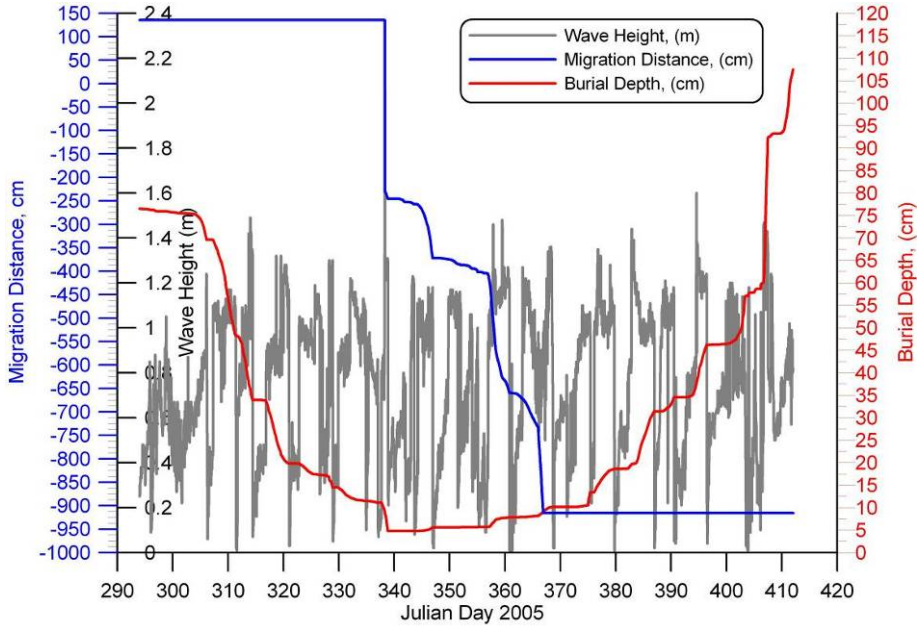

Figure 67. MM simulation of migration and burial sequence of 5”/38 surrogate #3, Inshore Group, Round Four, FRF Duck, 20 October 2005 – 16 February 2006.

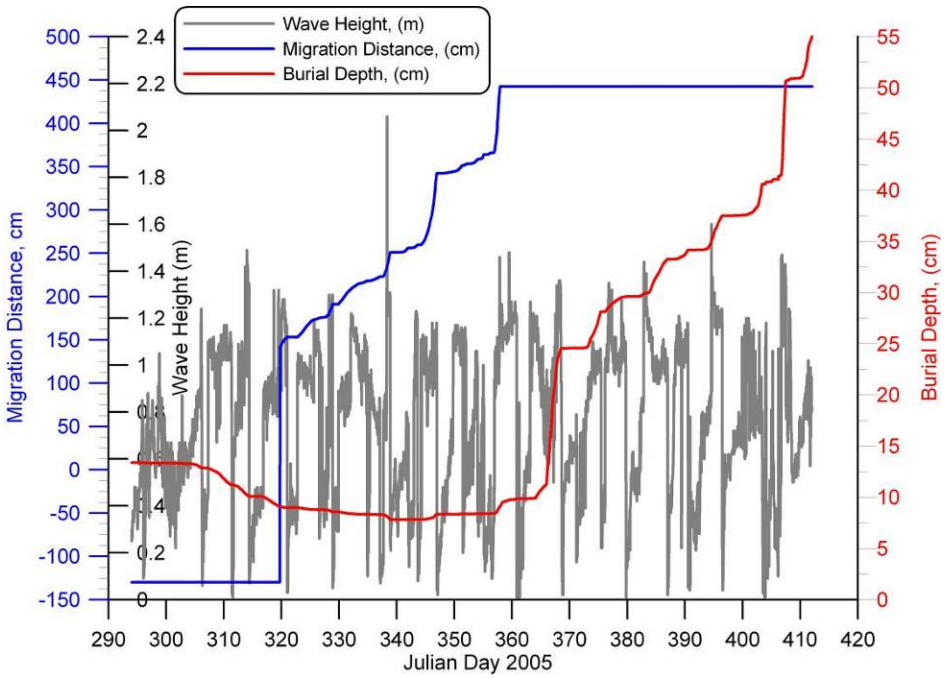

Figure 68. MM simulation of migration and burial sequence of 5”/38 surrogate #11, Offshore Group, Round Four, FRF Duck, 20 October 2005 – 16 February 2006.

With the Offshore Group (Figure 62, Figure 64, Figure 66, and Figure 68), migration was primarily on/off shore with the convention that transport off shore is taken as positive, while movement onshore is negative. So that migration and burial in both the Inshore and Offshore Groups can be compared to a common wave height reference, the wave heights plotted in Figure 61 through Figure 68 are from the wave rider buoy in 17m water depth (Sensor #630), prior to being shoaled into specific location of a particular surrogate. Burial depth is measured from the bottom of the surrogate at its basal end. The time axis in Figure 61 through Figure 68 is given in terms of Julian Day relative to the start of year 2005.

Some of the largest movements of the UXO surrogates (both in the Inshore and Offshore Groups) occurred in the first two days of Round One when burial was initially small immediately after installation. In this minimal burial state the UXO are particularly susceptible to mobility if sufficiently large waves occur to give rise to a supercritical transport state ($H_0 \geq 1.2$ m). Figure 61 indicates that this was indeed the case for surrogate #3 that was placed in the middle of the northern most row of the Inshore Group. The MM simulation computed that surrogate #3 moved a distance $\xi(i)$ = 186 cm from its initial lay-down position (diver surveys measured a net excursion of 2.0 m for surrogate #3 during Round One). The direction of movement calculated by the MM was principally long shore towards the north, counter to the prevailing long-term net littoral drift (cf. Figure 63), but in general agreement with diver surveys. It is also noted in Figure 65 that the high rate of initial migration for surrogate #13 was abruptly halted by burial lock-down, and that no further movement of the surrogate occurred during the remainder of Round One, as burial progressively increased to a burial depth of $h(i) =$ 23.4 cm, more than sufficient to totally bury the 5”/38 surrogate.

A larger migration excursion was played out during Round One in the Offshore Group. Figure 62 calculates that surrogate #11 at the seaward end of the Offshore Group initially moved $\xi(i)$ = 692 cm before burial arrested further movement. Divers measured net movement of surrogate #11 to be 7.8m during Round One. This movement was predominantly down-slope and offshore (cf. Figure 63), also in general agreement with diver acoustic ranging observations. The larger amount of movement of surrogate #11 versus surrogate #3 is apparently the result of steeper local bed slopes associated the seaward sloping face of a sand bar and trough bedform. Because the bedform migrated under the influence of the 1.4 m high shoaling waves, total burial of surrogate #11 was significantly more, computed to be $h(i) =$ 45.2 cm by the end of Round One (about double that realized for surrogate #3). High burial rates abruptly arrest high migration rates associated with the scour and roll progression involved with the migration mechanics of round bottom shapes like the 5”/38 naval projectiles, [28], [30], [32], and [33].

Once the UXO is fully buried, (as occurred by the end of Round One, cf. Figure 61 and Figure 62), subsequent movement is only possible if bottom profile variation of the type shown in Figure 55 results in re-exposure to a sufficient degree that releases the UXO from burial lock-down and permits it to undergo additional scour and roll progressions [28], [30]. In the MM, re-exposure of the UXO is the result of a complex interplay between the wave refraction/diffraction time history and the cycloid equilibrium profile algorithms. Computations of this interplay are

only possible in the Mode 3 operation of the model because it requires time variability in the wave forcing, and spatial variability in the bathymetry. In the FRF model runs of Rounds 1-6, the time variation of wave height and direction (when shoaled over the broad-shelf bathymetry, cf. Figure 55) produces time variability in the parameters of the type-b cycloid bottom profiles; and it is that profile variability that can re-expose a UXO and render it susceptible to further migration sequences. During all the diver surveys conducted in Rounds 1-6, the UXO surrogates were always buried (totally), and yet these surrogates were found in different locations during each survey round. The only explanation for how these buried surrogates moved between survey rounds is provided by the simulations of the MM that calculated interim re-exposure events that were not observed by divers.

Figure 63 shows one such re-exposure event occurring with surrogate #3 during Round Two at Julian Day 198 (17 July 2005). As the bar-berm profile re-adjusted to wave heights $H_0 \geq 1.6$ m, the burial depth was reduced to $h(i) \leq$ 7 cm, thereby exposing the 5”/38 surrogate and allowing it to scour and roll (cf. Figure 61). As the burial depth continued to decline to less than 4.5 cm, surrogate #3 executed a large amplitude scour and roll progression of several meters, retracing its migration route from Round One and trending along a general longshore pathway directed towards the south. It continued to migrate in this direction for several weeks but at a declining rate as the degree of burial gradually increased, resulting in burial lockdown on Julian Day 218 (6 August 2005), whence no further migration occurred. By the end of Round Two surrogate #3 had migrated a distance of $\xi(i)$ = 413 cm to the south of its initial deployment location at the stare of Round One. Altogether, MM calculates an incremental migration distance of $\Delta\xi(i) =$ 599 cm during Round Two, ending up totally buried at the end of Round Two at a relatively shallow burial depth of only $h(i) =$ 13.4 cm. The simulated migration distances in Figure 69 compare with a net movement of 4.2 m measured by divers for surrogate #3 over Rounds One and Two, and a measured incremental movement of 5.1 m for Round Two.

Migration and burial dynamics were also active on the sand bars of the Offshore Group during Round Two. Figure 64 shows that the MM predicted initially no further movement of surrogate #11 until the bar shifted and the UXO became exposed on Julian Day 201 (20 July 2005). Once exposed with only 5.7 cm of the surrogate buried, it abruptly moved almost 8 m in less than a day. This initial movement was shoreward, which was down slope on the shoreward face of the bar-trough bed form. This large initial excursion was the result of both gravity and radiation stress of the shoaling waves coupling together in the same direction. Once the surrogate had scoured and rolled to the trough of the bed form, migration was halted for a time, circa Julian Day 205 (24 July 2005). Thereafter, the surrogate gradually scoured and rolled about 3 m back seaward, eventually re-burying and becoming locked down under about 1 cm of overburden at a net distance of $\xi(i)$ = 215 cm from its initial starting position the beginning of Round One. This compares to a net transport of 1.9 m measured by divers from the beginning of Round One until the end of Round Two. The incremental movement calculated by the MM for surrogate #11 during Round 2 was $\Delta\xi(i) =$ 478 cm, as compared with 5.9 m measured by divers.

Unfortunately the acoustic ranging data for the positions of the most shoreward surrogates in the Inshore Group was too poor during Round Three to provide ground truth, but we do know from the measured profiles along ranges FRF # 76 and #85 that these surrogates were buried under about 0.75 m of sand overburden. Figure 65 provides insight from the MM calculations on what surrogate #3 in the Inshore Group likely did during Round Three. In the early portions of Round Three, surrogate #3 was buried under only a couple of centimeters of over burden, which was gradually eroded away as the bar-berm profile shifted, re-exposing and unlocking the surrogate circa Julian Day 243 (31 August 2005). Once this occurred, it abruptly moved about 2m back toward the north, followed by more gradual northward scour and roll progress until the degree of burial increased sufficiently by Julian Day 257 (14 September 2005) to re-establish burial lock down and arrest any further movement. Thereafter, the bar-berm profile continued to transition from a summer type equilibrium to a more winter type equilibrium configuration, increasing the depth of burial of surrogate #3 to $h(i) =$ 76.5 cm by the end of Round Three. During Round Three, the MM predicted an incremental movement of surrogate #3 of $\Delta\xi(i) =$ 277 cm toward the north, but still leaving the surrogate a net distance of $\xi(i)$ = 136 cm south of the initial placement at the start of Round One (Figure 65).

Round Three acoustic ranging measurements showed that surrogate #11 in the Offshore Group migrated shoreward an incremental distance of 3.76 m from its prior location at the end of Round Two. The MM simulation in Figure 70 calculated an incremental shoreward movement of $\Delta\xi(i) =$ 345 cm for surrogate #11 during Round-3, resulting in a net movement of $\xi(i)$ = 130 cm shoreward of the initial placement at the start of Round One. The time evolution of this movement was shown in Figure 70 to follow re-exposure and unlocking from shallow burial circa Julian Day 246 (3 September 2005), with continued gradual shoreward migration of the surrogate over the next 40 days. At Julian Day 285 (12 October 2005), surrogate #11 experienced burial lock down at its end point position for Round Three and subsequently buried under less than a centimeter of sand overburden. Thus, the computed direction and magnitude of migration of surrogate #11 were in general agreement with diver observations and the calculated burial depth was consistent with measured beach profiles along ranges FRF # 76 and #85 (cf. Figure 55).

A number of moderately high waves occurred during Round Four (20 October 2005 – 16 February 2006) that produced substantial movement of surrogates in both the Inshore Group (Figure 63) as well as the Offshore Group (Figure 68). In these plots, the time axis is in Julian Days relative to 2005, so that the days exceeding Julian Day 365 correspond to 2006. The Round Four MM simulation for surrogate # 3 in Figure 67 shows that it remained immobile in a state of deep burial until sufficient erosion had occurred to the bottom profile of the Inshore Group to cause re-exposure circa Julian Day 338 (4 December 2005). Once this occurred, surrogate #3 abruptly moved toward the north about 4 m, and continued a progressive northward migration for about a month when burial lock-down haltered further movement circa Julian Day 369 (4 January 2006). Thereafter, burial continued to advance as the bar-berm profile shifted further into a winter equilibrium state, leaving surrogate #3 buried as much as $h(i) =$ 107 cm by the end of Round Four. The incremental movement of surrogate #3 during Round Four was

calculated by the MM to be $\Delta\xi(i) =$ 1,051 cm, which compares well with a measured incremental movement of 10.4 m based on acoustic ranging measurements. The MM calculation of net movement of surrogate #3 from the beginning of Round One until the end of Round Four was $\xi(i)$ = 915 cm north of its initial placement. This agrees closely with a measured net movement of 9.1 m, suggesting that the MM calculations for surrogate #3 during Round Three (Figure 65), when no measurements were available, must have been accurate.

Similar accuracy during Round Four was also obtained with the MM for surrogate #11 in the Offshore Group. Figure 68 shows that surrogate #11 was re-exposed by bottom profile shifts on Julian Day 320 (16 November 2006) and begin migrating abruptly offshore at first, and continuing its offshore migration for another 40 days. Burial began increasing abruptly near the end of 2005, and surrogate #11 ceased further migration on Julian Day 358 (24 December 2005). Continued self-similar offshore shifts of the shore rise profile increased burial depth of surrogate #11 to $h(i) =$ 54 cm by the end of Round Four. The incremental movement of surrogate #11 during Round Four was predicted by MM to be $\Delta\xi(i) =$ 572 cm as compared to a measured value of 5.6 m. The net movement of surrogate #11 from the beginning of Round One until the end of Round Four was $\xi(i)$ = 443 cm offshore of its initial placement, as compared to a measured value of 4.0 m.

Note that on the time scale of Figures 61-68 there is a rapid movement that occurs (or stops) as the burial passes through the "lockdown" level (about 6 cm). On the horizontal scale of the display, movement over a period of a few minutes appears almost instantaneous.

A comparison of the predicted versus observed migration trajectories for Rounds 1-4 is shown in Figure 69 for all the surrogates in the Inshore Group, and in Figure 70 for all the surrogates in the Offshore Group. In these trajectory maps the initial position at the start of Round One is designated by a blue circle and the measured end point by a purple star. The measured legs of the trajectories for each round are indicated by the colored line segments, with Round One displacements indicated in green; Round Two displacements indicated in red; Round Three displacements indicated in yellow; and Round Four displacements indicated in purple. The modeled migration trajectories are shown as a dashed black line, with the predicted end-point at the end of Round Four indicated by a black star. The identification number of each surrogate in Figure 69 and Figure 70 can be deduced from Figure 59. In general the predicted trajectories show the correct trends with respect to the direction of net movement and are within 1m of the observed magnitude of movement, which in turn is within demonstrated measurement error using the acoustic ranging technique.

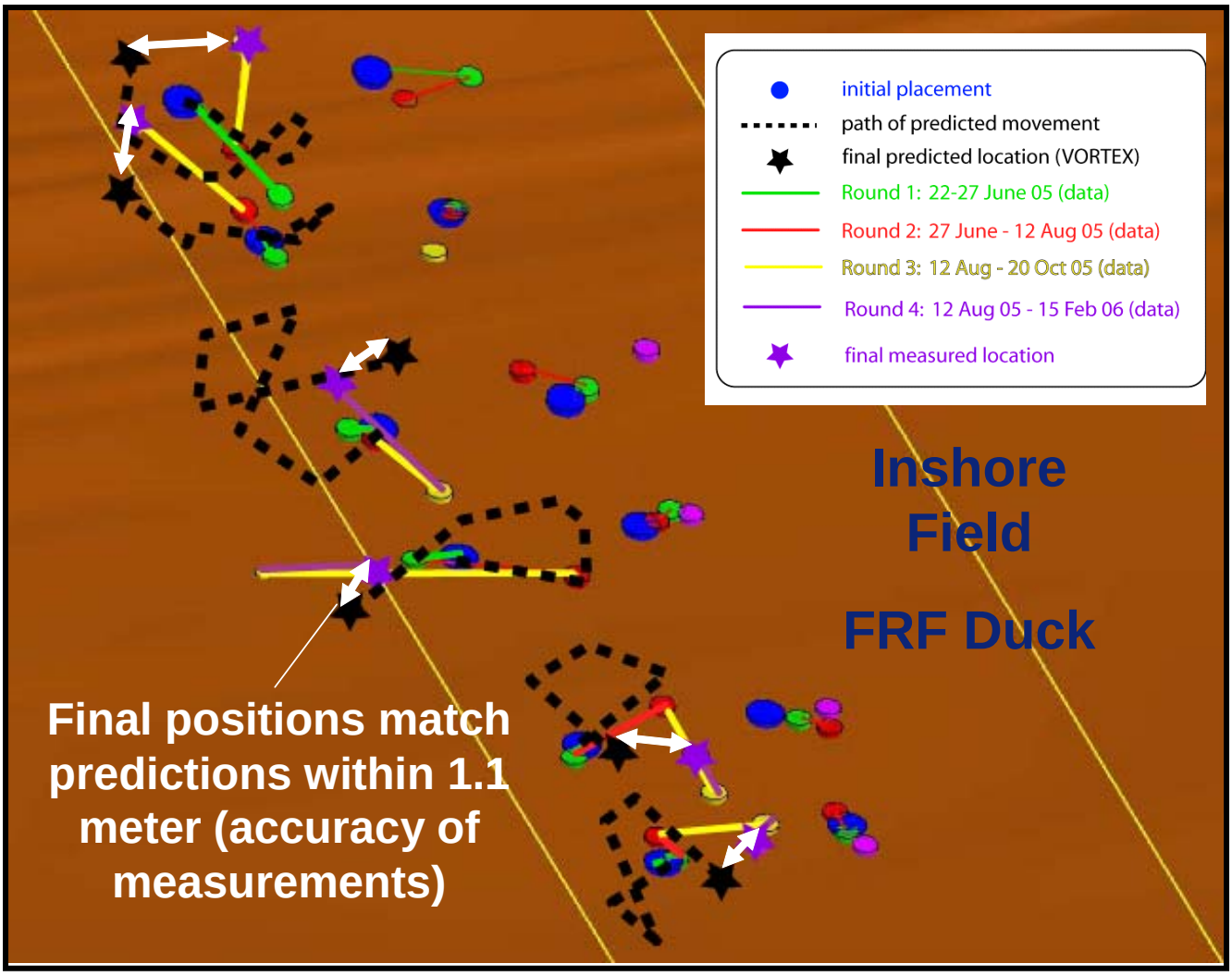

Figure 69. Predicted versus measured UXO migration in Inshore Field, FRF Duck, NC, Rounds One through Four, 22 June 2005 – 16 February 2006.

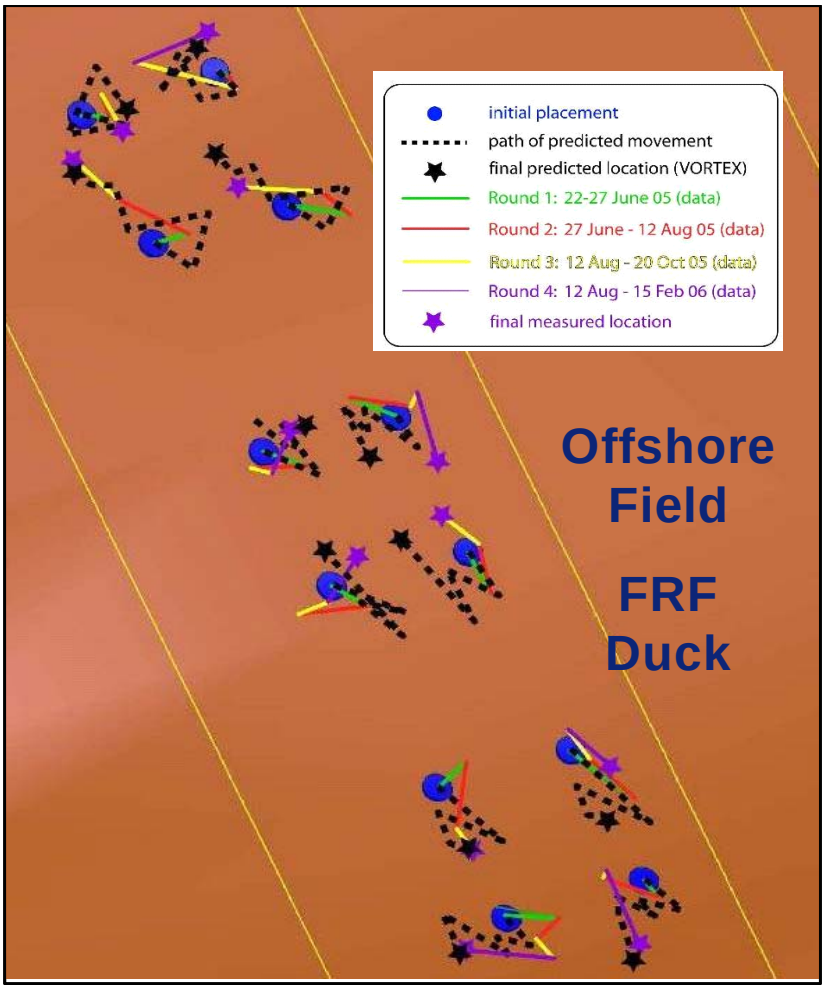

Figure 70. Predicted versus measured UXO migration in Offshore Field, FRF Duck, NC, Rounds One through Four, 22 June 2005 – 16 February 2006.

To quantify the statistical accuracy of the migration predictions of the MM, we construct probability density functions from the ensembles of measured and predicted movement. Figure 71 presents the probability density function (histogram) of the measured UXO migration distances for all 24 surrogates at FRF. A total of 80 realizations of migration distance were constructed from the diver measurements from Rounds 1-4. These are contrasted with the 96 simulated realizations of migration distance that make up the modeled probability density function. The peak, spread and shape of the predicted and measured probability density functions of migration in Figure 71are quite similar. The MM predicts a mean transport distance of 3.5 m as compared to an observed mean of 4.6m, an agreement within measurement error. The MM slightly over-predicts the spread in transport outcomes, predicting a maximum transport distance of 14.3 m and a minimum of 0.5m compared to an observed maximum of 12.6m and an observed minimum of 0.7m. However, the standard deviation of the modeled transport is

slightly less than observed, with the model giving σ_i = 1.9 m vs the observed σ_i = 2.6 m. This is to be expected when comparing a process-based model to stochastics from a field experiment.

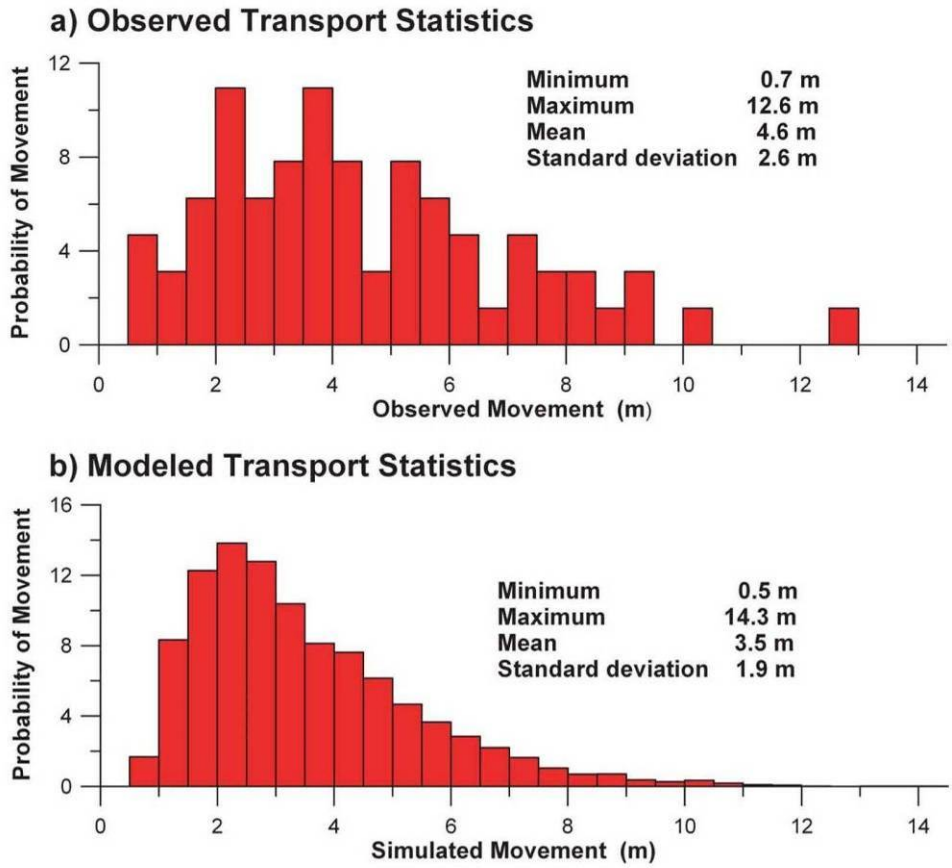

Figure 71. Predictive skill for all surrogate movement, Rounds 1-4, FRF Duck, NC. (a) Measured probability density function vs. (b) predicted probability density function.

Two of the 24 surrogates were not recovered after Round Four, and these were allowed to remain in place until 3 August 2006 in what was referred to as Rounds Five and Six. These included one surrogate from the Inshore Group (# 18) and the other from the Offshore Group (#23). While the positions of these were not monitored, their burial depth was determined at the time of extraction on 3 August 2006. To test the model's ability to make a long term prediction, we continued simulations of the migration and burial of these two surrogates from 16 February 2006 until 3 August 2006. Figure 72 gives the migration/burial prediction of surrogate #18 of the Inshore Group during Rounds Five and Six. We find that VORTEX predicted no additional migration following Round Four due to the very deep burial state. At the end of Round Four and beginning of Rounds Five and Six, the model predicted a burial depth of $h(i) =$ 251 cm. Over the course of Rounds Five and Six, the bottom profile transitioned from a winter equilibrium to a summer equilibrium and burial depth for surrogate #18 was predicted to decline to $h(i) =$ 43 cm by 3 August 2006. This compared to a measured burial depth of 0.51 m at the time surrogate #18 was extracted. In the Offshore Group, VORTEX predicted somewhat more active movement for surrogate #23 (Figure 73). Here the surrogate was re-exposed circa Julian Day 143 (23 May 2006) and migrated an incremental distance of $\Delta\xi(i) =$ 277 cm over a period of about 50 days before become re-buried to a depth of $h(i) =$ 18 cm by the end of Rounds Five and Six. This compares to a measured burial depth of 0.15 m for surrogate #23 at the time of extraction. Thus, the MM demonstrated a high degree of accuracy in predicting the burial of these two surrogates over a full calendar year.

The measured and predicted burial ensembles were assembled into probability density functions based on 98 separate observations and predictions. Figure 74 compares the predicted versus measured probability density functions for UXO burial at FRF during Rounds 1-6. The comparison with measured probability density function for burial in Figure 74a is quite satisfying, despite the small ensemble statistics. Again, the peak of the measured distribution, its breadth, and shape are all faithfully mimicked by the modeled distribution in Figure 74b. The model predicts a mean burial depth of 89.6 cm as compared to an observed mean of 84.9 cm. The model slightly under-predicts the spread in burial outcomes, predicting a maximum burial depth of 257.6 cm and a minimum of 11.3 cm. This compares to an observed maximum of 264.6 cm and an observed minimum of 1.85 cm. The standard deviations are virtually the same for both the observed and modeled distributions, σ_i = 58 -59 cm. These burial depths are significantly greater than what was observed during the brief deployment at Ocean Shores, Washington.

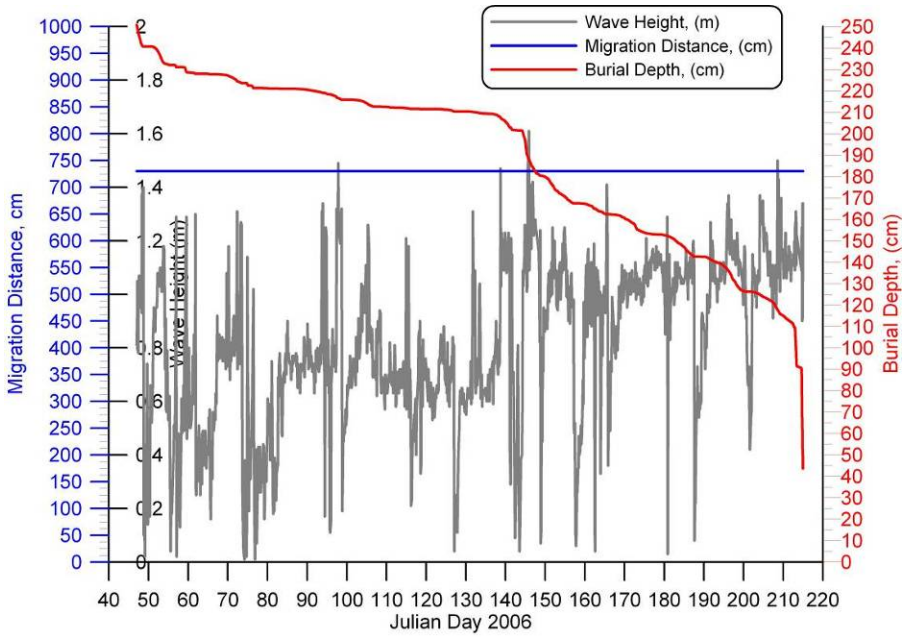

Figure 72. MM simulation of migration and burial sequence of 5”/38 UXO surrogate #18 in Inshore Group, during Rounds 5-6 at FRF Duck, NC, 16 February – 3 August 2006.

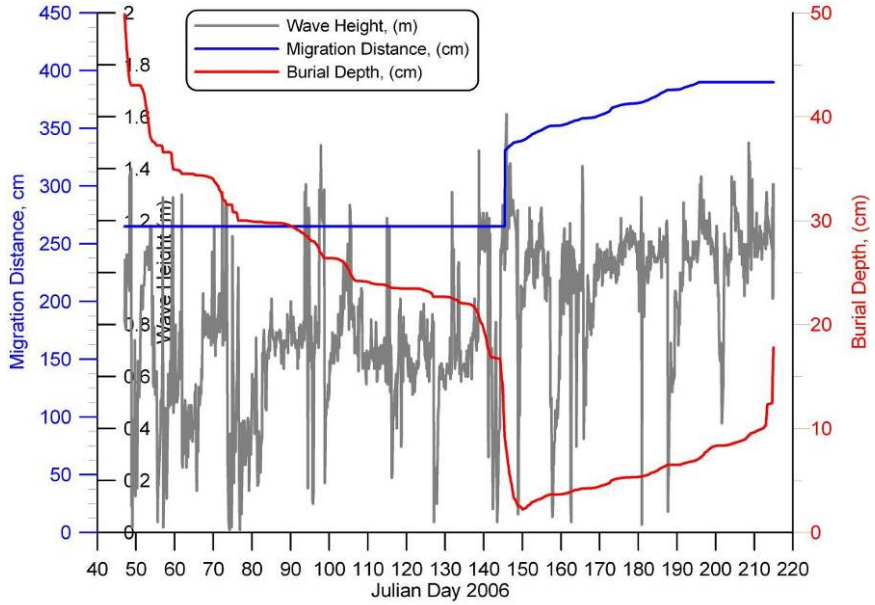

Figure 73. MM simulation of migration and burial sequence of 5”/38 UXO surrogate #23 in Offshore Group during Rounds Five and Six, FRF Duck, NC, 16 February – 3 August 2006.

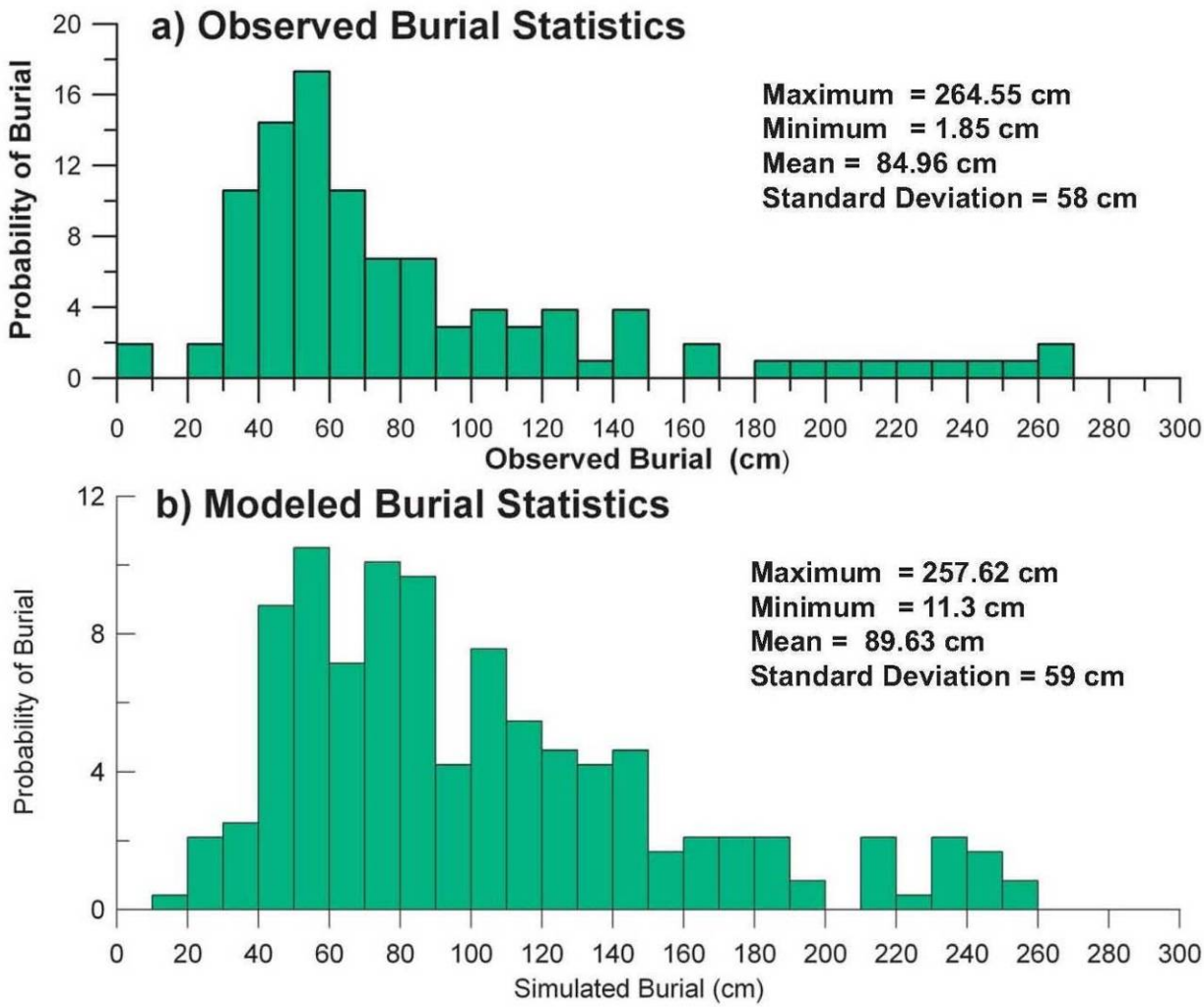

Figure 74. Predictive skill for surrogate burial, Rounds One through Four, FRF Duck, NC: (a) Measured probability density function, (b) predicted probability density function.

4.3.2 Predictive Skill of Model Predictions

A predictive skill factor, *R,* was computed from the mean squared error between the predicted and measured outcomes. The foundation reference for the skill factor, it's definition, and acceptable limits was originally treated in Gallagher, E.L., S. Elgar, and R. T. Guza (1998), "Observations of sand bar evolution on a natural beach", *J. Geophys. Res.*, *103*(C2), 3203–3215 [34].

It was later used in the equilibrium beach profile paper that now is considered the keystone reference for this type of modeling - Jenkins, S. A. and D. L. Inman, (2006), "Thermodynamic solutions for equilibrium beach profiles", *J. Geophys. Res.,* v.3, C02003, doi:10.1029, 21pp.[16]

Two approaches are applied to assess the predictive skill of the quantitative MM predictions of the magnitude of migration and burial of UXO surrogates at FRF. With the first approach, probability density functions are produced for migration and burial magnitudes predicted by the MM and compared with the probability density functions assembled from the observed outcomes of the experiment. Because the experimental outcomes involve small ensemble statistics, we merge the results of all 24 surrogates from the inshore and offshore test sites into a single set of probability density functions. By the second approach, we a compute predictive skill factor, *R,* is computed from the mean squared error between the predicted and measured outcomes.

Using the analytical statistical approach to error assessment, we compute the predictive skill factor *R* of the UXO migration distance, ξ, and burial depth *h* as quantified by an estimator adapted from the mean squared error. For burial depth the skill factor would have the following form adapted from [16]:

$$R_h = 1 - \frac{1}{N\hat{\sigma}_i}\left\{\sum_{1}^{i=N}\left[\hat{h}(i) - h(i)\right]^2\right\}^{1/2} \tag{5}$$

where $\hat{h}(i)$ is the measured burial depth for $i = 1, 2...N$ observations, $h(i)$ is the predicted burial depth for the ith observation, and σ_i is the standard deviation of all observations over the period of record. For migration distance the skill factor would have the form:

$$R_\xi = 1 - \frac{1}{N\hat{\sigma}_i}\left\{\sum_{1}^{i=N}\left[\hat{\xi}(i) - \xi(i)\right]^2\right\}^{1/2} \tag{6}$$

where $\hat{\xi}(i)$ is the measured migration distance for $i = 1, 2...N$ observations, $\xi(i)$ is the predicted migration distance for the ith observation. Based on these formulations and the predicted versus measured outcomes in Figures 19 & 21, the skill factor for migration at FRF was calculated at $R_\xi =$ 0.87 and $R_h =$ 0.93 for burial. For coastal processes modeling and mine burial prediction in particular, any skill factor in excess of 0.8 is considered to be within acceptable limits [16].

5.0 Conclusions

The field test was successful in its entirety. The following summary conclusions are based upon the analysis conducted to date.

- All 24 5”/38 surrogates were installed as planned and were tracked for 22 to 28 months, despite the fact that they were all found buried at each of 7 sets of measurements.
- Measurable movement occurred, generally within the range of initial predictions.

- The predicted depth of burial matched the measured depth consistently.
- The general nature of the horizontal movements matched the model predictions. After nearly two years, the average movement was within 24% of the predicted location (almost at the limit of accuracy of the tracking system).
- The presence of biofouling on the 5”/38 surrogates – and its absence on the 20mm surrogates – are both consistent with the Model predictions.

In addition, the following detailed conclusions were derived from the MM validation for the FRF Duck field test site:

- The trailing edge coast environment of the Outer Banks is a challenging UXO modeling problem that requires very large farfield model grids to adequately resolve the highly variable nearshore bathymetry that ultimately controls the burial/migration evolution. The far field grid is assembled from a 2,401 x 2,401 point array (5,764,801 grid points) formatted by latitude and longitude using 3 x 3 arc second grid cell resolution and yielding a computational domain of 168.1 km along the x-axis (longitude) and 222.3 km along the y-axis (latitude). This is the largest grid on which the MM has computed UXO transport and burial to date, and was necessitated by the broad-scale longshore fluxes of sediment and mass exchange occurring between the Hatteras and Ocracoke Littoral Cells. Spatial variation in wave forcing over the barrier island system of the Outer Banks is derived from refraction/diffraction analysis over the far field grid based on directional wave measurements from instrumentation maintained by FRF. This instrumentation includes a directional wave buoy in 17m water depth (Sensor #630), pier-mounted pressure sensors at 2m depth, (Sensor # 651) and an ADCP with pressure sensor array installed at 8m depth. The nearfield of the model was gridded for a fine to medium coarse sand bottom that was parameterized by 20 grain size bins according to the in situ grain size distribution. The FRF Duck sand is well sorted by the wave action, and mineral analysis indicates it is predominately quartz of glacial origin. The median grain size is 565 microns, and 70 % of the sediment is comprised of medium-coarse sand between 450 microns and 750 microns. The UXO surrogates were placed in two groups (inshore group and offshore group) along two cross-shore parallel lines next to FRF profile range lines # 76 and # 85. The in-shore field (surrogates #s 1-6 and 13-18) was located on the north side of the FRF Pier in a nominal depth of 2m to 3 m MSL, while the off-shore field (surrogates #s 7-12 and 19-24) was laid at depths between 6 m and 7 m MSL.

- Some of the largest movements of the UXO surrogates (both in the Inshore and Offshore Groups) occurred in the first two days of 1 when burial was initially small immediately after installation. In this minimal burial state the UXO are particularly susceptible to mobility if sufficiently large waves occur to give rise to a supercritical transport state ($H_0 \geq 1.2$ m). The high rate of initial migration was subsequently found to be abruptly halted by burial lock-down, whence no further movement of the surrogates occurred. Once the UXO is fully buried, (as observed during each diver inspection), subsequent

movement is only possible if bottom profile variation results in re-exposure to a sufficient degree that releases the UXO from burial lock-down and permits it to undergo additional scour and roll progressions. Three such re-exposure events were calculated by the MM during Rounds 1-4 of the experiment, and a forth was calculated for surrogate #23 during Rounds Five and Six.

- In the MM, re-exposure of the UXO is the result of a complex interplay between the wave refraction/diffraction time history and the cycloid equilibrium profile algorithms. Computations of this interplay are only possible in the Mode 3 operation of the model because it requires time variability in the wave forcing, and spatial variability in the bathymetry. In the FRF model runs of Rounds 1-6, the time variation of wave height and direction (when shoaled over the broad-shelf bathymetry) produces time variability in the parameters of the bottom profile algorithms; and it is that profile variability that can re-expose a UXO and render it susceptible to further migration sequences. The type-b cycloid algorithms in the MM were found to give the best fit to the FRF bottom profiles that are well known for having complex and highly variable bar-trough bed forms. The type-b cycloid has been built into the G-95/ FRF version of the VORTEX code (Appendix A) that was used exclusively for the model analysis of this study. An interesting feature of the calibrated cycloid profiles using the supporting survey data is that the closure depth was only $h_c \cong$ 6 m to 7 m, when normally it is about twice that value. The explanation for this beach profile anomaly was the unusually benign wave forcing that persisted throughout the experiment. The thickness of the critical mass (depth of permanent entombment) is $\xi_c =$ 220 cm for the inshore UXO group; $\xi_c =$ 140 cm for the offshore group; and the critical mass of sand (volume of sand that must be removed to expose buried UXO) is V_c = 600 m^3 to 1200 m^3 per meter of shoreline.

- The most accurate model predictions of migration were obtained with surrogate #3 in the Inshore Group and surrogate # 11 in the Offshore Group. The MM calculation of net movement of surrogate #3 from the beginning of Round One until the end of Round Four was $\xi(i)$ = 915 cm north of its initial placement. This agrees closely with a measured net northerly movement of 9.1 m using acoustic ranging techniques. The net movement of surrogate #11 from the beginning of Round One until the end of Round Four was $\xi(i)$ = 443 cm offshore of its initial placement, as compared to a measured value of 4.0 m of offshore movement.

- The most accurate model predictions of burial were obtained during Rounds 5-6 with surrogate #18 in the Inshore Group and surrogate # 23 in the Offshore Group. Over the course of Rounds 5-6, the bottom profile transitioned from a winter equilibrium to a summer equilibrium and burial depth for surrogate #18 was predicted to decline to $h(i)$ = 43 cm by 3 August 2006. This compared to a measured burial depth of 0.51 m at the time surrogate #18 was extracted. In the Offshore Group, VORTEX predicted active movement for surrogate #23. Here the surrogate was re-exposed circa Julian Day 143

(23 May 2006) and migrated an incremental distance of $\Delta\xi(i) =$ 277 cm over a period of about 50 days before become re-buried to a depth of $h(i) =$ 18 cm by the end of Rounds 5-6. This compares to a measured burial depth of 0.15 m for surrogate #23 at the time of extraction.

- Two approaches were applied to assessing the predictive skill of the quantitative model predictions of the magnitude of migration and burial of UXO surrogates at FRF. By the first approach, we construct probability density functions of migration and burial magnitudes predicted by the model and compare them with the probability density functions assembled from the observed outcomes of the experiment. By the second approach, we a compute predictive skill factor *R* from the mean squared error between the predicted and measured outcomes.

- A total of 80 realizations of migration distance were constructed from the diver measurements from Rounds 1-4. These are contrasted with the 96 simulated realizations of migration distance that make up the modeled probability density function. The peak, spread and shape of the predicted and measured probability density functions of migration are quite similar. The model predicts a mean migration distance of 3.5 m as compared to an observed mean of 4.6 m, an agreement within measurement error. The model slightly over-predicts the spread in migration outcomes, predicting a maximum migration distance of 14.3 m and a minimum of 0.5 m; compared to an observed maximum of 12.6 m and an observed minimum of 0.7 m. However, the standard deviation of the modeled migration is slightly less than observed, with the model giving $\sigma_i = 1.9$ m versus the observed $\sigma_i = 2.6$ m. This is to be expected when comparing a process-based model to stochastics from a field experiment.

- The measured and predicted burial ensembles were assembled into probability density functions based on 98 separate observations and predictions during Rounds 1-6. The peak of the measured distribution, its breadth, and shape are all faithfully replicated by the modeled distribution. The model predicts a mean burial depth of 89.6 cm as compared to an observed mean of 84.9 cm. The model slightly under-predicts the spread in burial outcomes, predicting a maximum burial depth of 257.6 cm and a minimum of 11.3 cm. This compares to an observed maximum of 264.6 cm and an observed minimum of 1.85 cm. The standard deviations are virtually the same for both the observed and modeled distributions, $\sigma_i = 58$ -59 cm.

- The skill factor for migration at FRF was calculated at $R_\xi =$ 0.87 and $R_h =$ 0.93 for burial. For coastal processes modeling, and mine burial prediction in particular, any skill factor in excess of 0.8 is considered to be within acceptable limits.

6.0 References

[1] Wilson, J., "Final Field Test Report (PMRF, Hawaii)", Sound & Sea Technology Report, (TBD), February 2008.

[2] Hammond, R., Jenkins, S.A., and J. Wasyl , "Underwater Munitions of Concern Migration and Burial Model: Phase 1 Report: Parameter Definition." 34 pp, June 2003.

[3] Wilson, J. , *"UXO Migration Field Test Point Mugu Lagrangian Drifters FINAL REPORT",* Sound and Sea Technology Report 04-13, 23 September 2004

[4] Wilson, J., et al., *"UXO Measurement Method Field Tests (MMFT1&2) and Mobility Model Modification FINAL REPORT",* Sound & Sea Technology Report 05-07 31 December 2005

[5] Jenkins, S.A. and D.L. Inman, "*Model for mine scour and burial: An illustrated abstract with technical appendix*", University of California, San Diego, Scripps Institution of Oceanography, SIO Reference Series 02-2, 42 pp.

[6] Wilson, J., *"ESTCP UXO Mobility Model FINAL REPORT*", Sound & Sea Technology Report (TBD), June 2008

[7] Dr. Gordon P. Watts, Jr., "*Magnetic Location of Unexploded Ordnance*, *Unexploded Ordnance Mobility and Burial Experiment*, *U.S. Army Corps of Engineers Field Research Facility*, *Duck, North Carolina"*, Tidewater Atlantic Research, Inc., Washington, North Carolina,10 December 2006

[8] USGS, "National Water Information System: Web Interface," http://waterdata.usgs.gov/nwis/, 2008.

[9] National Geophysical Data Center (NGDC), http://www.ngdc.noaa.gov/mgg/gdas/gd_designagrid.html, 2008.

[10] C. E. Nordstrom and D. L. Inman, "Sand level changes on Torrey Pines Beach, California," *U. S. Army Corps of Engineers, Coastal Engineering Research Center Miscellaneous Paper 11-75*, 1975.

[11] D. L. Inman, "Areal and seasonal variations in beach and nearshore sediments at La Jolla, California," *U. S. Army Corps of Engineers: Beach Erosion Board Technical Memorandum 39*, 1953.

[12] D. L. Inman and T. K. Chamberlain, "Particle size distribution in nearshore sediments," Finding Ancient Shorelines: *Society of Economic Paleontologists and Mineralogists*, Special Publication 3, pp. 106-129, 1955.

[13] D. K. Stauble, "Long-term profile morphodynamics: field research facility case history," *U. S. Army Corps of Engineers: Coastal Engineering Research Center Technical Report CERC-92-7*, 1992.

[14] D. K. Stauble and M. A. Cialone, "Sediment dynamics and profile interactions: DUCK94", *Coastal Engineering* - Proceedings of the twenty-fifth international conference, Vol. 4, ASCE, 1996.

[15] D. K. Stauble, "A review of the role of grain size in beach nourishment projects," U.S. Army Engineer Research and Development Center, Coastal and Hydraulics Laboratory, 2002.

[16] S. A. Jenkins and D. L. Inman , "Thermodynamic solutions for equilibrium beach profiles," *J. of Geophysical Res.*, vol. 111, C02003, doi:10.1029/2005JC002899, 21 pp., 2006.

[17] J. T. Kirby, "Higher-order approximations in the parabolic equation method for water-waves," *J. Geophysical Res*., vol. 91, no. C1, p. 933–952, 1986.

[18] R. A. Dalrymple, J. T. Kirby, and P. A. Hwang, "Wave diffraction due to areas of energy dissipation," *J. Waterway Port, Coast, and Ocean Engineering*., vol. 110, p. 67-79, 1984.

[19] M. S. Longuet-Higgins, "Mass transport in water waves," *Phil. Trans.*, Ser. A, vol. 245, p. 535-581, 1953.

[20] J. Lamoure and C. C. Mei, "Effects of horizontally 2-dimensional bodies on mass transport near sea bottom," *J. Fluid Mech.*, vol. 83, no. 3, pp. 415–433, 1977.

[21] M. S. Longuet-Higgins, "Steady currents induced by oscillations around islands," *J. Fluid Mech.*., vol. 42, no. 4, p. 701-720, 1970.

[22] J. J. Connor and J. D. Wang, "Finite element modeling of two-dimensional hydrodynamic circulation," *MIT Technical Report #MITSG 74-4*, p. 1-57, 1973.

[23] B. W. McCormick, *Aerodynamics, Aeronautics, and Flight Mechanics*. New York: John Wiley & Sons, 1979.

[24] M. Van Dyke, *Perturbation Methods in Fluid Mechanics*. Stanford, CA: Parabolic, 271 pp., 1975.

[25] A. J. Peace and N. Riley, "A Viscous Vortex Pair in Ground Effect," *J. Fluid Mech.*, vol. 129, pp. 409–426, Apr. 1983.

[26] R. A. Bagnold, “The flow of cohesionless grains in fluids, *Philos. Trans. R. Soc. London Ser. A*, *249*(964), 235–297, 1956.

[27] R. A. Bagnold, “Mechanics of marine sedimentation,” In *The Sea, Ideas and Observations on Progress in the Study of the Seas,* v*ol. 3, The Earth Beneath the Sea, History*, edited by M. N. Hill, pp. 507–528, Wiley, New York, 1963.

[28] S. A. Jenkins , D. L. Inman, M. D. Richardson, T. F. Wever, and J. Wasyl “Scour and Burial Mechanics of Objects in the Nearshore*,” IEEE Jour Oc Eng*, vol. 32, no. 1, pp78-90, Jan. 2007.

[29] J. J. Donohue and L. E. Garrison, “An Evaluation of Mine Behavior Observations in Four Test Areas,” Narragansett Marine Laboratory: Univ. Rhode Island, Reference 54-13, 1954.

[30] D. L. Inman and S. A. Jenkins, “Scour and Burial of Bottom Mines, A Primer for Fleet Use,” Scripps Institution of Oceanography: Univ. of California, San Diego, SIO Reference Series 02-8, 2002. Available: http://repositories.cdlib.org/sio/reference/02-8/

[31] Smith, A. M. 0., "Aerodynamics of High-Lift Airfoil Systems". AGARD CP 102, 1972.

[32] D. L. Inman and S. A. Jenkins, “A Chronology of Ground Mine Studies and Scour Modeling in the Vicinity of La Jolla,” Scripps Institution of Oceanography: University of California, San Diego, SIO Reference Series 96-13, 1996.

[33] R. F. Dill, “The Burial and Scouring of Ground Mines on a Sandy Bottom,” San Diego, CA: U. S. Navy Electronics Laboratory, Research Report NEL 861, 1958.

[34] Gallagher, E.L., S. Elgar, and R. T. Guza (1998), "Observations of sand bar evolution on a natural beach", *J. Geophys. Res.*, *103*(C2), 3203–3215.

Appendix A: UXO Mobility Model FORTRAN Code (FRF Duck)

```
c........UXO_transport_frf_duck_w_cycloid_29mar07.for
c***THIS PROGRAM IS CONFIGURED TO RUN ON A 29 Character wave file name (ie.
waves_frf_22jun05-15feb06.dat)
c   which has wave height in centimeters in non-uniform timesteps with a
c   mean interval of 6.44 hours*****
c
          DIMENSION time(5000),ang(5000),per(5000),wht(5000)
     dimension r(90601),s(90601),b(90601)
     dimension x(301),y(301),gama(301),gamb(301),gam(301)
     dimension z_mark(301,301)
     dimension gam2(301),gama_2(301),gamb_2(301)
     dimension scour(301,301,250),bot(301,301,250)
     dimension bury(5000),bur(5000)
            dimension u0(5000),u2(5000),whx(5000)
            character*12 bofile2
         character*5 fname(1500)
c
c9mar07
            dimension alam(5000),ucross(5000),vlong(5000),xcross(5000)
            dimension ylong(5000),shield(5000),theta(5000)
c
     character*20 ofile
     character*29 wavefile
c
c27mar07 cycloid stuff
            dimension dept(3001),wvnum(3001)
            dimension whtme(366)
      double precision  depce(366),depcp(366),ac(366),bc(366)
      character*6 fname2(366)
            character*1 cc
CCCC__________cycloid ellipse arrays_________________
            DIMENSION angc(2000),xd(2000)
         Dimension slope(2000),circle(2000)
         dimension cycloid(2000)
            character*20 ofile2
            character*12 breakshr
         dimension brkcol(2401),brkhgt(2401),brkang(2401),brkdep(2401)
         Dimension depmsl(2401)
         integer krow(2401),mslcol(2401)
c
1000  format(a12)
```

```
1001  format(a29)
1111  format(a20)
c
      open(19,file='UXO_transport_frf_duck_w_cycloid_29mar07.inp'
     &,status='old')
c***input parameters particular to wave induced burial
      read(19,1001)wavefile
      read(19,*)mstart
      read(19,*)mend
c***input parameters particular to UXO shape generation
      read(19,1000)ofile
      read(19,*)ix
      read(19,*)xinv
      read(19,*)jy
      read(19,*)yinv
      read(19,*)depth
      read(19,*)b_dia
      read(19,*)h
      read(19,*)point
c***input parameters particular to UXO scour
      read(19,*)z_plane
      read(19,*)delx
      read(19,*)dely
      read(19,*)cl
      read(19,*)cf
      read(19,*)g
      read(19,*)rhom
      read(19,*)alpha
      read(19,*)tauc
      read(19,*)str
      read(19,*)r_test
      read(19,*)s_test
      read(19,*)ak_bot
       read(19,*)tcon
       read(19,*)winu
       read(19,*)winl
       READ(19,*)cdir
       READ(19,*)effic
       read(19,*)akx
       read(19,*)htmin
       READ(19,1100)bofile2
       READ(19,*)ass
       READ(19,*)aks
       READ(19,*)tdown
```

```
      READ(19,*)tshift
      READ(19,*)eff2
      READ(19,*)eff3
      READ(19,*)akwave0
      READ(19,*)akwave2
      READ(19,*)icoast
c..9mar07
      READ(19,*)ax
      READ(19,*)ay
      READ(19,*)dbar
      READ(19,*)scrit
      READ(19,*)xuxo
      READ(19,*)yuxo
      READ(19,*)bplane
      READ(19,*)burmove
      READ(19,*)dir_thr
c
CYCLOID Inputs 27mar07
          read(19,*)gm
          read(19,*)ak
       read(19,*)beta
          read(19,*)akm
       read(19,*)akd
       read(19,*)vdepce
       read(19,*)bs
       read(19,*)nrange
      READ(19,*)ecc
      READ(19,*)akxc
      READ(19,*)crit
      READ(19,*)refdia
      READ(19,*)aka
      READ(19,*)dia2
      READ(19,*)akbr
      READ(19,*)ibrbm
      READ(19,*)zone
      READ(19,*)xshift
      READ(19,*)i_cycloid
      READ(19,'(a)')cc
      read(19,1111)ofile2
      read(19,1000)breakshr
      READ(19,*)krefrow
      READ(19,*)nuxorow
      READ(19,*)sx
      READ(19,*)sy
```

```
      READ(19,*)ktotal
CYCLOID END
      akd=akd*(refdia/dia2)**aka
c
c  xoffset is the distance in meters (sx = irowixshiftgrid cperpendicular to coastli
c
       pi=ACOS(-1.0)
          write(*,*)g,gm,mend
c....OPEN/READ Breaker/shoreline file ie, "duckbath.bra" determine column
c    of 0 MSL
      OPEN(UNIT=30,FILE=breakshr,STATUS='OLD')
      yoffset=(krefrow-nuxorow)*sy
      do 157 k=1,ktotal
     READ(30,*)krow(k),brkcol(k),brkhgt(k),brkang(k),brkdep(k),
    &mslcol(k),depmsl(k)
      if(krow(k).EQ.krefrow)krefcol=mslcol(k)
      if(krow(k).EQ.nuxorow)xoffset=(mslcol(k)-krefcol)*sx
157    continue
c
C.....open wave period-height-direction files
      OPEN(UNIT=2,FILE=wavefile,STATUS='OLD')
c...wave height read in cm
      mcount=0
      DO 105 m=1,5000
      READ(2,*,end=1105)time(m),per(m),wht(m),ang(m)
      mcount=mcount+1
      whx(m)=(wht(m)/((2.0*2.0*pi/per(m))**0.5))*((g/depth)**0.25)
      u0(m)=(whx(m)/2.0)*((g/depth)**0.5)
      u2(m)=akwave2*u0(m)
      alam(m)=(2.0**0.4)*(wht(m)**0.2)*(((2.0*pi/per(m))**2.0)/
    &(g*0.8))**0.2
105    CONTINUE
1105   write(*,*)mcount
      write(*,*)time(1),per(1),wht(1),ang(1)
      write(*,*)time(mcount),per(mcount),wht(mcount),ang(mcount)
c
      nblines=mcount
c
c
1100   format(a12)
C**************************begin UXO_br3 logic***************************
c
c..open time output file
      OPEN(UNIT=4,FILE=bofile2,STATUS='unknown')
```

```
c
c
91000   format(4f12.5)
c       write(*,*)nblines
c
      do 9155 n=1,nblines
      time(n)=time(n)-tcon
      bury(n)=0.0
      bur(n)=0.0
c..change absolute time to relative time by subtracting tcon
9155    continue
c
      ymine=htmin
      ss=0.0
      gr=0.0
      gr1=0.0
      gr2=0.0
c
c..9mar07
      xcross(1)=xuxo
      ylong(1)=yuxo
      write(*,*)xcross(1),ylong(1)
c***START OF BURY and BUR LOOP*************************
      DO 9406 n=2,nblines
      nm1=n-1
      if(icoast.EQ.3)then
      if(ang(n).GE.winu)ang(n)=winu
      if(ang(n).LE.winl)ang(n)=winl
      endif
      if(icoast.EQ.1)then
      if(ang(n).LE.winu)ang(n)=winu
      if(ang(n).GE.winl)ang(n)=winl
      endif
c..keep incident waves inside of window icoast=1 east facing, icoast=3 west coast
      np1=n+1
      delt=(time(np1)-time(n))*31536000.0
      theta(n)=ang(n)-cdir
      energy=1.0/8.0*g*whx(n)**2
      cn=0.5*g*per(n)/(2.0*pi)*SIN(theta(n)*2.0*pi/360.0)*
     &COS(theta(n)*2.0*pi/360.0)
c ..
      abcn=ABS(cn)
      asc=abcn*ass
      ptr=energy*cn*effic/(1.64*0.6*1000000.0*g*1000000.0)
```

```
c
c..correct instantaneous transport back to meters ptrm
      pt=ptr*delt
        if(time(n).LT.tdown)then
        gr1=gr1+ABS(pt)
        ELSE
        gr1=gr1-ABS(pt)*eff2
        ENDIF
      gr2=gr2+ABS(pt)*eff3
      gr=gr1+gr2
c
      ymine=htmin-(gr*htmin)
CCCCCCCCCC...inner loop
c
c
CC.5DEC06***HERE IS THE DEFINITION:
C  BURY(n) is the UXO sihlouette above seabed as a fraction of cross section
C  BUR(n) is the dimensional burial depth (cm) below seabed.
            bury(n)=ymine/htmin
         bur(n)=(1.0-bury(n))*h
         ucross(n)=u0(n)*COS(theta(n)*2.0*pi/360.0)
         vlong(n)=u0(n)*SIN(theta(n)*2.0*pi/360.0)
c..migration calculated in meters relative to initial position xuxo,yuxo using
C SST sign conventions (Solidworks).
        shield(n)=u0(n)**2.0/(1.65*g*b_dia)
        if(shield(n).GT.scrit.AND.bury(n).GT.burmove)then
        ylong(n)=vlong(n)*delt*ay/100.0+ylong(nm1)
          if(theta(n).LT.dir_thr)then
          xcross(n)=-1.0*ucross(n)*delt*ax/100.0+xcross(nm1)
          else
          xcross(n)=ucross(n)*delt*ax/100.0+xcross(nm1)
          endif
        else
        xcross(n)=xcross(n)
        ylong(n)=ylong(nm1)
        endif
c
        if(n.GE.mstart.AND.n.LE.mend)write(*,*)n,bury(n),bur(n)
    &,xcross(n),ylong(n),shield(n),theta(n)
9406      continue
c
c
      kbur=0
      DO 9408 n =1,nblines
```

```
      time(n)=time(n)+tshift
      write(4,92000)time(n),bury(n),bur(n),xcross(n),ylong(n),shield(n)
     &,theta(n)
          kbur=kbur+1
9408   continue
92000   format(7f15.5)
       rewind(4)
c
      write(*,*)kbur
c
C**************************end UXO_br3 logic***************************
c
c
C$$$$$$$$$$$$$$$$$$$$$ BEGIN TIMESTEP LOOP $$$$$$$$$$$$$$$$$$$$$$$$$$$$
      i1=0
      i2=0
      i3=0
      i4=0
      i5=0
      OPEN(UNIT=14,FILE=ofile2,STATUS='unknown')
c***can't run past the end of the wave record
      if(mend.GT.nblines)mend=nblines
      do 888 m=mstart,mend
      write(*,*)m,mend
C***DISPERSION RELATIONSHIP
c..convert wave height to meters for cycloid program
      whtme(m)=wht(m)/100.0
      mcountc=mcountc+1
c
c
c..for EVERY wave in time series do ALL OF THE FORTRAN
          freq=1.0/per(m)
       sigma=2.0*pi*freq
       shaldep=ak*gm*(per(m)**2.0)/(2.0*pi)
c
c
c..Wave number array generated for every depth 0-300m for each wave
       do 1010 i=1,3001
       dept(i)=(3001-i)*0.1
c..... depth array generated from 300 m to 0 m, by 0.1 m
        wvnum(i)=0.0
        if(dept(i).LE.0)go to 1090
        if(dept(i).LT.shaldep)then
         wvnum(i)=sigma/((gm*dept(i))**0.5)
```

```
        go to 1090
        endif
        yj=(sigma**2*dept(i))/gm
        xj=yj
c
       do 1030 k5=1,100
       ht=tanh(xj)
       f=yj-xj*ht
       if (abs(f) .lt. 0.000001) go to 1040
       fd=-1.0*ht-(xj/cosh(xj)**2)
       xj=xj-(f/fd)
1030     continue
c
c        write(*,1050)
1050     format(' subroutine disp does not converge!!! ')
1040      wvnum(i)=xj/dept(i)
1090     continue
1010     continue
C***END OF DISPERSION RELATIONSHIP
c********output file names 1-99999
c********i1=ones digit, i2=tens digit, i3=100s digit, i4=1000s, i5=10000s
     i1=i1+1
     if(i1.EQ.10)then
     i2=i2+1
     i1=0
     if(i2.EQ.10)then
     i3=i3+1
     i2=0
     if(i3.EQ.10)then
     i4=i4+1
     i3=0
     if(i4.EQ.10)then
     i5=i5+1
     i4=0
     endif
     endif
     endif
     endif
c
     in1=48+i1
     in2=48+i2
     in3=48+i3
     in4=48+i4
     in5=48+i5
```

```
      fname(m)=CHAR(in5)//CHAR(in4)//CHAR(in3)//CHAR(in2)//CHAR(in1)
      fname2(m)=CHAR(in5)//CHAR(in4)//CHAR(in3)//CHAR(in2)//CHAR(in1)
     &//cc
      write(*,*)fname2(m)
c...open cycloid profile output files 27mar07
       OPEN(UNIT=11,FILE=fname2(m),STATUS='unknown')
c
c
c
        ep=akm/(akm-1.0)
        depcp(m)=bs*whtme(m)*((beta/(bs*whtme(m)*akm))**ep)
          dst=vdepce
c
c
         do 400 n=1,100
c  find wave number associated with depce(m)
           kn=0
           do 600 ind=1,3001
           if(dept(ind).LT.depce(m).AND.kn.EQ.0)then
           kn=1
           wn=wvnum(ind)
           endif
600          continue
           if(n.EQ.1)then
           fun_hy=wn*depce(m)
           if(ibrbm.EQ.1)then
           depce(m)=akbr*whtme(m)
           else
           depce(m)=akd*whtme(m)/SINH(fun_hy)
           endif
           else
           kj=0
           do 601 ip=1,3001
           if(dept(ip).LT.depce(m).AND.kj.EQ.0)then
           kj=1
           wn=wvnum(ip)
           endif
601          continue
           fun_hy=wn*depce(m)
           if(ibrbm.EQ.1)then
           depce(m)=akbr*whtme(m)
           else
           depce(m)=akd*whtme(m)/SINH(fun_hy)
           endif
```

```
        endif
400     continue
c
       ac(m)=depce(m)/2.0
       bc(m)=depce(m)/2.0
       write(*,*)whtme(m),depce(m),wn
c
c
CCCC______cycloid ellipse
section_____________________________________________________
c
c   set eccentricity equal to parameter snum
c
      iuxo=0
      DO 777 n=2,nrange
      angc(n)=0.1*n
c   convert angc(n) to radians
      angc(n)=angc(n)*pi/180.0
c   apply stretching factor to cross shore coordinate xd...
      if(i_cycloid.EQ.1)then
c.TYPE-A
       fe=((2.0-(ecc**2.0))/2.0)**0.5
      rad=((SIN(angc(n)))**2.0)+((1.0-(ecc**2.0))
    &*((COS(angc(n)))**2.0))
      dr=-1.0*(ecc**2.0)*(SIN(angc(n))*COS(angc(n)))/rad
      dh=SIN(angc(n))+((1.0-COS(angc(n)))*dr)
      dx=1.0-COS(angc(n))+((angc(n)-(SIN(angc(n))))*dr)
      rc=(1.0-(ecc**2.0))**0.5*(ac(m)/(rad**0.5))
      xd(n)=((rc*fe*(angc(n)-(SIN(angc(n)))))/akxc)+xshift
      cycloid(n)=rc*(1.0-(COS(angc(n))))+(-1.0*zone)
      else
c.TYPE-B
       fe=((2.0-(ecc**2.0))/(2.0*(1.0-(ecc**2.0))))
      rad=((1.0-(ecc**2.0))*((SIN(angc(n)))**2.0))+
    &((COS(angc(n)))**2.0)
      dr=(ecc**2.0)*(SIN(angc(n))*COS(angc(n)))/rad
      dh=SIN(angc(n))+((1.0-COS(angc(n)))*dr)
      dx=1.0-COS(angc(n))+((angc(n)-(SIN(angc(n))))*dr)
      rc=bc(m)/(rad**0.5)
      xd(n)=((rc*fe*(angc(n)-(SIN(angc(n)))))/akxc)+xshift
      cycloid(n)=rc*(1.0-(COS(angc(n))))+(-1.0*zone)
      endif
c
c   apply stretching factor to slope
```

```
      slope(n)=(dh/dx)*(akxc/fe)
c   check slope(n) using slope of circlular cycloid
       dhc=SIN(angc(n))
       dxc=1.0-COS(angc(n))
c        circle(n)=(dhc/dxc)
      circle(n)=(dhc/dxc)*akxc
c   convert angc(n) back to degrees
       angc(n)=angc(n)*180.0/pi
c
c write cycloid at each xuxo in wave timeseries
       if(xd(n).GE.xuxo.AND.iuxo.EQ.0)then
        write(*,*)m,xd(n),cycloid(n)
        write(14,*)m,xd(n),cycloid(n)
       iuxo=1
       endif
c
c..add in xoffset, write cycloid profile
       xd(n)=xd(n)+xoffset
       write(11,*)xd(n),cycloid(n)
777    CONTINUE
       if(xd(nrange).LT.xuxo)then
        write(*,*)m,xd(nrange),cycloid(nrange)
       write(14,*)m,xd(nrange),cycloid(nrange)
       endif
c...End 27mar07
c
C***********************BEGIN SHAPE FILE LOGIC***************
CBurial Algorithm for bur in cm
c*****burial based on wave file
c
c..xinv and yinv already in cm
      xmid=(xinv*(ix-1))/2.0
      ymid=(yinv*(jy-1))/2.0
      if(bur(m).GT.h)then
      b_rad=0.0
      else
      b_rad=(b_dia/2.0)*(((h-bur(m))/h)**(1.0/point))
      endif
C
        open(3,file=ofile,status='unknown')
        DO 10 i=1,ix
        r(i)=((i-1)*xinv)-xmid
10        continue
c
```

```
      DO 15 j=1,jy
      s(j)=((j-1)*yinv)-ymid
15      continue
c
      k=0
      DO 20 i=1,ix
      do 30 j=1,jy
      k=k+1
      Ruxo=(r(i)*r(i)+s(j)*s(j))**0.5
c
      if(Ruxo.GT.b_rad)then
      b(k)=bplane
      else
      b(k)=h-bur(m)-(h*((Ruxo/b_rad)**point))
      endif
c
c
c
      write(3,920)r(i),s(j),b(k)
30      continue
20      continue
      rewind(3)
920     format(3f10.3)
C
c*****************Beginning on cn_scour_osc*******************
     b1=-1.0*3
     b2=-1.0*4
     b3=-1.0*5
     b4=-1.0*8
     b5=-1.0*10
     a0=1.0
     a1=5.410*(10**b1)
     a2=6.670*(10**b2)
     a3=1.173*(10**b3)
     a4=9.241*(10**b4)
     a5=2.729*(10**b5)
c
     gam0=0.5*cl*u0(m)*delx
c**oscilatory
     gam0_2=0.5*cl*u2(m)*delx
c**
     pi=3.14159
c
     open(9,file='z_mark.txt',status='unknown')
```

```
c
      ipts=ix*jy
c.....read 3 dimensional shape file
      icount=0
      do 100 k=1,ipts
      read(3,*)r(k),s(k),b(k)
      icount=icount+1
100   continue
c      write(*,*)icount
      rewind(3)
c
      kount=0
c.....read 3 dimensional shape file a second time to establish marker location
      do 110 i=1,ix
      do 120 j=1,jy
      read(3,*,end=111)dumr,dums,z_mark(i,j)
      kount=kount+1
120   continue
110   continue
111   continue
      write(*,*)kount
      rewind(3)
c
c
      if(m.NE.1)go to 166
      do 160 i=1,ix
      write(9,2000)(z_mark(i,j),j=1,jy)
160   continue
166   continue
c
c
      icount=0
      do 200 k=1,ipts
      icount=icount+1
c****part of sing point test
      if(r(k).EQ.r_test.AND.s(k).EQ.s_test)then
c.....re-initialize scour x-y grid
      do 131 i=1,ix
      do 141 j=1,jy
      scour(i,j,m)=0.0
141   continue
131   continue
      endif
c*******************************************************
```

```
      if(b(k).EQ.0.0)go to 200
      zmb=z_plane-b(k)
      zmb2=zmb**2
      zpb=z_plane+b(k)
      zpb2=zbp**2
c
      do 210 i=1,ix
      im1=(i-1)
c **calculate position relative to grid center offset by 1/2 grid cell to
c***prevent singularity at 0
      xgrid=im1*xinv-(xinv*ix/2)
      x(i)=xgrid-r(k)
      x1=x(i)
      x2=x(i)**2
      xs1=str*x(i)
      xs2=(str*x(i))**2
      gama(i)=a0+(a1*xs1)-(a2*xs1**2)+(a3*xs1**3)
      gamb(i)=(-1.0*a4*xs1**4)+(a5*xs1**5)
      gam(i)=(gama(i)+gamb(i))*gam0
      if(gam(i).LT.0.0)gam(i)=0.0
c**oscilatory vortex filament
      gama_2(i)=a0-(a1*xs1)-(a2*xs1**2)-(a3*xs1**3)
      gamb_2(i)=(-1.0*a4*xs1**4)-(a5*xs1**5)
      gam2(i)=(gama_2(i)+gamb_2(i))*gam0_2
      if(gam2(i).GT.0.0)gam2(i)=0.0
c***
c
      do 220 j=1,jy
      jm1=(j-1)
c **calculate position relative to grid center offset by 1/2 grid cell to
c***prevent singularity at 0
      ygrid=jm1*yinv-(yinv*jy/2)
      y(j)=ygrid-s(k)
      yps=y(j)+dely
      yps2=yps**2
      yms=y(j)-dely
      yms2=yms**2
      p1=gam(i)/(4.0*pi)
      aj24=p1*zmb/(x2+zmb2)*((yps/(x2+yps2+zmb2))-(yms/(x2+yms2+zmb2)))
      aj25=p1*zpb/(x2+zpb2)*((yps/(x2+yps2+zpb2))-(yms/(x2+yms2+zpb2)))
      u1=aj24+aj25
      aj26=p1*(zmb/(zmb2+yms2))*(1+(x1/(x2+zmb2+yms2)))
      aj27=p1*(zpb/(zpb2+yms2))*(1+(x1/(x2+zpb2+yms2)))
      aj28=p1*(zmb/(zmb2+yps2))*(1+(x1/(x2+zmb2+yps2)))
```

```
      aj29=p1*(zpb/(zpb2+yps2))*(1+(x1/(x2+zpb2+yps2)))
      v1=aj28+aj27-aj26-aj29
      tau0=rhom*cf*((2.0*u0(m)*u1)+(u1**2)+(v1**2))
c** oscilatory loop
      p1_2=gam2(i)/(4.0*pi)
      aj24_2=p1_2*zmb/(x2+zmb2)*
     &((yps/(x2+yps2+zmb2))-(yms/(x2+yms2+zmb2)))
      aj25_2=p1_2*zpb/(x2+zpb2)*
     &((yps/(x2+yps2+zpb2))-(yms/(x2+yms2+zpb2)))
      u1_2=aj24_2+aj25_2
      aj26_2=p1_2*(zmb/(zmb2+yms2))*(1+(x1/(x2+zmb2+yms2)))
      aj27_2=p1_2*(zpb/(zpb2+yms2))*(1+(x1/(x2+zpb2+yms2)))
      aj28_2=p1_2*(zmb/(zmb2+yps2))*(1+(x1/(x2+zmb2+yps2)))
      aj29_2=p1_2*(zpb/(zpb2+yps2))*(1+(x1/(x2+zpb2+yps2)))
      v2=aj28_2+aj27_2-aj26_2-aj29_2
      tau2=rhom*cf*((2.0*u2(m)*u1_2)+(u1_2**2)+(v2**2))
c**
      tau=tau0+tau2
      ajm=((tau-tauc)/tauc)*alpha
      if(tau.LT.tauc)ajm=0.0
      scour(i,j,m)=scour(i,j,m)+ajm
      if(z_mark(i,j).NE.0.0)scour(i,j,m)=0.0
      bot(i,j,m)=scour(i,j,m)*ak_bot
      if(z_mark(i,j).NE.0.0)bot(i,j,m)=bot(i,j,m)+z_mark(i,j)
c
220   continue
210   continue
200   continue
c
c
2000   format(301e15.6)
3000   format(f20.5)
c
c
      open(66,file=fname(m),status='unknown')
      do 300 i=1,ix
      write(66,2000)(bot(i,j,m),j=1,jy)
300   continue
      rewind(66)
      close(66)
c
888    continue
c$$$$$$$$$$$$$$$$$$$$$$$$$$ END TIMESTEP LOOP $$$$$$$$$$$$$$$$$$$$$$$$$$
c
```

```
c
c
      write(*,*)xoffset,yoffset
      stop
      end
```

Appendix B: FRF Duck Field Test Site Permits

NCDENR
North Carolina Department of Environment and Natural Resources
Division of Coastal Management
Michael F. Easley, Governor **Charles S. Jones, Director** William G. Ross Jr., Secretary

December 13, 2004

W. Coleman Long
Chief, Planning and Environmental Branch
Wilmington District, U.S. Army Corps of Engineers
P.O. Box 1890
Wilmington, NC 28402-1890

SUBJECT: Concurrence with Negative Determination for Tracking Inert Ordnance

Dear Mr. Long:

The Division of Coastal Management received (on December 2, 2004) a Negative Determination from the U.S Army Corps of Engineers (Corps) demonstrating that the proposal of the Naval Facilities Engineering Service Center at its facility in Duck in Dare County to track inert ordnance would not have coastal effects. It is the objective of the Division of Coastal Management to manage the State's coastal resources to ensure that proposed Federal activities would be compatible with safeguarding and perpetuating the biological, social, economic, and aesthetic values of the State's coastal waters.

The Division of Coastal Management (DCM) has reviewed the submitted information pursuant to the management objectives of the State's coastal program. DCM concurs that the proposed Federal activity is consistent, to the maximum extent practicable, with the enforceable policies of North Carolina's coastal management program.

Should the proposed activity be modified, a revised consistency certification could be necessary. Likewise, if further project assessments reveal environmental effects not previously considered by the proposed development, a revised consistency certification could be required. This might take the form of either a supplemental consistency determination pursuant to 15 CFR 930.46, or a new consistency determination pursuant to 15 CFR 930.36. If you have any questions, please contact Stephen Rynas at 252-808-2808. Thank you for your consideration of the North Carolina Coastal Management Program.

Sincerely,

Doug Huggett

Doug Huggett
Manager, Major Permits and Consistency Unit

cc: Ted Sampson, Division of Coastal Management

151-B Hwy. 24, Hestron Plaza II, Morehead City, North Carolina 28557-2518
Phone: 252-808-2808 \ FAX: 252-247-3330 \ Internet: www.nccoastalmanagement.net

An Equal Opportunity \ Affirmative Action Employer – 50% Recycled \ 10% Post Consumer Paper

DEPARTMENT OF THE ARMY
WILMINGTON DISTRICT, CORPS OF ENGINEERS
PO BOX 1890
WILMINGTON NC 28402-1890

CESAW-RG (1145-b) 10 February 2005

MEMORANDUM FOR Ms. Barbara Sugiyama, Principal Investigator, Naval Facilities Engineering Service Center, ESC411, 1100 23rd Avenue, Port Hueneme, California 93043

SUBJECT: Action ID 200510367, Department of the Army Permit for Naval Facilities Engineering Service Center

1. Enclosed is a Department of the Army (DA) permit to place unexploded ordnance models on the floor of the Atlantic Ocean, adjacent to the U.S. Army Corps of Engineers Field Research Facility and Pier, located at 1261 Duck Road, in Duck, Dare County, North Carolina, in accordance with your written request received 8 December 2004 and the ensuing administrative record.

2. If you require any change in the authorized work because of unforeseen or altered conditions or for any other reason, please revise the plans and send to this office promptly. Such action is necessary, as we must review and modify the permit for revised plans.

3. Carefully read your permit. The general and special conditions are important. Your failure to comply with these conditions could result in a violation of Federal law. Certain significant general conditions require that:

a. You must complete construction before 31 December 2008.

b. You must allow representatives from this office to make periodic visits to your worksite as deemed necessary to assure compliance with permit plans and conditions.

4. You must notify this office in advance as to when you intend to commence and complete work.

5. Please contact Mr. Raleigh W. Bland at the Washington Regulatory Field Office, at (252) 975-1616, extension 23, if you have questions.

Encls

CHARLES R. ALEXANDER, JR.
Colonel, EN
Commanding

CF(with encls):

Chief, Source Data Unit
NOAA/National Ocean Service
ATTN: Sharon Tear N/CS261
1315 East-west Hwy., Rm 7316
Silver Spring, MD 20910-3282

CF (w/special conditions and plans):

U.S. Fish and Wildlife Service
Fish and Wildlife Enhancement
Post Office Box 33726
Raleigh, North Carolina 27636-3726

Mr. Ron Sechler
National Marine Fisheries Service
Pivers Island
Beaufort, North Carolina 28516

Mr. Ronald J. Mikulak, Chief
Wetlands Protection Section - Region IV
Water Management Division
U.S. Environmental Protection Agency
61 Forsyth Street
Atlanta, Georgia 30303

Mr. Doug Huggett
Division of Coastal Management
North Carolina Department of
Environment and Natural Resources
151-B NC Hwy, Hestron Plaza II
Morehead City, North Carolina 28557

Mr. David Rackley
National Marine Fisheries Service
219 Fort Johnson Road
Charleston, South Carolina 29412-9110

DEPARTMENT OF THE ARMY PERMIT

RECEIVED
FEB 7 - 2005
REGULATORY
WILM. FLD. OFC.

Permittee **Naval Facilities Engineering Service Center**
Permit No. **200510367**
Issuing Office **CESAW-RG**

NOTE: The term "you" and its derivatives, as used in this permit, means the permittee or any future transferee. The term "this office" refers to the appropriate district or division office of the Corps of Engineers having jurisdiction over the permitted activity or the appropriate official of that office acting under the authority of the commanding officer.

You are authorized to perform work in accordance with the terms and conditions specified below.

Project Description: **Place inert unexploded ordinance models on the floor of the Atlantic Ocean.**

Project Location: **Adjacent to the U.S. Army Corps of Engineers Field Research Facility and Pier, located at 1261 Duck Road, in Duck, Dare County, North Carolina.**

Permit Conditions:

General Conditions:

1. The time limit for completing the work authorized ends on **December 31, 2008** If you find that you need more time to complete the authorized activity, submit your request for a time extension to this office for consideration at least one month before the above date is reached.

2. You must maintain the activity authorized by this permit in good condition and in conformance with the terms and conditions of this permit. You are not relieved of this requirement if you abandon the permitted activity, although you may make a good faith transfer to a third party in compliance with General Condition 4 below. Should you wish to cease to maintain the authorized activity or should you desire to abandon it without a good faith transfer, you must obtain a modification of this permit from this office, which may require restoration of the area.

3. If you discover any previously unknown historic or archeological remains while accomplishing the activity authorized by this permit, you must immediately notify this office of what you have found. We will initiate the Federal and state coordination required to determine if the remains warrant a recovery effort or if the site is eligible for listing in the National Register of Historic Places.

4. If you sell the property associated with this permit, you must obtain the signature of the new owner in the space provided and forward a copy of the permit to this office to validate the transfer of this authorization.

5. If a conditioned water quality certification has been issued for your project, you must comply with the conditions specified in the certification as special conditions to this permit. For your convenience, a copy of the certification is attached if it contains such conditions.

6. You must allow representatives from this office to inspect the authorized activity at any time deemed necessary to ensure that it is being or has been accomplished in accordance with the terms and conditions of your permit,

Special Conditions:

SEE ATTACHED SPECIAL CONDITIONS

Further Information:

1. Congressional Authorities: You have been authorized to undertake the activity described above pursuant to:

(X) Section 10 of the Rivers and Harbors Act of 1899 (33 U.S.C. 403).

( ) Section 404 of the Clean Water Act (33 U.S.C. 1344).

( ) Section 103 of the Marine Protection, Research and Sanctuaries Act of 1972 (33 U.S.C. 1413).

2. Limits of this authorization.

a. This permit does not obviate the need to obtain other Federal, state, or local authorizations required by law.

b. This permit does not grant any property rights or exclusive privileges.

c. This permit does not authorize any injury to the property or rights of others.

d. This permit does not authorize interference with any existing or proposed Federal project.

3. Limits of Federal Liability. In issuing this permit, the Federal Government does not assume any liability for the following:

a. Damages to the permitted project or uses thereof as a result of other permitted or unpermitted activities or from natural causes.

b. Damages to the permitted project or uses thereof as a result of current or future activities undertaken by or on behalf of the United States in the public interest.

c. Damages to persons, property, or to other permitted or unpermitted activities or structures caused by the activity authorized by this permit.

d. Design or construction deficiencies associated with the permitted work.

e. Damage claims associated with any future modification, suspension, or revocation of this permit.

4. Reliance on Applicant's Data: The determination of this office that issuance of this permit is not contrary to the public interest was made in reliance on the information you provided.

5. Reevaluation of Permit Decision. This office may reevaluate its decision on this permit at any time the circumstances warrant. Circumstances that could require a reevaluation include, but are not limited to, the following:

a. You fail to comply with the terms and conditions of this permit.

b. The information provided by you in support of your permit application proves to have been false, incomplete, or inaccurate (See 4 above).

c. Significant new information surfaces which this office did not consider in reaching the original public interest decision.

Such a reevaluation may result in a determination that it is appropriate to use the suspension, modification, and revocation procedures contained in 33 CFR 325.7 or enforcement procedures such as those contained in 33 CFR 326.4 and 326.5. The referenced enforcement procedures provide for the issuance of an administrative order requiring you to comply with the terms and conditions of your permit and for the initiation of legal action where appropriate. You will be required to pay for any corrective measures ordered by this office, and if you fail to comply with such directive, this office may in certain situations (such as those specified in 33 CFR 209.170) accomplish the corrective measures by contract or otherwise and bill you for the cost.

6. Extensions. General condition 1 establishes a time limit for the completion of the activity authorized by this permit, Unless there are circumstances requiring either a prompt completion of the authorized activity or a reevaluation of the public interest decision, the Corps will normally give favorable consideration to a request for an extension of this time limit.

Your signature below, as permittee, indicates that you accept and agree to comply with the terms and conditions of this permit.

Jan 31, '05

(PERMITTEE) **NAVAL FACILITIES ENGINEERING SERVICE CENTER** *(DATE)*

This permit becomes effective when the Federal official, designated to act for the Secretary of the Army, has signed below.

11 Feb 05

(DISTRICT ENGINEER) **CHARLES R. ALEXANDER, JR., COLONEL** *(DATE)*

When the structures or work authorized by this permit are still in existence at the time the property is transferred, the terms and conditions of this permit will continue to be binding on the new owner(s) of the property. To validate the transfer of this permit and the associated liabilities associated with compliance with its terms and conditions, have the transferee sign and date below.

(TRANSFEREE) *(DATE)*

*U.S. GOVERNMENT PRINTING OFFICE: 1986 - 717-425

SPECIAL CONDITIONS

a. If, in the opinion of the Secretary of the Army or his authorized representative, said structure or work shall cause unreasonable obstruction to the free navigation of the navigable waters, the Permittee will be required, upon due notice from the Corps of Engineers, to remove, relocate, or alter the structural work or obstructions caused thereby.

b. The Permittee must place the tethering devices in such a manner so as not to create a risk of entanglement by sea turtles feeding or foraging in the vicinity of the pier.

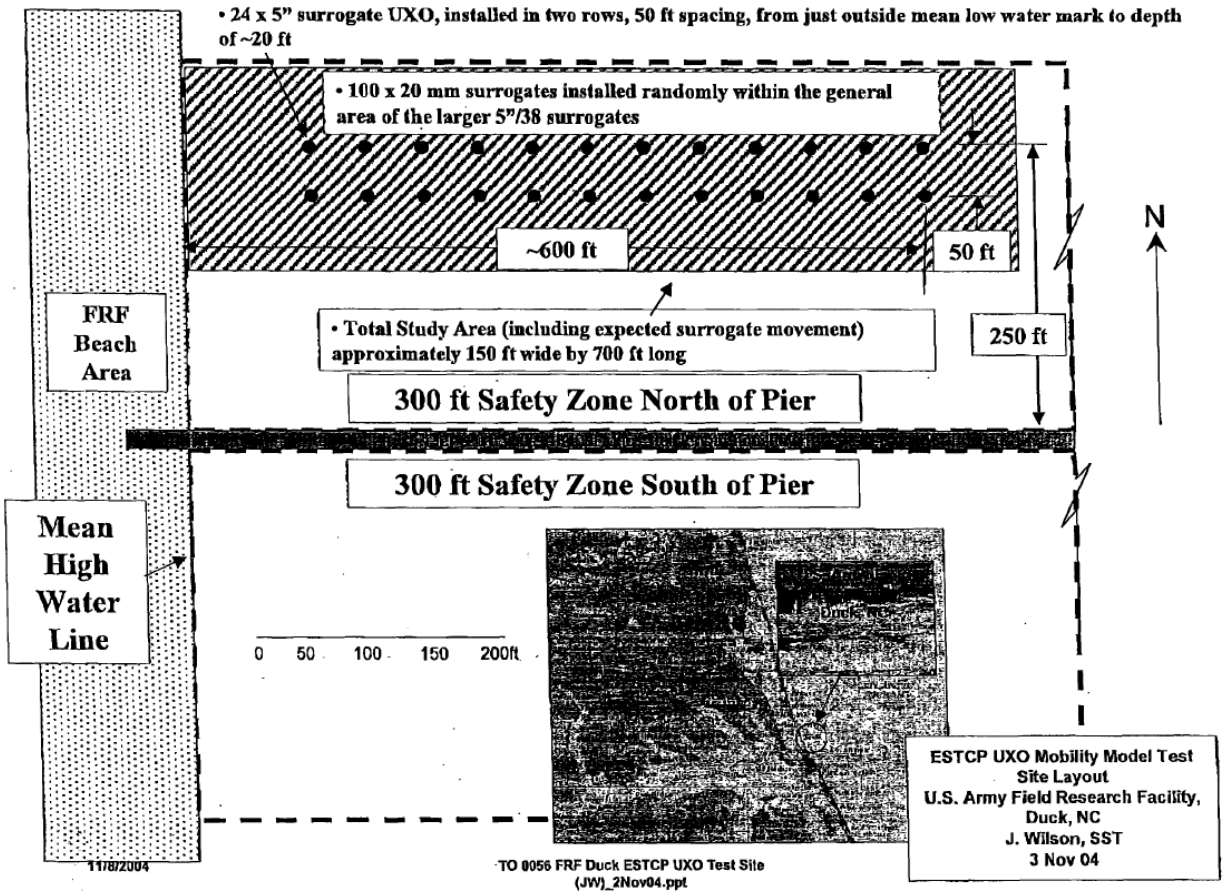

NOTIFICATION OF ADMINISTRATIVE APPEAL OPTIONS AND PROCESS AND REQUEST FOR APPEAL

Applicant: **Naval Facilities Engineering Service Center**	File Number: **200510367**	Date: **JAN. 19, 2005**
Attached is:		See Section below
X	INITIAL PROFFERED PERMIT (Standard Permit or Letter of permission)	A
	PROFFERED PERMIT (Standard Permit or Letter of permission)	B
	PERMIT DENIAL	C
	APPROVED JURISDICTIONAL DETERMINATION	D
	PRELIMINARY JURISDICTIONAL DETERMINATION	E

SECTION I – The following identifies your rights and options regarding an administrative appeal of the above decision. Additional information may be found at http://usace.army.mil/inet/functions/cw/cecwo/reg or Corps regulations at 33 CFR Part 331.

A: INITIAL PROFFERED PERMIT: You may accept or object to the permit.

- ACCEPT: If you received a Standard Permit, you may sign the permit document and return it to the district engineer for final authorization. If you received a Letter of Permission (LOP), you may accept the LOP and your work is authorized. Your signature on the Standard Permit or acceptance of the LOP means that you accept the permit in its entirety, and waive all rights to appeal the permit, including its terms and conditions, and approved jurisdictional determinations associated with the permit.
- OBJECT: If you object to the permit (Standard or LOP) because of certain terms and conditions therein, you may request that the permit be modified accordingly. You must complete Section II of this form and return the form to the district engineer. Your objections must be received by the district engineer within 60 days of the date of this notice, or you will forfeit your right to appeal the permit in the future. Upon receipt of your letter, the district engineer will evaluate your objections and may: (a) modify the permit to address all of your concerns, (b) modify the permit to address some of your objections, or (c) not modify the permit having determined that the permit should be issued as previously written. After evaluating your objections, the district engineer will send you a proffered permit for your reconsideration, as indicated in Section B below.

B: PROFFERED PERMIT: You may accept or appeal the permit

- ACCEPT: If you received a Standard Permit, you may sign the permit document and return it to the district engineer for final authorization. If you received a Letter of Permission (LOP), you may accept the LOP and your work is authorized. Your signature on the Standard Permit or acceptance of the LOP means that you accept the permit in its entirety, and waive all rights to appeal the permit, including its terms and conditions, and approved jurisdictional determinations associated with the permit.
- APPEAL: If you choose to decline the proffered permit (Standard or LOP) because of certain terms and conditions therein, you may appeal the declined permit under the Corps of Engineers Administrative Appeal Process by completing Section II of this form and sending the form to the division engineer. This form must be received by the division engineer within 60 days of the date of this notice.

C: PERMIT DENIAL: You may appeal the denial of a permit under the Corps of Engineers Administrative Appeal Process by completing Section II of this form and sending the form to the division engineer. This form must be received by the division engineer within 60 days of the date of this notice.

D: APPROVED JURISDICTIONAL DETERMINATION: You may accept or appeal the approved JD or provide new information.

- ACCEPT: You do not need to notify the Corps to accept an approved JD. Failure to notify the Corps within 60 days of the date of this notice means that you accept the approved JD in its entirety, and waive all rights to appeal the approved JD.
- APPEAL: If you disagree with the approved JD, you may appeal the approved JD under the Corps of Engineers Administrative Appeal Process by completing Section II of this form and sending the form to the division engineer. This form must be received by the division engineer within 60 days of the date of this notice.

E: PRELIMINARY JURISDICTIONAL DETERMINATION: You do not need to respond to the Corps regarding the preliminary JD. The Preliminary JD is not appealable. If you wish, you may request an approved JD (which may be appealed), by contacting the Corps district for further instruction. Also you may provide new information for further consideration by the Corps to reevaluate the JD.

SECTION II – REQUEST FOR APPEAL or OBJECTIONS TO AN INITIAL PROFFERED PERMIT

REASONS FOR APPEAL OR OBJECTIONS: (Describe your reasons for appealing the decision or your objections to an initial proffered permit in clear concise statements. You may attach additional information to this form to clarify where your reasons or objections are addressed in the administrative record.)

ADDITIONAL INFORMATION: The appeal is limited to a review of the administrative record, the Corps memorandum for the record of the appeal conference or meeting, and any supplemental information that the review officer has determined is needed to clarify the administrative record. Neither the appellant nor the Corps may add new information or analyses to the record. However, you may provide additional information to clarify the location of information that is already in the administrative record.

POINT OF CONTACT FOR QUESTIONS OR INFORMATION:

If you have questions regarding this decision and/or the appeal process you may contact: Mr. Raleigh Bland Washington Regulatory Field Office P.O. Box 1000 Washington, North Carolina 27889-1000	If you only have questions regarding the appeal process you may also contact: Mr. Arthur Middleton, Administrative Appeal Review Officer CESAD-ET-CO-R U.S. Army Corps of Engineers, South Atlantic Division 60 Forsyth Street, Room 9M15 Atlanta, Georgia 30303-8801

RIGHT OF ENTRY: Your signature below grants the right of entry to Corps of Engineers personnel, and any government consultants, to conduct investigations of the project site during the course of the appeal process. You will be provided a 15-day notice of any site investigation, and will have the opportunity to participate in all site investigations.

_____ Signature of appellant or agent	Date:	Telephone number:

DIVISION ENGINEER:
Commander
U.S. Army Engineer Division, South Atlantic
60 Forsyth Street, Room 9M15
Atlanta, Georgia 30303-3490

DEPARTMENT OF THE NAVY

NAVAL FACILITIES ENGINEERING SERVICE CENTER
1100 23RD AVE
PORT HUENEME CA 93043-4370

IN REPLY REFER TO:

April 26, 2005

MEMORANDUM for Colonel Charles Alexander, Department of the Army, Wilmington District, Corps of Engineers, Post Office Box 1890, Wilmington, North Carolina 28402

SUBJECT: Permit Number 200510367, Commencement of Work

1. The Naval Facilities Engineering Service Center (NFESC) plans to commence work at the U.S. Army Corps of Engineers Filed Research Facility in Duck North Carolina on or near June 20, 2005. Part of this effort involves placing inert unexploded ordinance on the floor of the Atlantic Ocean and will be performed in compliance with permit number 200510367.

2. Please address any questions or concerns to myself at (805) 982-1668 (e-mail barbara.sugiyama@navy.mil)

Barbara M. Sugiyama

cc:
Mr. Raleigh W Bland (ACOE Wilmington District, Washington Regulatory Field Office)
Ms. Alexandra Devisser (NFESC, Code ESC51)
Mr. Carl Miller (FRF)
Mr. Jerry Haskins (ERDC)

Appendix C: Test Hardware

NOTE: This discussion of Test Hardware - with accompanying photographs - appears in the UXO Measurement Method Field Test Plan of 29 March 2004 (reference 4 of this report).

Preliminary brainstorming for materials to be used in construction of surrogate UXO called for the use of concrete, lead, rebar, and tin. This design was appealing on a cost basis but required a lot of steps. Using a concrete matrix with an SG (specific gravity) of 2.3 the design would have to incorporate lead to reach the desired overall SG and CG (center of gravity). Concrete is also prone to water erosion and requires strength members to make it strong. These strength members combined with use of lead and tin (for the cylindrical portion of the UXO) make a very complicated modeling process. With some research it was found that there exists a resin type moldable plastic that is machineable and has a high SG. This plastic is also very strong and resistant to water absorption. The strength enables the design to be much simpler allowing modeling to be much more accurate. The high SG permits the avoidance of lead use for the core. (See Table B-1 for typical plastic properties.)

Table B-1 Hapco, Inc., Hapcast 3738/60 Properties

Viscosity @ 25° C	9,000 cps
Hardness Shore D	85-90
Ultimate Compressive Strength	16-18,000 psi
Linear Shrinkage inch/inch	.001
Specific Gravity	2.5
Color	Black
Machinability	Very good

Properties of HapCast 3738/60
Courtesy of Hapco, Inc. <http://www.hapcoweb.com>

2.5 pound cast iron weight-plates (identical to ones used for fitness) were selected as the SG equalizer because of their diameter, cost, and high density ($7.0\, g/cm^3$). The center rod is a standard weight lifting handle with nutlike screwing weight-locks to hold the weight-plates in place. This cast iron core facilitates the correct specific gravity and center of mass. Placement of the cast iron weight-plates must be 1.65 inches from the base of the rod and rod end must be flush the end of the mold to reach ideal center of mass. Pouring the Hapcast 3738/60 into the mold with correct placement of the cast iron core will result in properties listed.

Mass properties of Assembly UXO
Output coordinate System: -- default -- Density = .18 pounds per cubic inch Mass = 54.22 pounds Volume = 302.7 cubic inches
Center of mass: (Inches) X=0.00 Y-7.72 (19.61 cm) Z=0.00

The underwater acoustic tracking system used had two basic subsystems. The first was the active acoustic pinger on each surrogate plus a multi-frequency diver-held receiver. That was used to allow the diver to select each surrogate's frequency, listen for the ping, and then follow it to position himself over the surrogate. The second sub-system was the Benthos acoustic positioning system. The diver held the Benthos receiver close to the surrogate and received range data from each of 2 or 3 fixed Benthos transponders. Those ranges were later converted into a location for each surrogate.

Sonotronics USR-96 Narrow Band Scanning Receiver:

The USR-96 is built by SONOTRONICS, 3169 S Chrysler Ave, Tucson, AZ 85713 (Email: sales@sonotronics.com, www.sonotronics.com). It offers wide tuning range and narrow band reception ideal for use in noisy environments. Additionally, the USR-96 may be set to scan 10 preset frequencies to reduce the labor in manual tracking. The two line LCD displays both frequency and interval. The USR-96 is available as a part of the **MANTRAK Kit**, bringing all of the tools together necessary for manual tracking.

FREQUENCY: 30 - 90 kHz, 250 Hz steps.
BANDWIDTH: 500 Hz, 7 pole response.
OUTPUT: Headphone jack, RS-232 output.
POWER: Internal rechargeable batteries with charger.
SIZE: 6.3 in. x 6.3 in. x 4.5 in. deep
INPUT: BNC connector
SENSITIVITY: 1 uVolts for 30 dB (S+N)/N ratio.
DISPLAY: 2 x 16 LCD

Sonotronics Model DH-4 directional hydrophone:

This unit provides the greatest range and precision in locating tags in lakes and oceans, and permits rejection of local noise caused by dams or pumping stations in rivers and streams. The DH-4 is the primary hydrophone for both fixed stations and manual tracking.

SENSITIVITY: -84 dBV ref 1 uBar.
BEAM WIDTH: +/-6 degrees at half power points.
SHAFT LENGTH: User supplies mounting shaft (1 inch PVC).
OUTPUT: BNC connector on 10-foot coaxial cable (other lengths available).
CABLE: *Replaceable* RG-58 C/U.

Sonotronics UDR Underwater Diver Receiver:

The UDR allows a diver to approach an object or target marked with a pinger, even in low visibility environments. The UDR comes with waterproof headphones. The unit has variable gain control to maintain good signal strength and directionality during approach to the target. It also has a volume control and a backlit display. The unit is user programmable for frequency selection and gain range.

Length: (From Display to outer rim) 16cm
Width: (At outer rim) 11cm
Height: (Bottom of Handle to top of unit) 20cm
Weight (Air): UDR: 900g, Headphones: 415g
Sensitivity: 20uV, (S+N)/N = 30dB
Frequencies: 30 to 90 kHz
Controls: Gain control, volume control, and frequency control. User can preprogram the unit before the dive for a variety of applications.

Sonotronics EMT-01-2 Equipment Marker Acoustic Pingers:

The EMT transmitters are a set of standard models packaged and configured for equipment marking applications.

The EMT series transmitters come standard with flat ends and 3/16" mounting holes on each end. Other custom packaging options are possible. Each EMT pinger is individually numbered, with different frequencies and pinger intervals so that differentiation can take place in the "in field" environment.

Model	Length	Diameter	Weight	Range	Depth Rating
EMT-01-1	99mm	19mm	39g	Up to 1km	2.5km

FREQUENCY RANGE: 77-83 kHz
RANGE: Up to 3km
SOURCE LEVEL: 146dB re 1μPa at 1 meter (14dB below NMFS 160dB standard for impact on marine mammals)
SIZE: 104x18mm

WEIGHT: 15g
BATTERY LIFE: 18 months

Specifications for the FRF Duck instrumentation (wave measurements, beach profilers, etc.) are available at the FRF Duck website.

Appendix D: Data

Figure 75 depicts the conversion of the Benthos range measurements to surrogate locations.

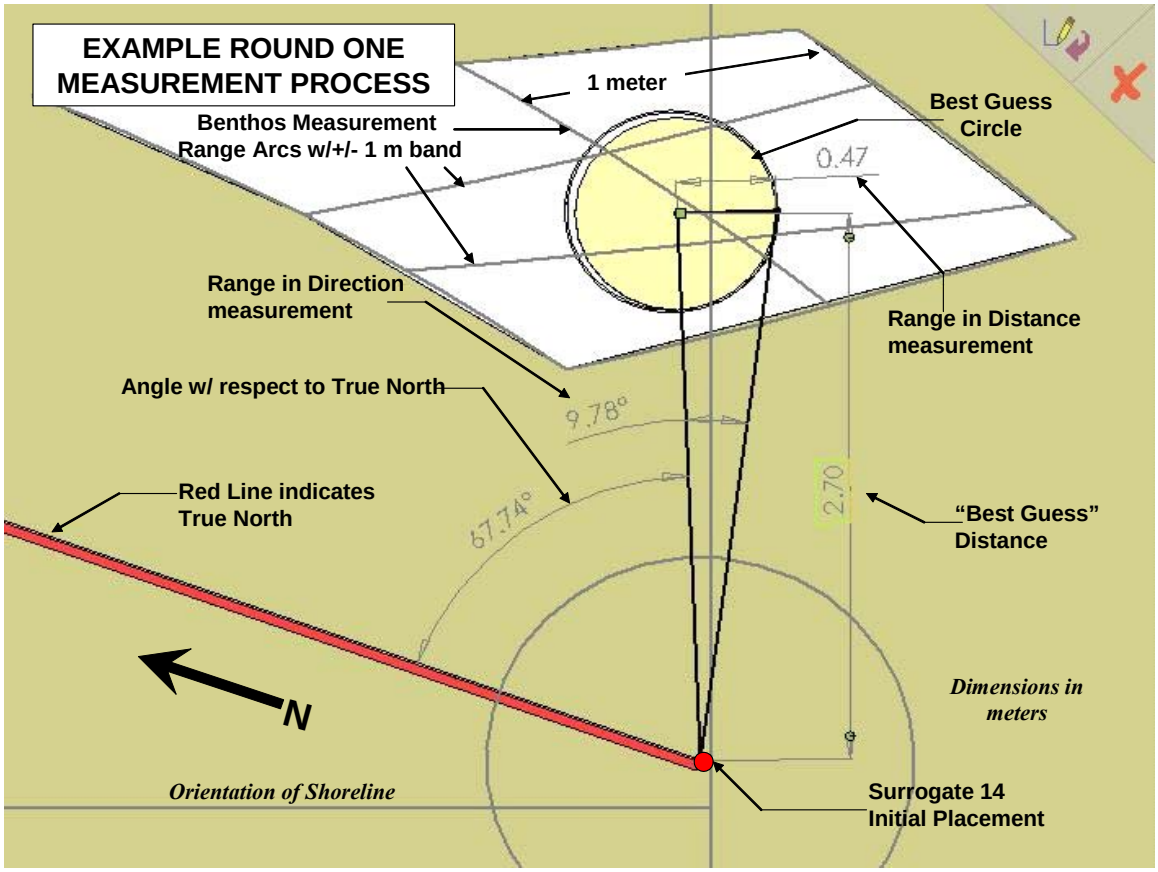

Figure 75. Converting Benthos range measurements to surrogate location.

Table 9. Round Two measurements determined cumulatively from the installation point to the reference stakes.

12 AUG 05 UXO Surrogate Location Measurements at FRF Duck, NC

				Benthos Transducer Measurement (m)		
Surrogate	freq (kHz)	Code	Interval	stake 220m	stake 260m	stake 300m
1	70			10	47	83
2	81			12	32	72
3	78			24	14	52
4	72			49	12	33
5	69			72	44	12
6	82			86	48	10
Date:	Time:	Recorder:		**Hand Measurement with Tape (ft.)**		
Surrogate	Notes (Burial depth, Orientation):			stake 220m	stake 260m	stake 300m
1						
2						
3						
4						
5						
6						
				Benthos Transducer Measurement (m)		
Surrogate	freq (kHz)	Code	Interval	stake 620m	stake 660m	stake 700m
7	71			11	47	87
8	75			14	35	74
9	72			33	13	49
10	74			48	13	33
11	71			73	36	11
12	79			85	48	7
Date:	Time:	Recorder:		**Hand Measurement with Tape (ft.)**		
Surrogate	Notes (Burial depth, Orientation):			stake 220m	stake 260m	stake 300m
7						
8						
9						
10						
11						
12						
				Benthos Transducer Measurement (m)		
Surrogate	freq (kHz)	Code	Interval	stake 220m	stake 260m	stake 300m
13	77			6	42	81
14	78			9	38	74
15	77			22	11	48
16	79			52	13	26
17	77			69	29	9
18	78			86	46	9
Date:	Time:	Recorder:		**Hand Measurement with Tape (ft.)**		
Surrogate	Notes (Burial depth, Orientation):			stake 220m	stake 260m	stake 300m
13						
14						
15						
16						
17						
18						
				Benthos Transducer Measurement (m)		
Surrogate	freq (kHz)	Code	Interval	stake 620m	stake 660m	stake 700m
19	79			11	51	90
20	70			9	42	77
21	76			37	10	50
22	81			50	16	33
23	73			77	10	9
24	69			89	51	12
Date:	Time:	Recorder:		**Hand Measurement with Tape (ft.)**		
Surrogate	Notes (Burial depth, Orientation):			stake 220m	stake 260m	stake 300m
19						
20						
21						
22						

An example of the Round One movement plus the incremental movement derived from the Round Two measurements is shown for Surrogate #7 in Figure 76 below. The path is shown incrementally by starting at the initial placement location, signified by the solid blue circle, and then progressing along the path of the two green arrows, first to the solid yellow circle in Round One and then to the solid red circle in Round Two.

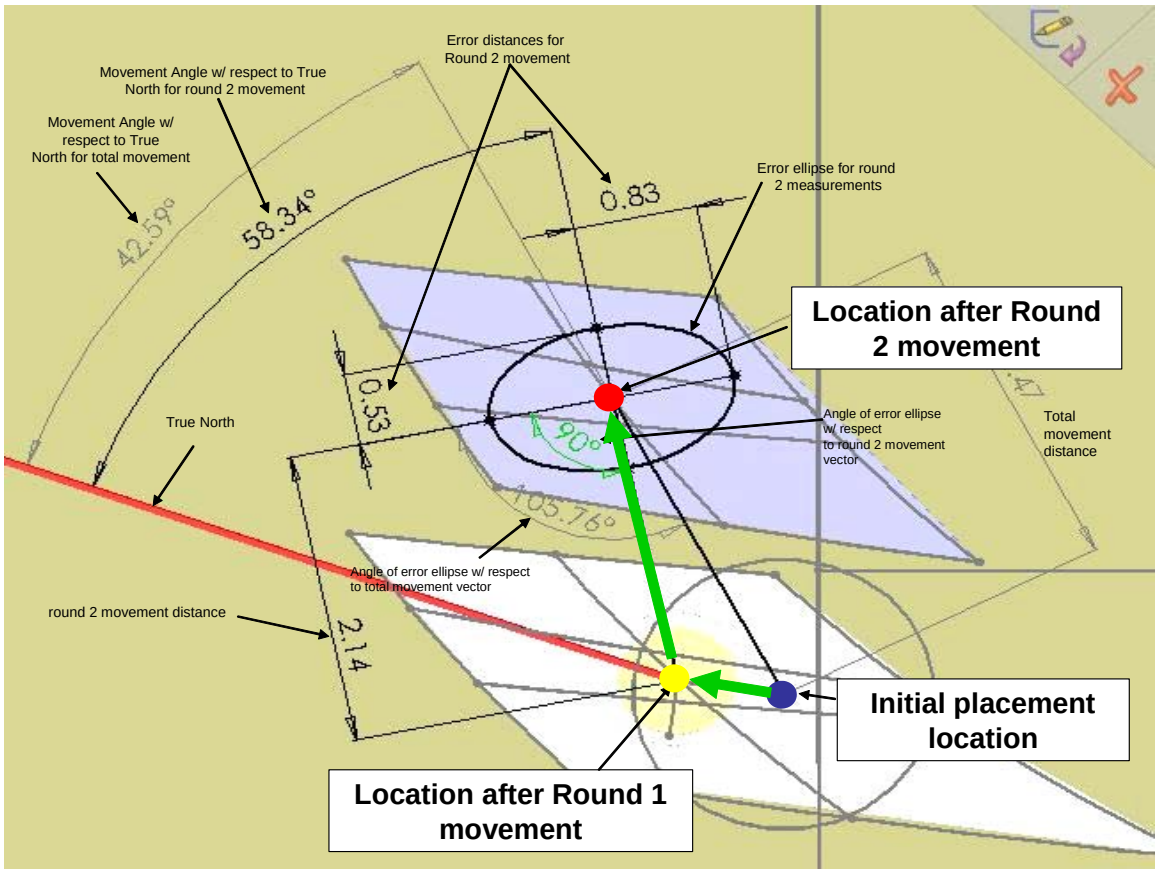

Figure 76. Surrogate #7 movement from the initial location, to Round One, and then to Round Two.